

Growth and Characterization of
ZnSe On GaAs and Si Substrates Using
Metal Organic Chemical Vapour Deposition Technique.

by

© Jayatirtha H. N.
Department of Electrical Engineering
McGill University
Montreal, Canada.

July 1989

A Thesis

Submitted to the Faculty of Graduate Studies and Research
in partial fulfillment of the requirements for the
Degree of Master of Engineering.

Study of ZnSe/(GaAs, Si) heterojunctions using MOCVD technique

Abstract

This work is based on the heterojunctions of zinc selenide grown on gallium arsenide semiconductor. The heterojunctions formed between them pose interesting junction properties because of the minimum lattice mismatch. A pulsed organometallic chemical vapour deposition technique is used to grow good quality zinc selenide thin films of the order of few microns, both on gallium arsenide and silicon substrates. In order to fully understand the interface properties of such structures the junctions were characterized by various techniques.

Experiments of X-ray diffraction were performed on samples of ZnSe:GaAs and ZnSe:Si grown at different substrates temperatures. The X-ray experiments revealed a preferred [111] orientation of ZnSe thin films on GaAs and Si substrates. Examination of the samples of ZnSe grown on Si substrates under SEM showed a variation of film morphology with the growth temperature. The SEM and X-ray experiments suggested that the optimum growth temperature for good quality and uniform ZnSe thin films was 350°C.

Optical measurements were performed on ZnSe:GaAs diodes in order to determine in a quantitative way the band structure of the heterojunctions. The results suggested that the depletion of electrons occurred on the GaAs side and accumulation of electrons

in the ZnSe side.

The electrical characterization of ZnSe:GaAs diodes was done using current-voltage (I-V) and differential capacitance-voltage (C-V) methods. The results of the I-V analysis lead us to believe that the current transport across the junction occurs due to a tunneling mechanism. The C-V analysis also allowed us to determine the value and uniformity of donor concentration in the grown film. The results suggested that the junction is abrupt and that the depletion region extends into the lightly doped side of the junction. In order to further understand the nature of impurity profile in the grown film, photoluminescence measurements were performed on ZnSe:GaAs diodes both at low and high temperatures. The spectra indicated a low level of residual impurity in all the cases. Finally, an energy band model for the ZnSe:GaAs heterostructure is adopted to account for the various observed results.

Résumé

Ce travail consiste principalement en l'étude d'hétérojonctions semiconductrices d'arséniure de gallium (GaAs) recouvertent de séléniure de zinc (ZnSe). Vu la correspondance étroite des reseaux cristallins, on observe des propriétés de jonction intéressantes lors de la formation de ce type d'hétérojonctions. On utilise une technique de deposition à l'aide de vapeurs chimiques organo-metalliques, pour faire croître des films minces de quelques microns de ZnSe sur du silicium (Si) et sur du GaAs. Afin de bien comprendre les propriétés d'interface de telles structures, les jonctions ont été caractérisées par plusieurs techniques.

Des expériences par diffraction de rayon-X ont été effectuées sur des échantillons de ZnSe:GaAs ainsi que de ZnSe:Si, obtenus pour différentes températures des substrats. Les expériences aux rayons-X révèlent une orientation préférentielle [111] du film de ZnSe sur les deux types de substrats. L'examen de croissance de ZnSe sur les substrats de Si à l'aide d'un microscope à balayage électronique démontre la variation de la morphologie des films avec la température de croissance. Les expériences de microscopie et de diffraction de rayons-X suggèrent que la température de croissance optimum pour l'obtention de films minces, uniformes et de bonne qualité de ZnSe est de 350°C. Des expériences optiques ont été exécutées sur des diodes ZnSe:GaAs afin de déterminer de façon quantitative la structure de bande des hétérojonctions. Les résultats suggèrent

une baisse de concentration électronique du côté du GaAs et une hausse de la concentration du côté du ZnSe.

La caractérisation électrique des diodes ZnSe:GaAs consiste en la caractéristique volt-ampère (I-V) et la mesure différentielle capacité-voltage (C-V). Les caractéristiques volt-ampère nous amènent à croire que le transport du courant à travers la jonction se produit par un mécanisme à effet tunnel. Les analyses capacité-voltage nous permettent de déduire l'uniformité ainsi que la valeur, de la concentration des donneurs dans le film. Les résultats suggèrent que la jonction est abrupte et que la région de faible concentration s'étale vers le côté faiblement dopé de la jonction. Afin de mieux comprendre la nature du profil d'impuretés dans le film, des mesures de photoluminescence ont été exécutées sur les diodes ZnSe:GaAs à basse température ainsi qu'à température ambiante. Dans tous les cas, le spectre indique un faible niveau d'impuretés résiduelles. Finalement, un modèle de bande d'énergie pour l'hétérojonction ZnSe:GaAs est adopté pour expliquer les différents résultats observés.

Acknowledgements

I am gratefully indebted to my thesis supervisors Professor D. Walsh and Dr. I. Shih for their encouragement, ideas, enthusiastic discussions and constant help throughout the course of this project.

I am very much thankful to Drs. K. Mazuruk and M. Benzaquen for their help in crystal growth, critical appraisal of data and most valuable suggestions throughout this work.

I also extend my thanks to visiting Professor, H. Aharoni, from Ben Gurion University, Israel for his active participation and guidance to make this work successful.

I very much appreciate the good times I shared with my fellow graduate students during this work and I thank them all for their help and cooperation from time to time in both academic and other matters.

Finally I am very much grateful to my parents for their patience and moral support.

Table of Contents

	Page No.
Abstract	I
Resume	III
Acknowledgements	V
Table of Contents	VI
CHAPTER 1 Introduction	1
CHAPTER 2 Types of Epitaxial Growth	3
2.0 Introduction	3
2.1 Types of Epitaxy	6
2.2 Band Model of GaAs & ZnSe	9
CHAPTER 3 Factors Affecting OMCVD	11
3.1 Factors Affecting Growth	11
3.2 Introduction to Heterojunctions	22
CHAPTER 4 Fabrication of Heterojunctions	30
4.1 Vacuum Evaporation Technique	30
4.2 OMCVD Technique	33
4.3 Growth by OMCVD Technique	41
4.4 Growth of ZnSe on Si and GaAs Substrates by OMCVD	48
4.5 OMCVD Growth System	49
4.6 External Contacts	58
CHAPTER 5 Experimental Results	59
5.1 Thickness and X-ray Measurements	59
5.2 Photo-Electric Measurements	74
5.3 I-V Measurements	80
5.4 C-V Measurements	90
5.5 Photoluminescence Spectra	92
5.6 SEM Analysis	98
5.7 Energy Band Model	98
CHAPTER 6 Conclusions	101
References	103

CHAPTER 1

INTRODUCTION

This study deals with the growth and characterization of ZnSe thin films on gallium arsenide and silicon substrates. Both ZnSe and GaAs are direct band gap semiconductors with a minimum lattice mismatch that makes them good candidates for the formation of heterojunction having interesting electrical and optical properties. The main emphasis of research is on understanding the growth mechanism of good quality ZnSe thin films using organometallic chemical vapour deposition technique necessary for the formation of good quality interface for the electronic device application. Although no attempt has been made in the present work on the fabrication of a specific electronic device, a study of optical and electrical properties of such heterojunctions is considered in view of potential device application.

The second chapter of the thesis gives a brief introduction to heterostructures and describes various techniques employed in the growth of thin films. Energy band structures of gallium arsenide and zinc selenide are considered.

The third chapter is dedicated to the understanding of the OMCVD technique for the growth of thin films and the factors that affect the growth parameters. A brief description of formation and properties of n-n heterojunction are also given. An account

of band off-set and band deformation at the interface is given in light of conduction band off-set that occurs at the ZnSe:GaAs interface.

Chapter four deals with all the steps involved in the fabrication of ZnSe heterojunctions both by vacuum evaporation and OMCVD techniques on silicon and gallium arsenide substrates. Experimental results and analysis are given in chapter five. Emphasis is based on characterization of ZnSe:GaAs heterojunctions using various methods such as x-ray and SEM for structural properties, photoluminescence and photo-electric for optical properties and current-voltage, capacitance-voltage measurements for electrical properties. Finally an energy-band diagram is adopted based on the observed properties for the ZnSe : GaAs system.

A brief summary of all the steps involved in this work and a few useful comments on the important precautions that are necessary at the time of fabrication, concludes this thesis.

CHAPTER 2

TYPES OF EPITAXIAL GROWTH

2.0 Introduction :

Heterojunctions are formed whenever two different materials of different energy gaps are brought into contact. Depending on the types of material used for the formation of the heterojunction four kinds of junctions are possible between two different semiconducting materials namely n-N, p-P, n-P, p-N heterostructures. Such contacts have interesting electrical and electro optical properties and find many application in devices such as high speed band-pass photodetector, light emitting devices and injection lasers [1].

In order to form effective heterojunctions, some of the properties of the materials involved in the junction formation such as energy band gap, dielectric constant, lattice constant and the degree of crystal perfection must be obtained.

Most of the III-V compound semiconductors such as gallium arsenide crystallize in zinc blend structure where each atom is surrounded by four equidistant neighbours which lie at the corner of a tetrahedron as shown in the figure 2-1.

Goldschmidt first prepared GaAs in 1920s, and found it to have a zinc blend structure [2]. This material has fcc translational symmetry, with a basis of one GaAs molecule at origin, and the

other at $1/4 \ 1/4 \ 1/4$ of the fcc unit cube. GaAs cleaves most readily on $\{110\}$ family planes. Goryunova noted that GaAs can also cleave on $\{111\}$ planes and between (111) and (011) [3]. Of the eight planes in the $\{111\}$ family for GaAs, four are $(111A)$ planes containing only gallium atoms. The other four planes are $(111B)$ comprised entirely of arsenic atoms as shown in the fig.

2-2. Most of the II-VI compound semiconductors such as zinc selenide crystallize both in zinc blend and wurtzite structure as shown in fig. 2-3. In order to form heterojunctions, identical combinations of structures is essential. Failure to observe this may result in change in electrical properties of the junction.

Both gallium arsenide and zinc selenide are direct band gap semiconductors having the same crystallographic structures. The lattice mismatch is less than one percent which makes them prime candidates for the heterojunction formation. The following table summarizes some of the important properties of both these compounds at room temperature.

Table 1 Properties of ZnSe and GaAs at room temperature

Material	Type	Band gap (eV)	Lattice constant (Å)	Mobility ($\text{cm}^2/\text{v}.\text{sec}.$)
GaAs	III-V	1.42	5.654	5-8000
ZnSe	II-VI	2.67	5.667	5-600

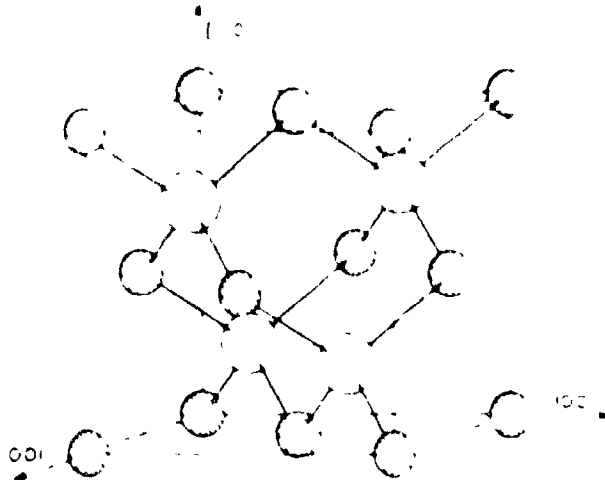


Fig. 2-1 Structural arrangement of Ga and As atoms. [2]

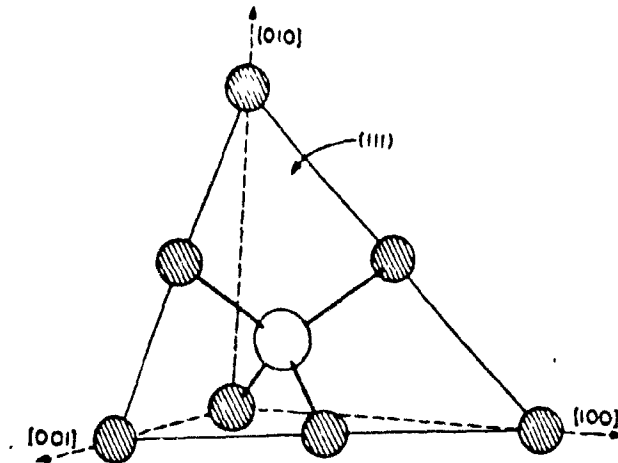


Fig. 2-2 FCC translational symmetry for GaAs. [3]

If the lattice mismatch is significant, then defects such as interfacial dislocations are generally present and they have effects on band bending and recombination of minority carriers at the hetero interface.

2.1 TYPES OF EPITAXY :

In order to achieve a good heterojunction, several techniques have been widely used and some of the important methods are listed below.

2.11 Liquid Phase Epitaxy (LPE):

This technique involves precipitation of a material from a supercooled solution onto an underlying substrate. The composition of the layer formed on the substrate depends mainly on the equilibrium phase diagram and to lesser extent on the orientation of the substrate. The main points are

- 1) the composition of melt
- 2) the growth temperature and
- 3) the growth time.

This method was first developed by Nelson in 1963 [4]. Advantages of this method includes the simplicity of the equipment and higher deposition rate.

2.12 Vapour Phase Epitaxy (VPE):

In vapour phase epitaxy method, the materials to be deposited are in the vapour form at room temperature. Under the suitable conditions of temperature and pressure, they react and deposit on

to the substrate to form an epitaxial layer of the film. This technique was first demonstrated by Tietjenend [5] and Anik [6]. Advantages include 1) high degree of flexibility in introducing the dopants, 2) good control of composition gradient by accurate flow adjustment.

2.13 Organometallic Chemical Vapour Deposition (OMCVD):

In this technique, the semiconductor films of III-V and II-VI compounds are produced by decomposing appropriate group III and group II organometallic compounds in the presence of the appropriate group V and group VI hydrides or alloys. In addition, the group II organometallic and group VI hydrides are commonly used as dopants for the III-V compounds. Very good quality films can be grown using this method under controlled temperatures and time of growth. This method was used for the first time to grow gallium arsenide by Manasevit and Simpson in 1969 [7], using trimethyl gallium and arsine as the source materials.

2.14 Molecular Beam Epitaxy (MBE):

Molecular beam epitaxy is a process involving the reaction of one or more thermal beams of atoms or molecules with the crystalline surface under ultra high vacuum conditions. The knowledge of surface physics and the observation of surface structure variations resulting from the relation between the atom arrival rate (beam flux) and the substrate temperature allows considerable understanding of preparation of high quality films with the compilation of atomic layers upon one another [8].

In 1958, Gunther described the growth of III-V materials using this technique [9]. The main advantages of this method includes

- 1] precise control over layer thickness and doping profile
- 2] high uniformity over large area of substrate.

2.15 Vacuum Evaporation :

In vacuum deposition method, the substance to be deposited is taken in the form of a powder in a suitable boat, placed in the vacuum chamber evacuated to a low pressure of few micro torr. A suitable current is passed through the system to heat up the boat and to evaporate the material on the substrate. Fairly good quality films can be grown using this method [10].

2.16 Interface Alloy Technique :

In interface alloy method, the material to be alloyed in is taken in the molten form and brought into contact with the second material. The formation of the junction takes place by the process of diffusion at the interface of the two materials. This technique is however not very popular [11].

In order to fabricate a good junction, both the materials used should have a similar thermal coefficient of expansion during the growth process in order to avoid defects resulting from over stress and strain on the grown layers. In order to grow films of good quality, cleanliness is almost important at each step of growth in all these techniques.

Out of the techniques mentioned above, OMCVD and LPE are widely used. Both these techniques give a unique opportunity for low temperature deposition, resulting in the great improvement in the photoelectric properties of grown layers.

2.2 BAND MODEL OF GALLIUM ARSENIDE AND ZINC SELENIDE :

The band structure of gallium arsenide has been theoretically calculated by Kane et al [12] using perturbation theory. These calculations have revealed that GaAs is a direct gap semiconductor with a band gap of 1.42 eV at room temperature and has an important secondary minimum at about 0.36 eV above the lowest minimum as shown in fig. 2-4.

Zinc selenide on the other hand, has a band gap energy of 2.67 eV at room temperature. Analysis of scattering mechanism in ZnSe has shown the presence of considerable ionic component in the binding. Fig. 2-5 shows the energy band of ZnSe along the [111], [100] and [110] symmetry axes first proposed by Cohen and Bergstresser [13] using pseudo potential method.

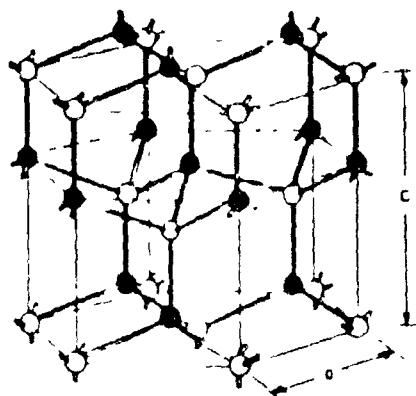


Fig. 2-3 Wurtzite structure of ZnSe. [3]

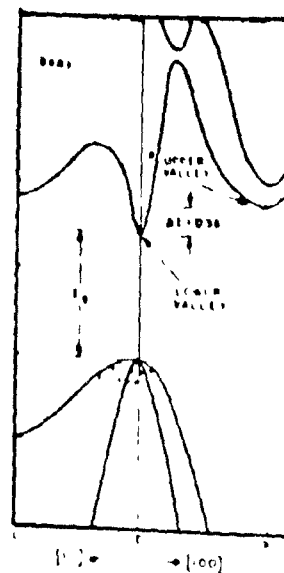


Fig. 2-4 Second minima of GaAs. [12]

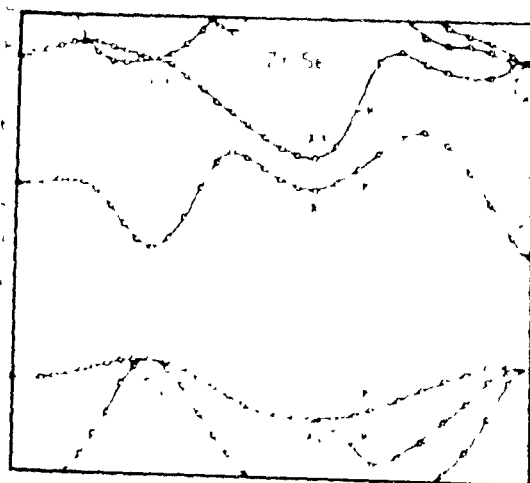


Fig. 2-5 Energy band of ZnSe along the [111], [100] and [110] symmetry axes. [13]

CHAPTER 3

FACTORS AFFECTING OMCVD

3.1 Factors Affecting Growth :

In order to obtain good quality films using the OMCVD technique, the following factors have to be optimized as they affect the growth results significantly.

3.1.1 Reaction pressure :

Reaction pressure plays an important role in the growth of high quality thin films of ZnSe. It has been observed that low pressure favours the growth of defect free thin films by minimizing the premature reaction between dimethylzinc (DMZ) and hydrogen selenide (H_2Se) in the presence of a carrier gas such as HCl. These components can react at room temperature and hence it is necessary to minimize the number of collisions between molecules in the period 't', the time between gas mixing and contact between the substrate. Low pressure creates conditions for high translational velocity of the reactant molecules thus minimizing the value of 't' and the number of collisions between molecules in this period. For the growth of ZnSe on (100) GaAs, Fugita et.al. [14] have shown that the growth rate falls by approximately a factor of 3 in going from 10 to 0.1 torr from (7.5 to 2.5 $\mu m/hr.$) for flow rates of 10 standard cubic centimeter per minute (sccm) for DMZ and 50 sccm for H_2Se . The substrate temperature was maintained at 350°C. It was observed that the quality of the layer increases dramatically with

pressure reduction.

3.12 Substrate Temperature :

The carrier concentration in ZnSe films prepared by OMCVD is mainly determined by the substrate temperature. It varies between 10^{17} and 10^{14} cm^{-3} below 350°C . This may be due to the fact that chlorine atoms in the carrier gas HCl might have remained in the reactor. In addition it has been reported that the carrier concentration monotonically decreased with the increase in film thickness. Such a decrease in the carrier concentration may give rise to dominant donor species in unintentionally doped ZnSe [15].

The electron mobility in the hetero epitaxial films increases with the film thickness since the stress and/or defects in the films induced by the effect of lattice mismatch between the substrate and the grown layer reduce with the increase in the film thickness. Increase in the electron mobility can also be attributed to improvement of the crystallinity of the films grown at higher substrate temperatures. It has been observed that [16] the value of electron activation energy does not change significantly during the growth process. The electron mobilities in such films have been reported to be $300\text{-}400$ $\text{cm}^2/\text{v}\cdot\text{sec}$. at room temperature for thickness of $1\text{-}3$ μm .

3.13 Molar Ratio of Se/Zn Source Gas :

The molar ratio between Se source and the Zn source is

significant in varying the film properties. Molar ratio is simply defined as the ratio between source gases of H_2Se and DMZ which are introduced into the reactor. Since both the gases are admitted into the reaction chamber during the growth process, the composition of the gases in the reaction mixture varies to a considerable extent based on gas pressure, spreading angle and the distance from the substrate surface where these gases decompose to form suitable reaction products. Thus the effect of the $|H_2Se|/|DMZ|$ molar ratio on the film properties has a tendency to vary the carrier concentration significantly.

In the growth of III-V compounds such as GaAs by OMCVD the gas composition ratio of TMG/ AsH_3 can have effect on the material properties. As in the previous case, the higher molar ratio of arsine to gallium has a net effect of reducing the carrier concentration. The number of methyl radicals present is reduced by the increased rate of hydrogen transfer from the greater number of AsH_3 species to the radicals to form methane. The methyl radicals are the source of carriers and hence, less carriers are available for incorporation.

3.14 Morphology :

The next criterion is the morphology of the grown films. Substrates used for epitaxy play an important role. The ideal substrate is the one which has lattice constants same as that of the epitaxial layer as in homoepitaxy. Hence the substrate chosen for the growth of epitaxial films considerably affect the

morphology of the grown films. However, the more recent studies on ZnSe [17] showed that $\text{ZnS}_x\text{Se}_{1-x}$ and GaAs lattice matched very closely when $x = 0.06$ using the former as the substrate material. The penetration of gallium into the substrate was significant and the penetration depth increased with the substrate temperature during deposition.

3.15 Lattice Mismatch :

In order to grow high quality ZnSe layers on GaAs, the mismatch between the two materials should be minimum; the mismatch at room temperature is significantly large. Such a large mismatch between the ZnSe and the GaAs is related to the high donor concentration frequently observed in undoped ZnSe on GaAs [18]. The explanation is that the Ga atoms may diffuse from the GaAs substrate into the epilayer during growth due to the mismatch. High quality ZnSe free of misfit dislocation can be grown if the grown layers are thin enough to be strain free. The misfit between ZnSe and the GaAs is of the order of 0.3 % at room temperature and slightly increases with temperature. The misfits can be accommodated by a periodic set of dislocations i.e. parallel lattice planes will be incorporated into the GaAs lattice. Holt [19] has pointed out that the distance between these planes is of the order of a few hundred atomic units. It was also pointed out by him that the ZnSe:GaAs diodes exhibit typical current-voltage characteristics having a weak temperature dependence.

It has been shown by Hiroshi M. et al. [20] that the lattice of

ZnSe grown on GaAs using OMCVD thinner than 0.15 μm expands in the growth direction involving the elastic strain so that ZnSe can be lattice-matched to the smaller lattice of GaAs at the interface. On the other hand the layers thicker than 1 μm have the same lattice constant as that of bulk ZnSe, implying that the strain is released by introducing misfit dislocations. These results clearly indicate the importance of lattice match for growing high quality thick layers. This could be improved by growing $\text{ZnS}_x\text{Se}_{1-x}$ alloy exactly lattice matched to GaAs or growing ZnSe onto $\text{In}_x\text{Ga}_{1-x}\text{As}$ or $\text{In}_x\text{Ga}_{1-x}\text{P}$ substrates which are lattice matched to ZnSe [21].

However, it is worth while to point out that some of the chemical reactions used in OMCVD can occur prematurely upstream from the required deposition zone and at a temperature lower than that of the substrate, resulting in non uniformity of the grown layers. Such non uniformities have been observed in films of ZnSe grown using DMZ and H_2Se and mainly attributed to the occurrence of premature reaction between the alkyls and the hydrides [22]. These premature reactions lead to the formation of adducts which, if sufficiently volatile, can be transported after in-situ formation. The successful use of adducts has been demonstrated for the growth of III-V compounds but not as yet for the II-VI compounds.

P.J. Wright et.al. [23] have shown that the growth of $\text{ZnS}_x\text{Se}_{1-x}$ offers the possibility of growing layers which are lattice

matched to these substrates and potentially free from residual strain. However, the major difficulty in the alloy growth is that the relationship between the $H_2S:H_2Se$ ratio in the gas phase and the S:Se ratio in the solid phase is non-linear. Control of the gas phase ratio ($x=0.052$) to achieve lattice matching with GaAs proved relatively simple because the gas phase concentrations of the two hydrides are relatively high. The uniformity of composition through the layers was confirmed by EDAX studies across a cleaved section.

Heterocyclic compounds are shown to be useful as sources of the group VI elements in their reaction with DMZ for the growth of crystalline layers of ZnSe in the standard technique of OMCVD. The problems of premature reaction observed between the group VI hydrides and DMZ is insignificant when heterocyclic compounds are employed. In this case, the reaction is brought between DMZ and a sulphur containing heterocyclic compound namely selenophene (C_3H_2Se). With this method, good quality single crystal ZnSe has been grown on GaAs(100) single crystal substrate. The use of the heterocyclic compounds to produce either single crystal or polycrystalline layers on a wide range of substrates at relatively low temperatures suggests considerable potential for using heterocycles in production of the current range of thin layer devices using II-VI compounds; these include electroluminescent panels, optical filters, anti-reflection coatings and transparent conducting layers [24].

The main advantage of heterocyclic compounds over the conventional use of hydrides lies in the fact that the pre reaction observed in the later is almost completely absent. This absence indicates a reduced reactivity of the group VI atoms in the cyclic structures compared to the simpler hydrides, an observation which is supported by slightly higher temperatures required for deposition when the heterocyclic compounds are used. Nevertheless, since the heterocyclic structures do not contain "active" hydrogen atoms as do hydrogen selenide, their total reactivity towards DMZ must reduce. This effect may be further enhanced by the presence of group VI atoms in the ring structure.

3.16 Interface Formation :

The next consideration in the growth by OMCVD is the physics of interface formation during thin film deposition. We have considered here both the techniques of vacuum evaporation and OMCVD as well. Kinetic theory shows that the atoms evaporated from an open boat as in vacuum evaporation, have a Maxwellian velocity distribution and a mean kinetic energy of $3/2 kT$. At a temperature of 800°C , this energy is of the order of about 0.2 eV [25]. Only a negligible number of atoms have energies greater than 1 eV. Hence the energy available from the stopping of thermally evaporated atoms is not enough to clean physically adsorbed gases from the surface. This is the reason why the kinetic energy of the thermally evaporated atoms may be neglected when considering the sticking coefficients or nucleation and

growth phenomenon. In the presence of lattice relaxation, the energy needed for the diffusion of atoms into the lattice is of the order of 1 to 5 eV. Such penetration may create vacancies in the substrate lattice or increase the number of foreign interstitial atoms and in turn may result in the formation of dislocation loops [26].

The overall result of these processes is a change in the free energy and the structure of the substrate surface which in turn affects the number of nucleation sites and the surface free energy and results in the change of bond strength between the substrate and the resulted film. These effects change properties such as film stress, sticking coefficient and film structure etc. In the case in which there is a solid solubility of one material into the lattice of the other the interfacial region can be established by diffusion; the activation energy for diffusion coming from any source such as heating of the substrate as in the case of OMCVD.

3.17 Thermodynamics :

It has been shown that for understanding any vapour growth process thermodynamics play a very important role [27]. However, the thermodynamic study of OMVPE are not common because such reactions are normally considered as a non equilibrium or kinetically controlled process. Hishachi Seki et al. [28] have shown that the chemical equilibrium is established at the vapour-solid interface for the growth of all common III-V compounds and

alloys. An equilibrium model has been established by the above workers to relate the vapour and the solid compositions. Details of the model has not been dealt here. The result of this analysis is in agreement with the data cited in literature.

It has been shown that the distribution relation of III-V alloys in MOVPE is determined mainly by the Gibbs free energy of formation of binary compounds and by the input V/III ratio. For preparing III-V compounds in a reproducible manner, a precise control of the V/III ratio is of considerable importance. The study concluded that the equilibrium model proposed, showed that under normal growth conditions i.e. $V/III > 1$, the growth is independent of the deposition temperature and V/III ratio, and the rate increases linearly with the increase of the input partial pressures of the group III source. These are quite in agreement with the experimental observations. It was also noticed that a drastic variation of equilibrium partial pressure occurred at $V/III = 1$. This has been attributed to the changes of solid stoichiometry and the carbon contamination of grown layers. In fact, it has been experimentally observed that the abrupt change of the conduction type from p to n with the increase of V/III ratio without intentional doping in the growth of GaAs.

3.18 Thermal Expansion Coefficient:

Another factor which is very important in the the growth of ZnSe on gallium arsenide is the thermal expansion of both the materials during the growth process. In order to grow good

quality films free from strained layers, it is important that both the materials should have the same coefficient of thermal expansion. The investigation of thermal expansion of GaAs and ZnSe, which are isotronic of the germanium series was carried out by Novikova [29] in 1960. Figure 3-1 shows the plots of α versus absolute temperature for both gallium arsenide and zinc selenide. For GaAs, it can be seen that α decreases with the decreasing temperature, becoming equal to zero at $T = 55$ K and passing into the region of negative values. At $T=40$ K, the value of α is $-0.5 * 10^{-5}$ per degree.

For ZnSe, it can be seen that the value of α becomes negative at $T < 64$ K, and has a minimum value of $-3.10 * 10^{-5}$ per degree at $T=36$ K. These results show that the expansion coefficients of GaAs and ZnSe are in the close vicinity. The thermal expansion coefficient for GaAs has been reproduced and is predicted theoretically as a function of temperature. The corresponding phonon shift occurred in the case of gallium arsenide grown under pressure.

The aspects described above in chapters 2 and 3 of ZnSe and GaAs forms the basis of fundamental considerations in describing the formation and characterization of heterojunctions. We now deal with the basic concepts of heterojunctions with special reference to n-n heterostructures as is the case in this study.

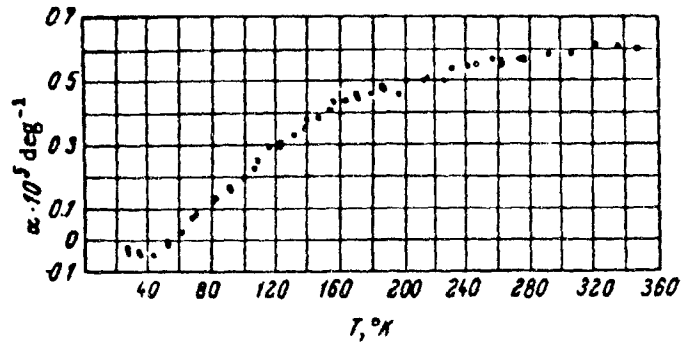
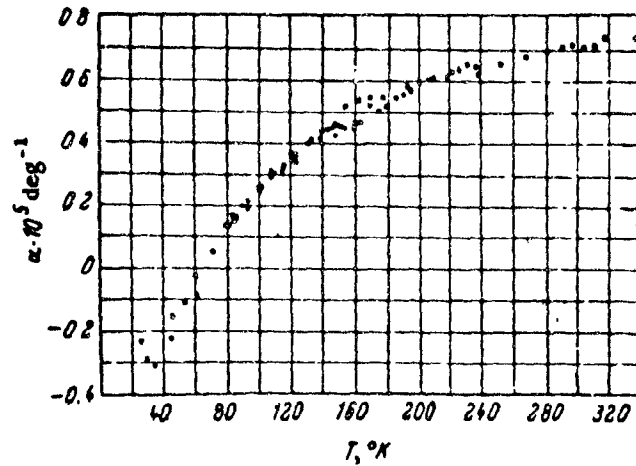
Experimental values of α for GaAs.Experimental values of α for ZnSe.

Fig. 3-1 Plot of expansion coefficient vs. absolute temperature for GaAs and ZnSe. [29]

3.2 INTRODUCTION TO HETEROJUNCTIONS :

The energy band model as proposed by R.L. Anderson has been discussed here with a particular reference to the n-n structure which forms the basis of our study.

3.21 Shockley-Anderson Model.

Shockly-Anderson [30] proposed a model describing the energy band at the hetero interface of the two junctions. From a device physics point of view the most important aspect of semiconductor hetero-interface, is the energy band diagram at the interface. The model assumes that the transition from one semiconductor takes place over atmost a few lattice constants. For such abrupt interfaces, the canonical "energy" band is the above model as shown in fig. 3-2. Its characteristic reature is an abrupt change in energy gap at the interface, leading to discontinuities or offsets in the conduction and valence band edges. The magnitudes of these offsets are assumed to be characteristic properties of semiconductors pair involved, essentially independent of doping levels and hence of Fermi level considerations, but possibly dependent on the crystallographic orientation and on other factors influencing the exact arrangements of atoms near the interface. Away from the interface, the band energies are governed by the requirement that a bulk semiconductor must be electrically neutral, which fixes the band energies relative to the Fermi level.

Fig. 3-3 shows a band diagram for an n-n heterostructure based on

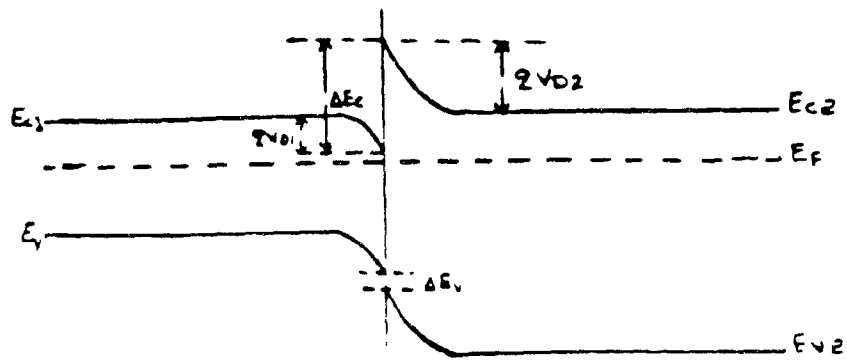


Fig. 3-2 Canonical energy band model for abrupt junctions. [30]

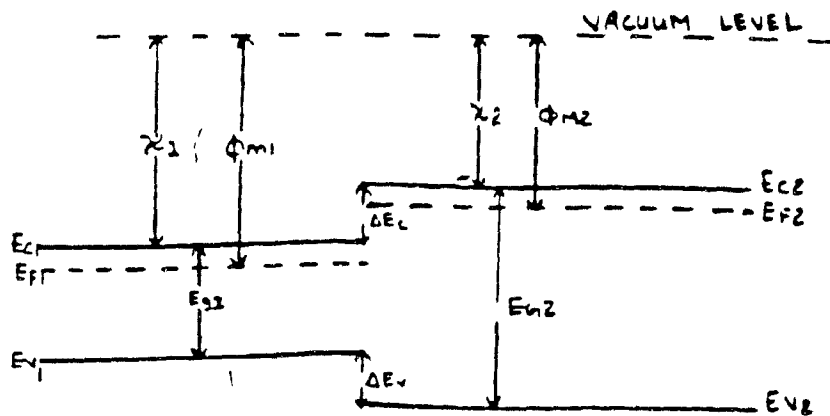


Fig. 3-3 Band diagram of isolated n-n heterostructure. [30]

Anderson's model. The conduction band offset then leads to a shallow potential notch and a Schottky barrier like potential spike barrier, both of which play large roles in the electrical properties of such junctions. The band offsets are the dominant aspect of heterostructure interfaces, and their existence is in fact the principal reason why heterostructures are incorporated into semiconductor devices. In fact, the band offsets act as potential barriers, exerting strong forces on electrons and holes. Basically the band offset forces may be made either to assist or to counteract the classical electrostatic forces.

Normally the presence of an interface charge has an effect of deforming the energy bands. Fig. 3-4 shows the deformation in such cases as applied to n-n heterostructures for both signs of the charge. From the figure it is clear that the negative interface charge would raise the height of the spike barrier and a positive charge lowers it. These charges in general have a significant effect on the overall barrier heights seen by the carriers and hence on the properties of any heterostructure device employing the offset barriers.

Interface charges may result either from the accumulation of chemical impurities at the interface during the growth, or due to the structural defects at the interface resulting from the strain on the grown layers. Also, this could be largely attributed to an additional mechanism that occurs at the hetero interfaces when two semiconducting materials combine from different columns of the periodic table, in which case there exists a large net

interface charge.

3.22 Energy Band Profile :

Consider the energy band profile of two isolated semiconductors as shown in the figure 3-3. The two materials are assumed to have a different band gaps E_g , different dielectric constant ϵ , different work function ϕ and different electron affinity χ . The work function is defined as that energy required to remove an electron from Fermi level to the position just out side of the material (vacuum level). The electron affinity is defined as the energy required to remove an electron from the conduction band to the vacuum level. The difference in energy in conduction band edges is denoted by ΔE_C and that between the valence band edges is represented by ΔE_V , as shown in the figure.

Whenever these two materials are brought into contact, the junction formation takes place and the band bending occurs at the interface depending on the type of materials involved in the junction formation. Figure 3-5 shows the energy band diagram between the n-ZnSe and n-GaAs at thermodynamic equilibrium.

Since the work function of the wide band semiconductor (ZnSe in the present case) is the smaller, the energy bands will be bent as shown in the fig. 3-5. Number of states available in the conduction band is small and so the excess electrons in the material of greater work function will occupy states in the conduction band. Since there are a large number of states available in the conduction band, the transition region extends

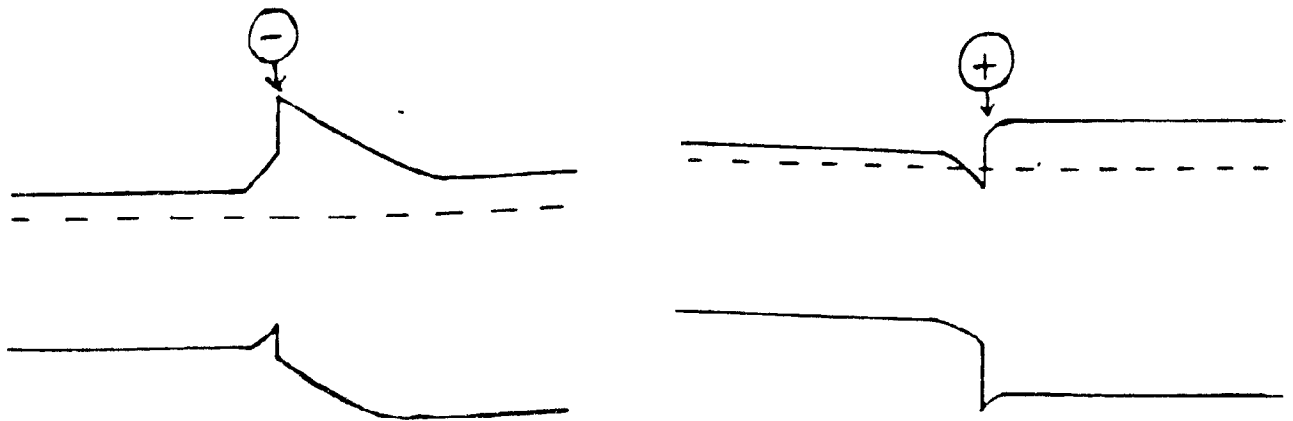


Fig. 3-4 Deformation of energy band diagram as applied to n-n heterojunctions. [31]

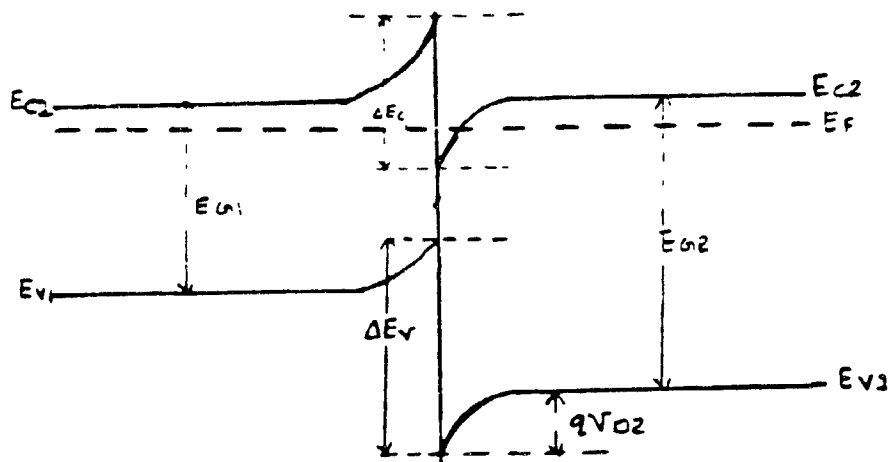


Fig. 3-5 Energy band diagram of n-n heterojunction at static equilibrium. [30]

only a small distance into the narrow band material and the voltage is mainly supported by the material with the smaller work function. The current-voltage characteristics of such junctions clearly indicate that there must be a discontinuity of conduction bands in such a way that the electron affinity of the larger band semiconductor (ZnSe in the present case) should be greater than the electron affinity of the of the smaller gap material (GaAs in the present study). This agrees well with the qualitative analysis by Swank [31], which shows that the electron affinity of zinc selenide to be equal to 4.09 eV and the electron affinity of gallium arsenide as 3.65 eV.

Figures 3-6 and 3-7 show the two cases in which the n-n heterojunctions have been biased differently. In the forward bias case the n-ZnSe is biased positively with respect to n-GaAs and the ZnSe side accumulates electrons. In the reverse bias condition, the ZnSe side is biased negatively with respect to the GaAs side. The valence band offset in the second case is more pronounced than in the first case. For the n-n heterojunction in the reverse bias case we normally consider only a tunneling transport of electrons predominating from the notch of the conduction band discontinuity of ZnSe into the GaAs. If there exists an accumulation layer at the ZnSe side, the possibility of electron tunneling with higher energies only has to be taken into consideration or else the effective barrier height would be smaller than the expected conduction band offset E_c .

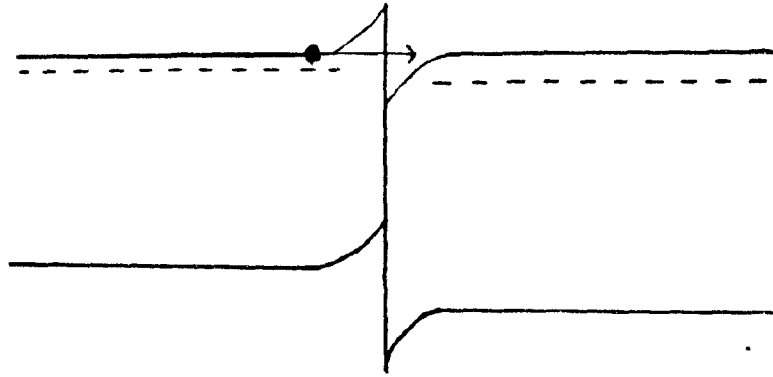


Fig. 3-6 Heterojunction with a forward bias.

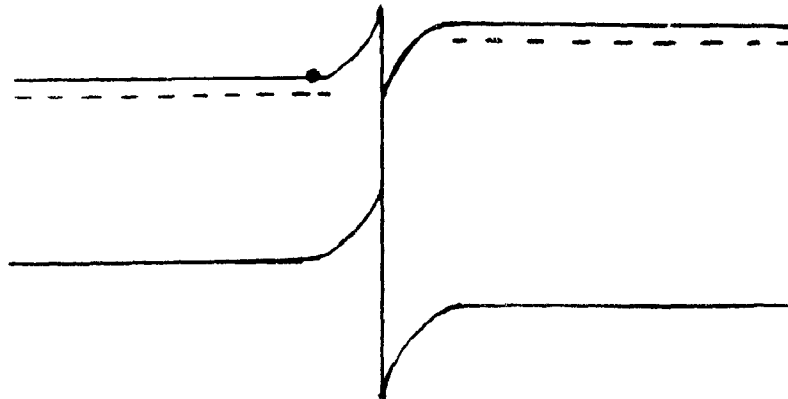


Fig. 3-7 Heterojunction with a reverse bias. [32]

Heterojunctions between n-ZnSe and n-GaAs have been prepared and the growth habits of ZnSe on GaAs monocrystals have shown that the epitaxial deposits of ZnSe can be obtained on (111) and (110) faces of GaAs. Thermodynamic calculations have shown that the partial pressure of selenium is much higher than the partial pressure of zinc [32]. This favours the creation of acceptors and as a consequence of self compensation, one should expect zinc selenide films of relatively high resistivity. However, MOCVD grown n-type ZnSe can be very conductive. This is possible if some kind of diffusion of gallium from the gallium arsenide substrate into zinc selenide has occurred.

The current voltage characteristics in heterojunctions are influenced by various mechanisms depending on the band discontinuities at the interface and the density of interface states. If the barrier to the holes is much higher than that for the electrons, then the current will consist of almost entirely of electrons; or if the density of interface states is very high then the dominant current will be generation-recombination current from the interface. The dominating current can also result from tunneling mechanism if the width of the barrier is very thin. It can also be attributed to the thermionic emission if the inter-face acts as a metal-semiconductor contact. We now proceed to to the fabrication of our junctions.

CHAPTER 4

FABRICATION OF HETEROJUNCTIONS

We employed two techniques to form heterojunctions of ZnSe on silicon and gallium arsenide substrates respectively. The first method used to form the junction was vacuum evaporation technique and the second being the organometallic chemical vapour deposition technique. Both the methods have been dealt in detail in this chapter.

4.1 VACUUM EVAPORATION TECHNIQUE

Vacuum evaporation is one of the most widely used deposition techniques. As described earlier in chapter two, this technique consists of vapourization of solid material by heating it to sufficiently high temperature and condensing it on to a cooler substrate to form a film. Heating of the material can be carried out directly or indirectly by a variety of methods. The most common method is to use a filament wire or boat which is electrically heated to evaporate the material. Such evaporation sources are normally made of refractory materials such as W, Mo, Ta etc. with or without a ceramic coating. The choice of the filament or the boat materials is primarily determined by the evaporation temperature and the resistance to alloying and chemical reactions with the evaporant. In this study, to evaporate ZnSe powder we employed Mo boat made in our laboratory.

Direct heating of the evaporant in the boat can be done easily

by passing current through it. In the case of evaporation of elements, the evaporated species consists of neutral single atoms which vapourize in the form of poly atomic clusters. In the case of alloys and compounds as in this study, vapourization is accompanied by dissociation or decomposition because of differences in vapour pressure of various constituent elements or because of thermal instability. However, if the constituents are equally volatile, congruent evaporation occurs. The composition of the vapour and the film differ from that of the source if evaporation is not congruent. This difference may be further aggravated if the condensation coefficient of the various constituent vapour atoms or molecules differ from each other. The tendency to dissociate is greater at high evaporation temperatures and low ambient pressures.

4.11 Langmuir Model :

According to Langmuir-Dushman theory of the kinetics of evaporation [33], the rate of free evaporation of atoms or molecules from a clean surface of unit area in vacuum is given by

$$N_e = 3.513 * 10^{22} * P_e (1/MT)^{1/2} \text{ molecules sec}^{-1} \text{ cm}^{-2}$$

where, P_e = equilibrium vapour pressure (in torr) of the evaporants under saturated vapour conditions at a temperature T.

N = Number of evaporated molecules per second

M = Molecular weight of the vapour species,

T = Absolute temperature

The rate of condensation of the vapours (or the deposition rate)

depends not only on the evaporation rate but also on the source geometry, its position relative to the substrate and the condensation coefficient. Langmuir model can be pictorially depicted as shown in the figure 4-1.

Because of the collision with the ambient gas molecules, a fraction of the vapours proportional to $\exp(-d/\lambda)$

where d = distance between two molecules and,

λ = mean free path between successive collisions

is scattered and hence randomized in direction within a distance 'd' during their transfer through the gas. The mean free path through air at room temperature is about 45 and 4500 cm respectively. Thus lower pressures are essential to ensure a straight line path for most of the evaporated species and for substrate to source distance of 8 to 20 cm in a vacuum chamber. Good vacuum is also necessary for producing contamination free deposits.

Another parameter of interest in understanding the degree of vacuum on the purity of films is the impingment rate of ambient gas molecules. Experimental results have shown that [34], under normal conditions of vacuum (10^{-6} torr) and deposition rate ($1\text{\AA}/\text{sec}$), the impingment rate of gas molecules is relatively large, so that if the sticking coefficient of the gas is not very small, a significant amount of gas absorption could occur. However, the sticking coefficient of gas molecules is very small, there by making the normal pressure good enough for

deposition of clean films. Of this number a certain fraction will rebound from the surface, while the remainder will collide with the surface, give up their excess energy as phonon, and become adsorbed. Most of the impinging atoms are initially adsorbed. The adsorbed atom may acquire sufficient thermal energy to overcome the local attractive forces binding it to its immediate site and migrating to a new position on the surface. the surface mobility of the atom will depend on the magnitude of local attractive forces and on the cleanliness of the surface as well. On glass, ZnSe tends to exhibit considerable surface mobility. Eventually an atom may acquire sufficient thermal energy to evaporate from the surface or it may bond to another surface atom to form a diatomic complex. This complex may acquire additional atoms and grow into larger nucleus, or an atom may evaporate from the complex. As the complex continues to grow, surface life time will increase and that the surface mobility will decrease. Thus, once the nuclei have formed, further growth into larger aggregates occurs because of the greatly increased surface lifetime of the associated atoms. We now discuss the OMCVD technique.

4.2 ORGANOMETALLIC CHEMICAL VAPOUR DEPOSITION TECHNIQUE (OMCVD):

The important characteristic of OMCVD is that it necessarily involves a heterogeneous chemical reaction at the surface of the substrate without requiring vacuum as an essential condition for deposition. Continuously flowing carrier gases and / or chemical reactions induced by temperatures and concentration gradients between the substrate and the surrounding gaseous ambient are

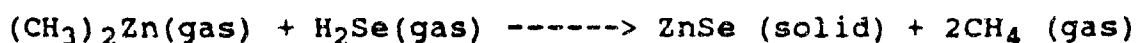
responsible for the transfer of the vapour to the substrate. CVD may be carried out in pressures ranging from several atmospheres down to high vacuum. This technique involves the exposure of substrate to the appropriate reactant vapours and their reaction near or at the substrate surface to produce a film of the solid phase reaction product. The deposition condition should be such that the reaction occurs only near the surface and not in the gaseous phase to avoid formation of powderly deposits. The morphology of the deposits is strongly influenced by the nature of the chemical reaction and the activation mechanism.

Basically any chemical reaction between the reactive vapours which yields a solid phase reaction product can be used for CVD. The substrate may in some cases, take part in the reaction if the temperature is sufficiently high. (e.g. formation of silicon dioxide on silicon substrate) The selection of a practically suitable reaction is dictated by several constraints. One has to take into account the fact that the actual course of the reaction may be much more complex and involves formation of intermediate species in accordance with the reaction kinetics, which depends on several factors such as flow rates, partial gas pressures, deposition temperature and temperature gradients and nature of the substrates. Some of these important aspects have been already discussed in detail. A general decomposition reaction can be written as



In this study, we have used DMZ (dimethyl zinc) and hydrogen

selenide (H_2Se) as source gases which, under suitable conditions of temperature and pressure, combine in the vacuum reactor to form solid ZnSe deposit and methane gas according to the reaction shown below.



ZnSe deposits on the surface of the substrate. Chemical reaction occurs by the decomposition process activated by heat (pyrolytic decomposition). Most of the metal hydrides and the organometallic compounds decompose at temperatures $< 600^\circ\text{C}$. For decomposition at low pressures or with a large concentration of the decomposition products, higher substrate temperatures may be required. Such an increase in the substrate temperature is beneficial in improving crystallinity, purity and adhesion of the film to the substrate. Despite the simplicity of the decomposition process, difficulties may arise due to the formation of more than one non volatile reaction product such as carbon in the case of organometallic compounds.

4.21 Growth of ZnSe thin films by Vacuum Evaporation :

In order to study the properties of zinc selenide thin films we first grew ZnSe on glass and silicon substrates respectively using vacuum evaporator. The scheme of the evaporation is shown in figure 4-2. High purity ZnSe (purity 99.9999 %) was employed for this purpose. Coarse ZnSe was made into a fine powder by proper grinding and a molybdenum boat was used for the purpose of source evaporation. Boat was thoroughly etched using a proper etchant. The glass substrates and silicon (111) wafers were

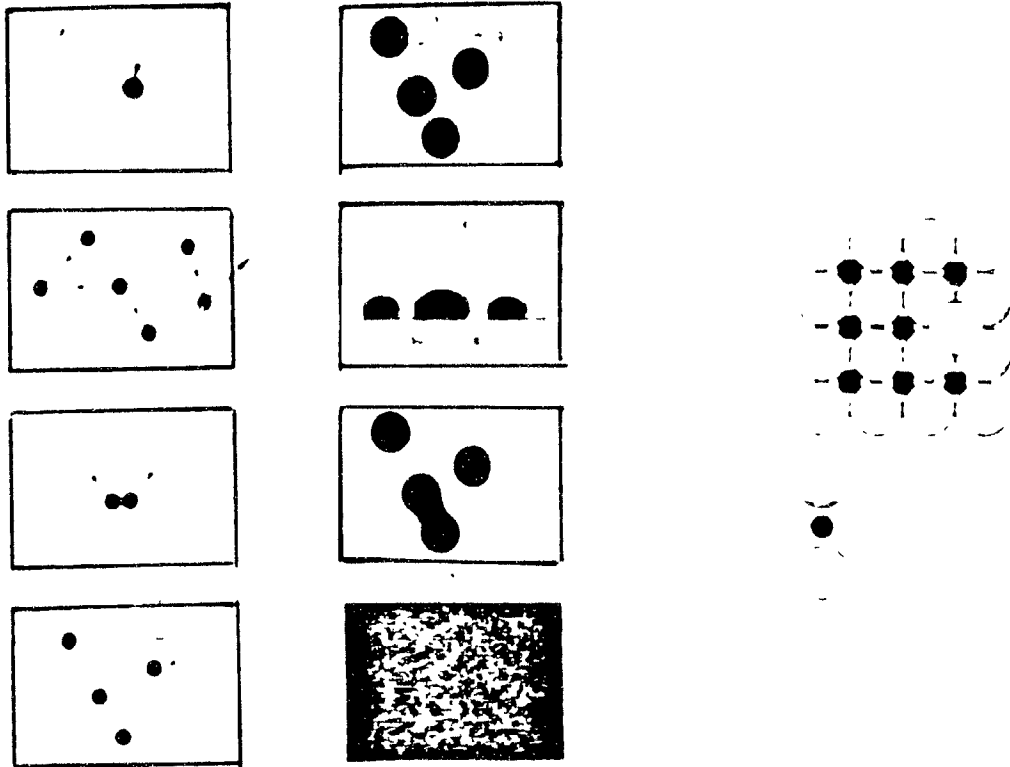


Fig. 4-1 Kinetics of film formation on the substrate. [33]

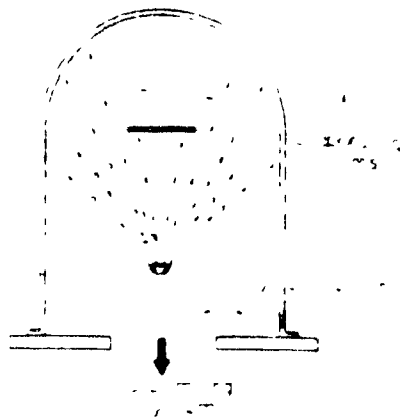


Fig. 4-2 Vacuum evaporator.

properly degreased by successively washing them first with trichloroethylene followed by rinsing in acetone for five minutes. They were then rinsed with de-ionized water and dried in air. The samples were then loaded into the system which is a conventional vacuum unit provided with an oil diffusion pump and a rotary pump to achieve a good vacuum. The substrate holder was made of stainless steel bar provided with aluminum clamps to hold the samples onto it. The boat containing the evaporant was clamped firmly between the ends of an electrode heated electrically. The evaporator together with the bell jar was properly cleaned before operation. Cleanliness was maintained at every step of the experiment. The system was first evacuated using a rotary pump and then to a high vacuum using a diffusion pump having a speed of 500 l/s. With a liquid nitrogen trap, a pressure of 1×10^{-5} torr was achieved without much difficulty. The boat together with the contents was then heated by passing electric current of suitable magnitude (40 amperes) which first melts ZnSe and then evaporates it on to the substrates.

In order to protect the substrate from a possible oxide contamination resulting from the evaporation of possible impurities present within the system, a shutter is used to cover the boat completely till the material melts completely. Since ZnSe has a fairly high melting point corresponding to 1560°C only small quantity of it (1 gm) was used for the evaporation. The substrate was held at a distance of about 9 cm from the source. The evaporation was performed till all of the material evaporated

from the boat. The system was then cooled for a sufficiently long time in order to avoid air contamination.

Depending on the source position and the distance of each substrate from the source, we grew ZnSe films of varying thicknesses on four substrates, two for glass and two for silicon. The thickness was measured using a DEKTECK system, by etching one end of the film using a suitable etchant. The measurements showed the thickness in the range of 2-13 microns on the glass substrates.

4.22 Resistivity Measurement :

The electrical resistivity measurements were made using a four point probe. However, in all the cases, the electrical resistivity of the as grown films was very high of the order of 10^8 ohm-cm on all the samples. This could have probably resulted from its strong tendency towards self-compensation.

In order to reduce the resistivity of the grown film, we used indium sulphide as a dopant material as indium sulphide has a vapour pressure close to that of zinc selenide and also all the group III-B metals such as indium, aluminum and gallium give rise to donor levels in ZnSe [47]. We grew three films of ZnSe doped with In_2S_3 with different weight percentage. The three samples had 5, 3, 1 weight percent of In_2S_3 mixed with ZnSe. In order to ensure thorough mixing of both the materials, the two compounds were first weighed accurately using a Metler's electronic balance and the powders properly mixed to get a uniform mixture of the

two compounds. The evaporation was carried out as before under identical conditions of pressure.

4.23 Heat Treatment :

In order to improve the crystallinity quality, annealing was done in the nitrogen atmosphere for a period of half an hour at 420°C in a small open tube furnace. The films were then examined for resistivity. The calculated In density in films varied from 5×10^{21} to $1 \times 10^{19} \text{ cm}^{-3}$. The films showed excellent optical quality but in all these samples there was no improvement in the lateral resistivity even after annealing. The annealing of these samples was further continued with those grown on silicon substrate for a period of 24 and 36 hours respectively at 500°C. Again no evidence of any significant change in the resistivity was noticed.

The effort to reduce the resistivity was further continued by using excess metallic zinc as a dopant in these films. This was performed by taking a small piece of zinc (99.999 % pure) together with the sample in a small quartz ampoule about 3 cm long and 1 cm in diameter. The contents were evacuated to 10^{-3} torr using a diffusion pump and the ends properly sealed with the help of oxy-acetylene torch. These ampoules were then heat treated in air at 500°C for 8, 16, 24 and 36 hours respectively. In all these cases, again the resistivity measurement either showed no significant improvement or a slight temporary improvement in conductivity in a few samples which disappeared

within a few days. These results show that the resistivity of as grown samples is high. The transmittance measurements were also made on these samples.

4.24 Transmittance Measurements :

A monochromator supplied with a tungsten source lamp was used for this purpose. The lamp could be illuminated to the required degree of illumination using a power supply. The sample of ZnSe grown on glass substrate was placed at normal incidence at a suitable distance from the point of incidence and the current was measured using a microammeter in contact with the sample. The readings were first calibrated using a standard silicon photovoltaic cell. The range of wavelength selected was from 400 to 1100 nm and for each wavelength, the light intensity was measured by measuring the current using a microammeter. In order to study the transmittance of the ZnSe films with a minimal margin of experimental error, the light intensity was first measured by putting a plane glass in front of the Si detector. For the same setting of wavelength the sample of ZnSe grown on glass was then inserted into the slot of the monochromator exactly under similar conditions and the corresponding measurement made. For each wavelength recorded, measurements were simultaneously made on both the samples through the whole range of measurement. In order to calculate the transmission factor, the ratio of photocurrent of ZnSe/glass to that measured on the plain glass was considered for each wavelength recorded. Finally a plot of transmittance versus wavelength was obtained as shown in the figs. 4-3 to 4-5.

The same procedure was applied to measure the photovoltage and the photocurrent on ZnSe grown on silicon wafers and the gallium arsenide wafers as discussed further. From the plots of transmittance versus wavelength for different samples the estimate of the band gap of ZnSe was confirmed to be 2.7 eV.

In order to understand the growth structure and orientation of the thin films of ZnSe on glass and silicon substrate, X-ray measurements were made on these samples. The measurements were done using ED-2000 diffractometer. CuK radiation was used as a source of radiation and the sample mounted on a suitable holder was rotated between the range of 2θ equal to 5 to 70 degree using the proper intensity of radiation and a suitable angular rotation speed of the diffractometer. The intensity of diffraction was recorded as a function 2θ on the chart recorder. The X-ray spectra of films grown on both glass and silicon substrates are shown in figures 4-6 and 4-7 respectively. The silicon substrates employed for this purpose had the orientation $\langle 111 \rangle$. In both the cases the films of ZnSe were grown using vacuum deposition technique. The discussion of the results will be given further in this thesis.

4.3 GROWTH BY OMCVD TECHNIQUE :

We now discuss the growth of ZnSe on silicon and on GaAs substrates using OMCVD technique including all the steps involved in the process.

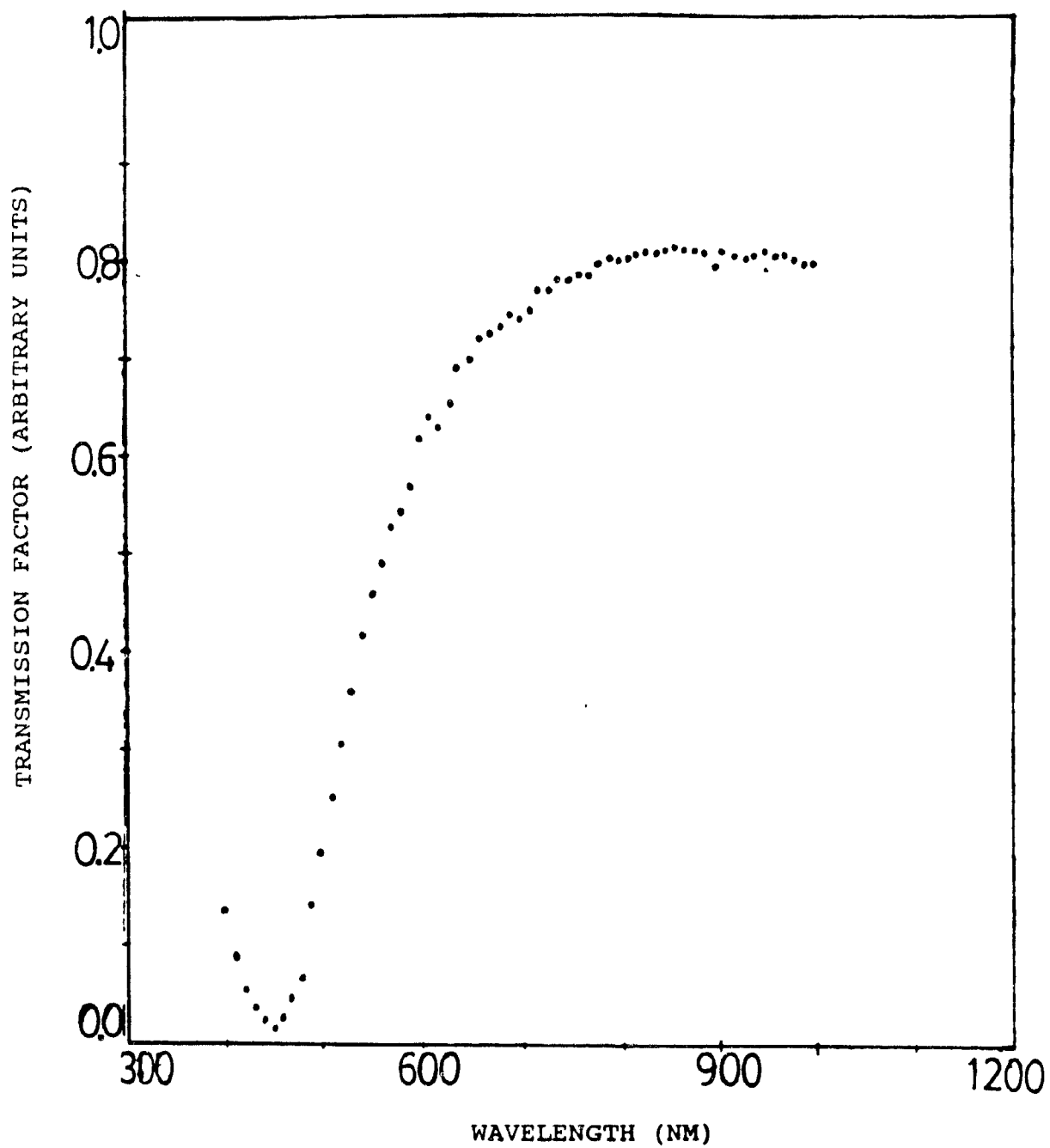


Fig. 4-3 Plot of transmittance vs. wavelength for sample 1.

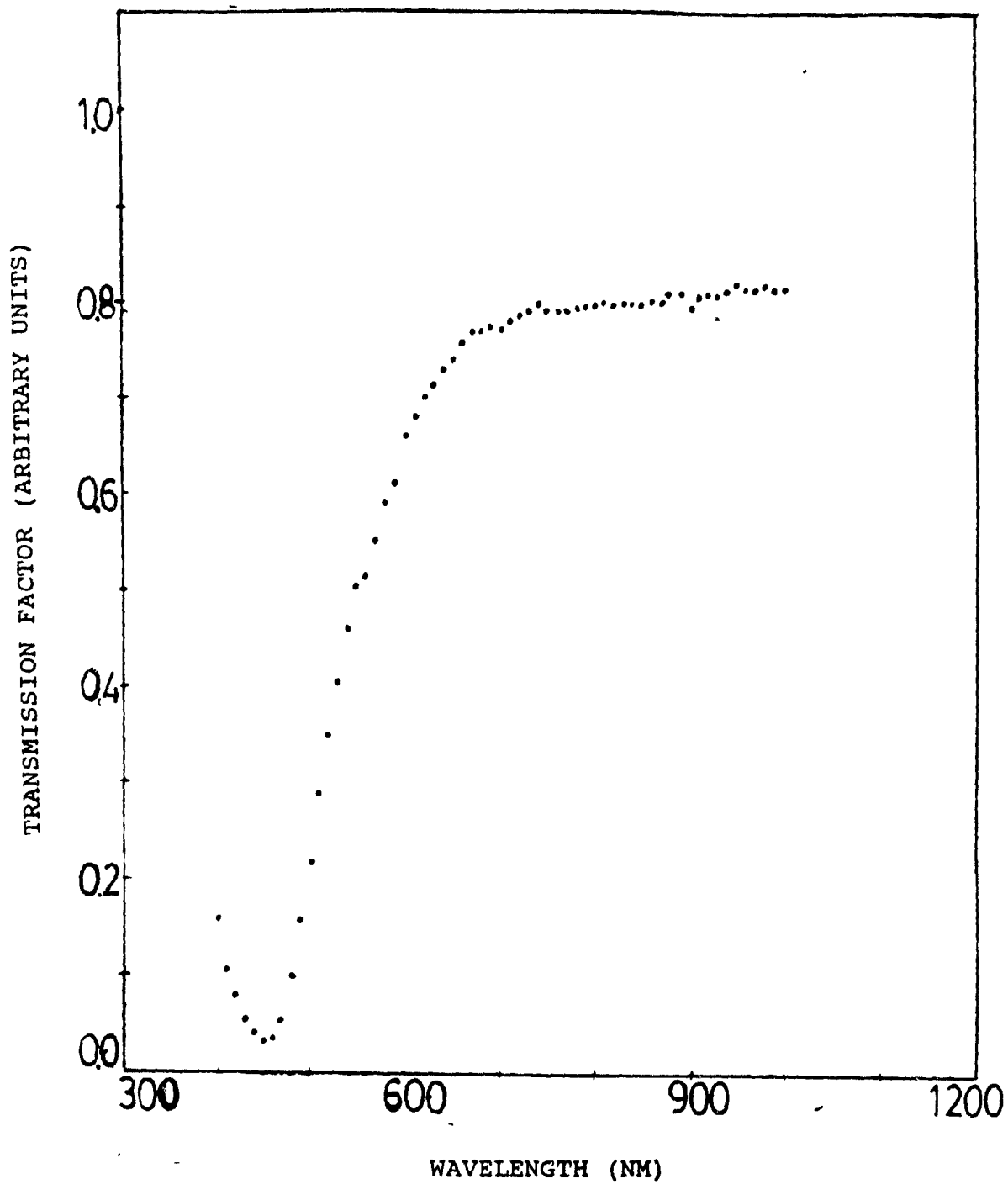


Fig. 4-4 Plot of transmittance vs. wavelength for sample 2.

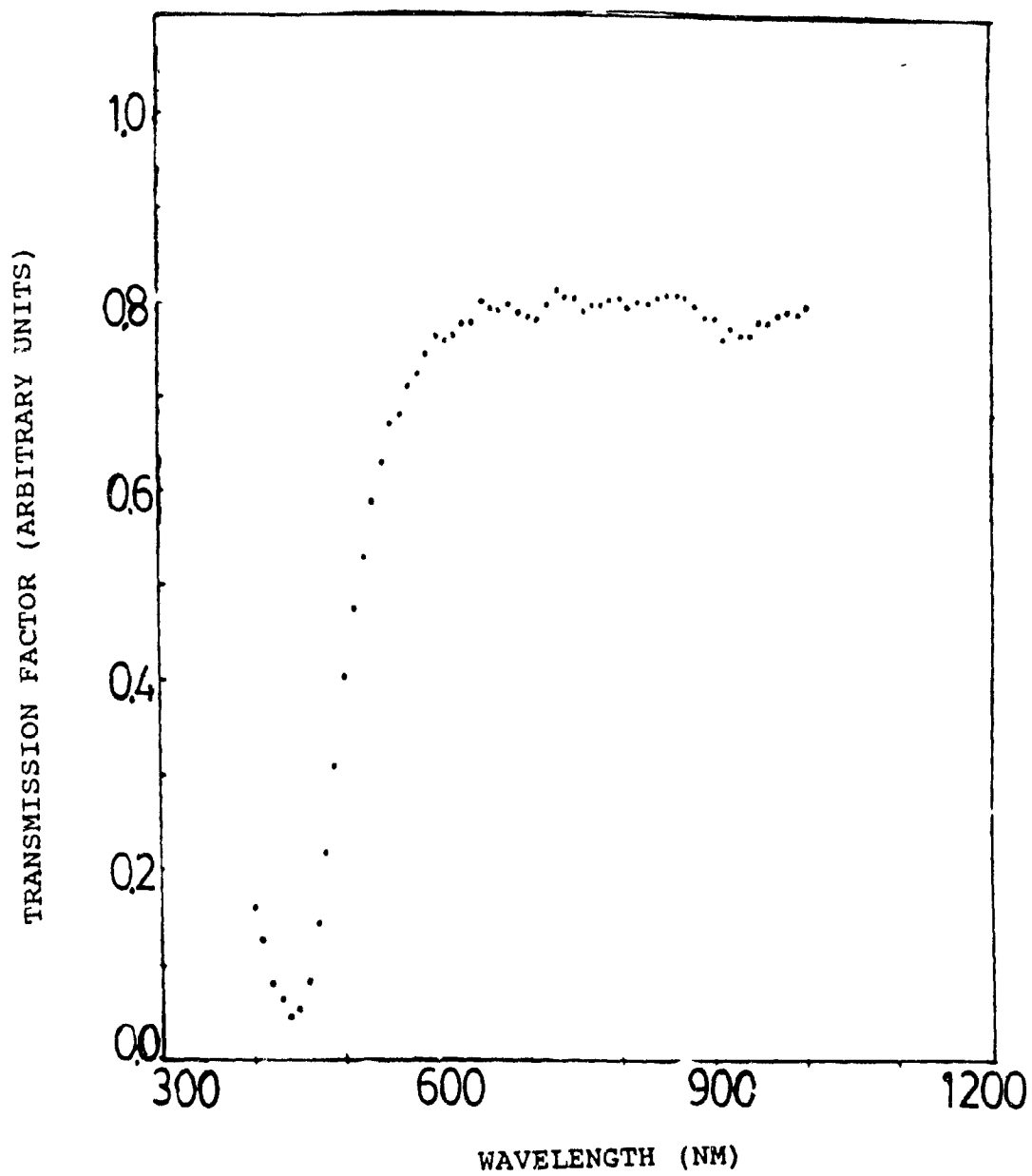


Fig. 4-5 Plot of transmittance vs. wavelength for sample 3.

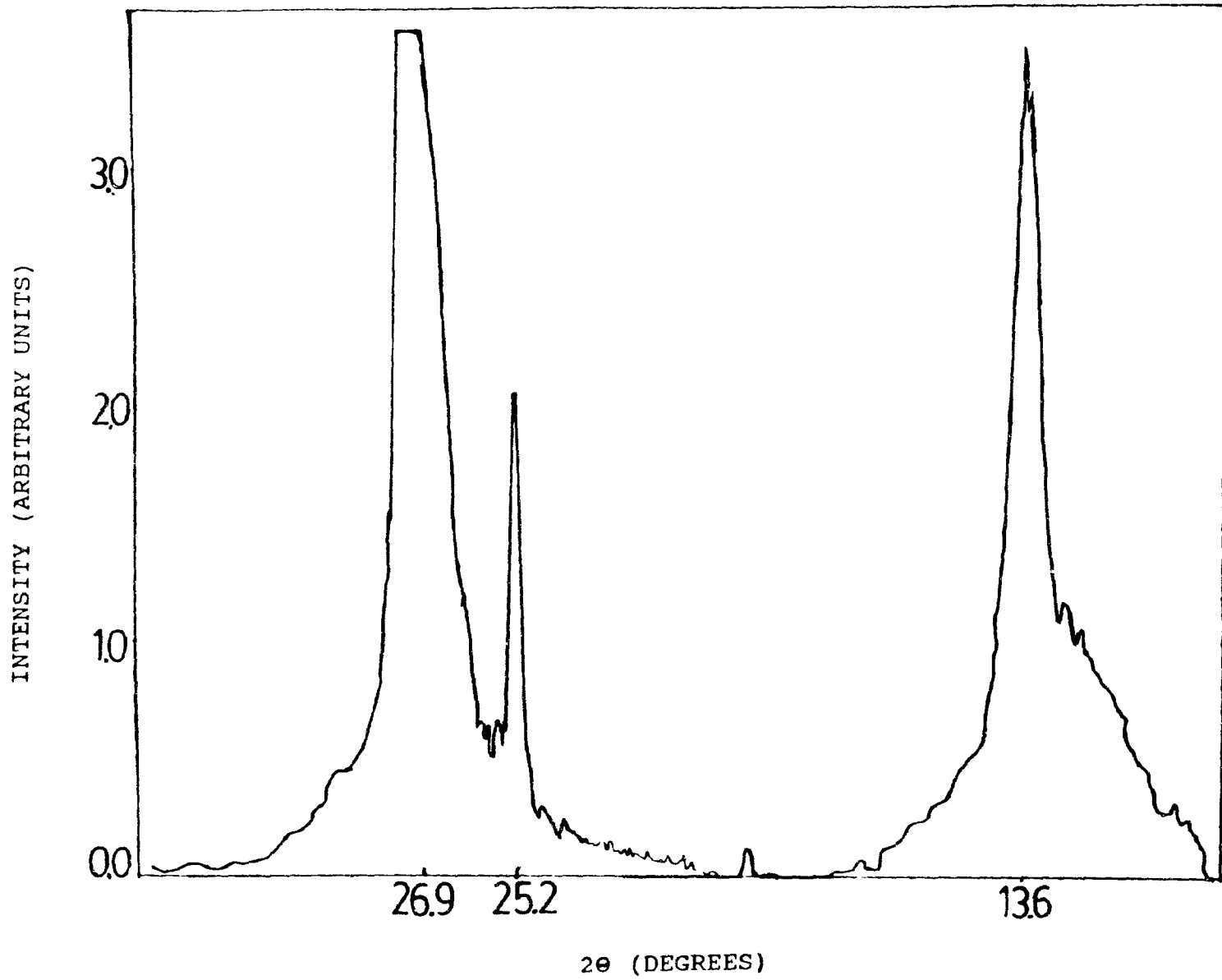


Fig. 4-6 X-ray spectra of ZnSe deposited on corning glass.

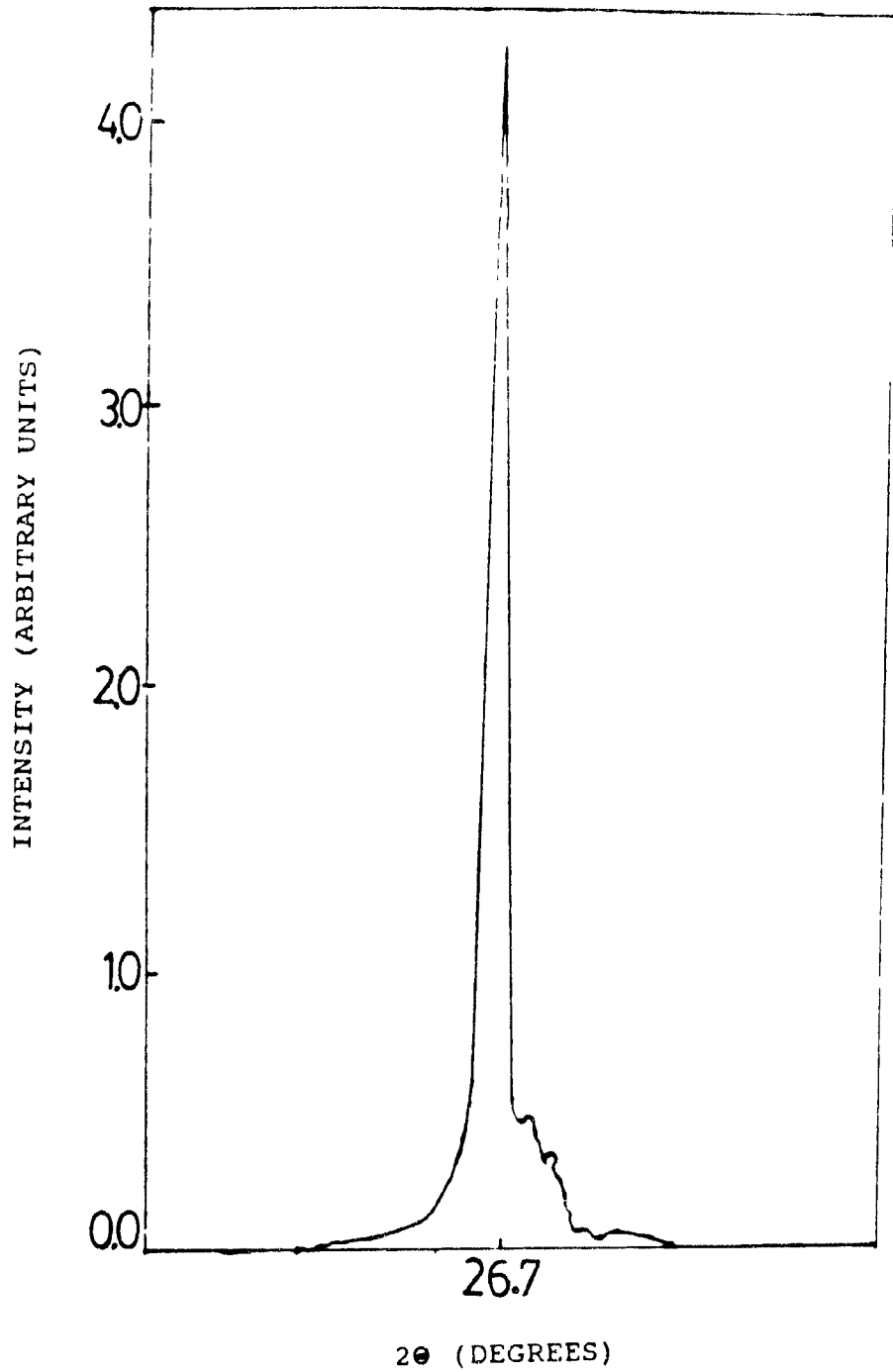


Fig. 4-7 X-ray spectra of ZnSe deposited on <111> Si.

Cleaning Procedure:

In this study, the substrates employed were those of silicon (100) and chemically polished semi insulating gallium arsenide with (100) orientation. The first step is to clean the substrates in order to remove all the residual grease and the organic material off the surface of the sample. This was done by first rinsing the substrates of silicon and gallium arsenide in a beaker containing trichloroethylene (TCE) preheated to 60°C, for a period of ten minutes. This was followed by further rinsing of the substrates for 5 minutes in acetone. Finally, the substrates were washed with de-ionised water and dried using spinner for 30 seconds. Twizers used for this purpose were thoroughly cleaned prior to the handling of these substrates with acetone and de-ionized water. Hand gloves were used to avoid dust contamination and all the cleaning took place under the fume hood. The quartz tubes used for the heat treatment was cleaned with a solution of aqua regia.

Etching Procedure:

In order to minimize the surface defects, the silicon and the gallium arsenide substrates were chemically etched using a standard solution of ($H_2SO_4 : H_2O_2 : H_2O$) in the proportion of 5:1:1. The substrates were then washed with deionized water and blown dry prior to insertion in to the OMCVD reactor. It is also important to etch away the excess ZnSe deposition from the wafers and the walls of the reactor completely. For this purpose, the standard technique applied in the previous case cannot be applied

because it has been reported by Gunther et al. [35] that the ZnSe films contain less vacancies which pose serious problems to etching it from the substrate surface without destroying the surface properties. Also, studies have shown that dilute hydrochloric acid (HCl) can be used with fair amount of success. However, small quantities of H_2O_2 has been successively used for large area etching although traces of film were left unetched owing to the presence of small number of vacancies.

4.4 OMCVD GROWTH OF ZnSe FILMS ON Si AND GaAs SUBSTRATES :

As described earlier, OMCVD is a process where one of the reactants in the form of metalorganics is transported to the surface of the substrate placed in the evacuated reaction chamber with the help of a carrier gas. Metal organics are the compounds with the metal covalently attached to hydrocarbon chains as in the case of dimethyl zinc (DMZ). Methyl chains are the most commonly used hydrocarbon group and often are the source of lower valence elements from the group II, III and V of the periodic table. Near the surface of the heated substrate, the cracking of the bond takes place, releasing the metal which immediately combines with the hydrogen based compound forming the desired product that gets adsorbed onto the substrate. However, in some cases such as ZnSe, the compound formation takes place prior to reaching the substrate and gets chemisorbed to the surface by the act of linking chemical bonds. The epitaxial growth begins when the adsorbed atom(s) or molecule(s) combine together by forming stable covalent bonds between them thus initiating the process of

nucleation. The adsorbed atoms also diffuse across the surface by the energy imparted to them from collisions with solid surface atoms thermally vibrating about their mean position. Thus it is not only the growth kinetics that govern the nucleation but also the physics and chemistry of the growth process.

4.5 OMCVD GROWTH SYSTEM :

Volatile organometallics stored in stainless steel bubblers are cooled to their liquid temperatures so that control on transport may be exercised. High purity hydrogen gas is passed through a purifier prior to being bubbled through metalorganics in order to carry its vapour to the reaction chamber. Hydried sources were taken directly from their gas cannisters along a stainless steel piping network directly to the chamber. Each reactant used has its own port to the central chamber to ensure that the mixing occurs only inside the chamber. All the flows were properly regulated by electronically controlled flow regulators. All the valves connecting the stainless steel tubings were thoroughly sealed in order to prevent gas leakages. It is also extremely important to exercise great care while the unit is in operation because any form of damage could be extremely hazardous owing to the toxic nature of the gases involved. Fig. 4-8 shows the actual design of our OMCVD unit used to grow the ZnSe films.

The system consists of different inlets to the main reaction chamber for transporting various reactants. Stainless steel tubing of one eighth inch diameter was used for the piping

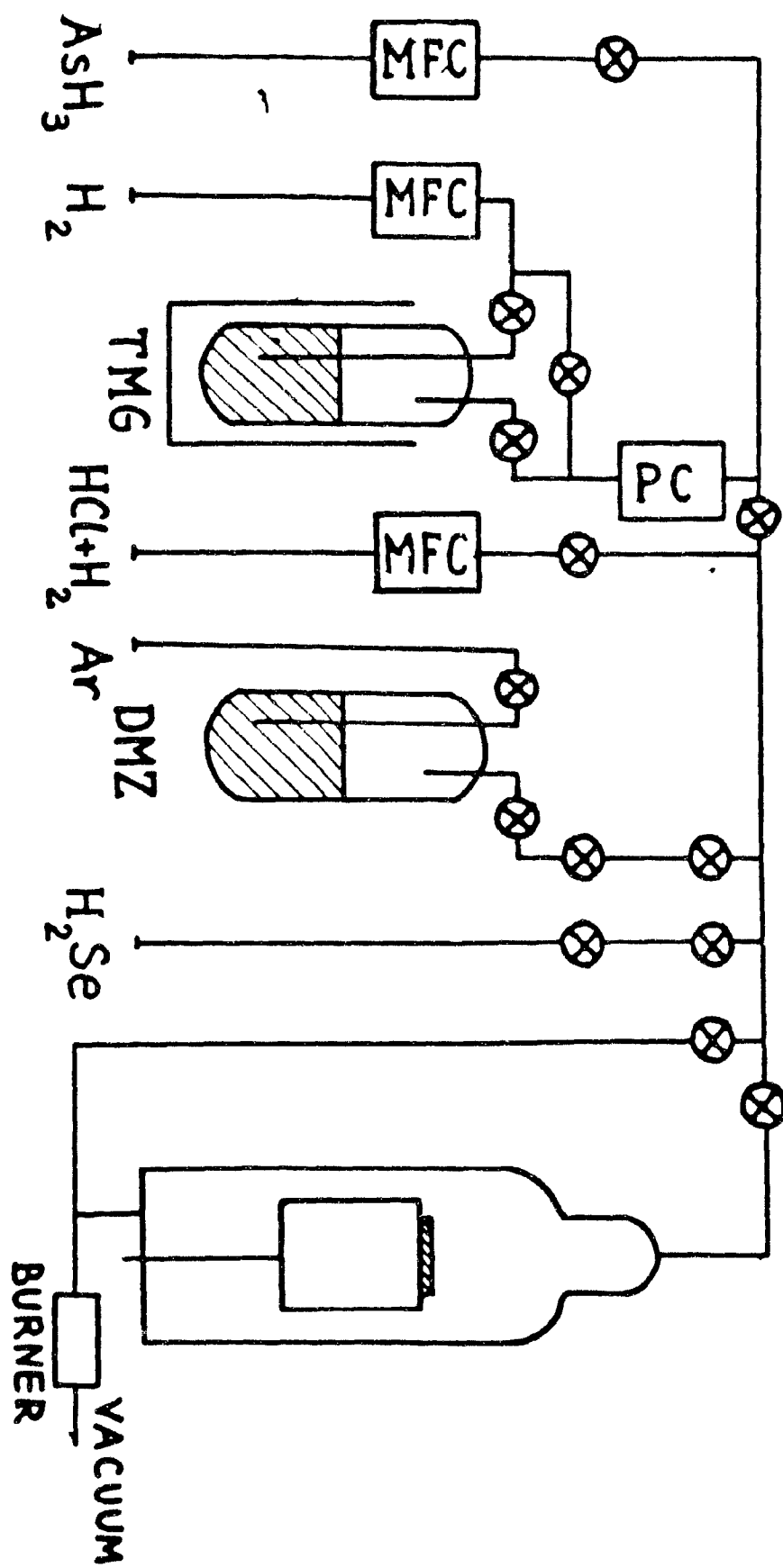


Fig. 4-8 MOCVD reactor.

network joined by steel valves and controllers to control precisely the pressure and the mass flow rates of reactants. Injection cells were incorporated for the purpose of dopant injection during the growth. A vertical reaction chamber 50 mm in internal diameter and 90 mm long is used to obtain a uniform gas flow pattern near the substrate. A graphite susceptor heated with a halogen lamp and accompanied by an electronically controlled thermocouple is used to heat the substrate. The maximum surface temperature attainable was upto 800°C. This system was operated at a pressure of 1 torr. Volatile liquids of DMZ and TMG were held at 25°C. All the reactants to the chamber were mixed and introduced into the reaction chamber from a single gas line, the outlet of which was located at 100 mm above the substrate. The gas flow was monitored through mass flow controller (MFC) and pressure controlled with pressure controller valves (PC). The growth temperature had a range from 300 to 350°C.

4.51 Preparation and purification of Alkyls for II/VI Compound Semiconductors:

Purity of semiconducting layers is determined by the purity of the precursors (metal alkyls or hydrides). In the preparation of dimethyl zinc (DMZ), there is a possibility that copper contamination may occur. Lewis et al. [36] devised a technique of synthesizing DMZ from a reaction of zinc chloride with methyl iodide in high boiling ethers. The reaction proceeded smoothly and high yields of methyl zinc was achieved after distillation.

In achieving reproducible growth of high quality ZnSe by MOCVD, it is important to prevent premature reactions by selecting appropriate source material combination. It has been well established that zinc alkyls and hydrogen selenide react easily even at room temperature forming ZnSe powder on the reactor wall before they reach the surface. The use of a double alkyl zinc helps in minimizing the formation of the adduct [37].

It has been also noted that at higher temperatures the growth rate is independent of growth temperature. At lower temperatures the growth rate changes exponentially with temperature. This implies that the diffusion controlled mass transport-limited growth and kinetically controlled growth takes place at temperature higher and lower than 400°C respectively. The ideal growth temperature for MOCVD grown ZnSe is in the range of 300-400°C. We will now discuss in brief the steps involved in the growth of ZnSe and GaAs using the MOCVD system.

The reactor shown in figure 4-8 is used for the growth of GaAs and ZnSe. Although no deposition of gallium arsenide was made since GaAs and silicon substrates were used directly in the reactor, only a brief account of GaAs deposition will be outlined below.

Trimethylgallium (TMG) is used as a source of gallium and arsine AsH_3 is used as a source of arsenide for the deposition of GaAs in this technique. The substrate to be used is loaded into the reactor on the graphite susceptor and the chamber is evacuated to a low pressure of the order of 1 torr. The substrate is then

etched thermally in the reactor with the carrier gas (hydrogen) at a fairly high temperature for about 30 minutes. The flow rate is normally maintained at 1.5 litres/minute. After etching, the substrate is slowly cooled to the growth temperature. The substrate temperature is monitored by an electronically controlled thermocouple. When the temperature approaches near the growth point, the valves of the TMG and AsH₃ are opened and the gas flow monitored at proper flow rate. With these conditions of growth no unwanted deposition occurs upstreams.

The actual mechanism lies in the fact that TMG first decomposes by the successive removal of methyl radical giving gallium in the vapour form which combines with arsine to form GaAs. The equation of the reaction is as follows;



Owing to the tight covalent bond between the metal and the hydrocarbon and between the arsine and hydrogen it is not necessary always that the decomposition be complete. This situation often leads to the formation of adduct such as arsenic hydride. These problems can however, be resolved by using hydrocarbons such as diethylzinc and diethylselenide where the bonding is relatively weaker.

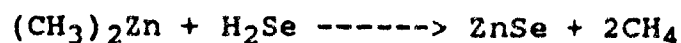
In order to achieve the films of required type of conductivity doping can be done only at the growth stage by introducing appropriate dopants in the gaseous form into the mixture over the surface of the substrate. Excess H₂Se could be used to produce

n-type and excess DMZ for p-type layers. Depending upon the need, suitable dopants in the form of gas also can be employed. However, the actual mechanism and the reactive kinetics involved here is not well understood. TMG was kept at -10°C and arsine diluted in hydrogen to within 5 %, was kept at maximum flow to establish the necessary arsenic over pressure. All the samples were grown under low pressure and the average growth rate was about 2.5 microns per hour. A vertical quartz reactor was used with success in growing epilayers of n-type with carrier concentration of 10^{19} cm^{-3} and p-type with 10^{15} cm^{-3} . A home made graphite pedestal was mounted at the centre of the cylindrical quartz reactor tube of 5 cm diameter and 15 cm in length. The graphite susceptor was heated with a halogen lamp. The quartz reactor allowed for an easy cleaning and efficient fluid dynamics.

We now discuss the growth of ZnSe epilayers. The procedure remains the same as discussed for the case of gallium arsenide.

The layers of ZnSe were grown successively on both silicon (100) and SI gallium arsenide substrates of (100) orientation.

Substrates were cleaned by the standard technique as described earlier. In this case layers were grown using palladium diffused hydrogen through DMZ cooled to -10°C and mixing the metal organic vapours with hydrogen selenide gas diluted in hydrogen within the reaction chamber. The reaction equation is as under;



The suitable temperature is around 350°C . Sritheran et al. [38]

reported that reaction between DMZ and H_2Se at room temperature can have a disadvantage. This disadvantage is the formation of the product which reduces the flow of reactants to the growth surface by condensing out of the gas stream. This difficulty however, was overcome by introducing the reactants into reaction chamber separately and allowing the mixing to occur close to the surface of the substrate thereby protecting layer quality and surface morphology. Conductive layers of ZnSe were grown by using excessive H_2Se which makes it n-type. Growth rate varied from 1 to 3 microns per hour. At low substrate temperatures resistive layers were grown owing to the greater partial pressures of Se compared to that of Zn. This favours the creation of acceptors and as a consequence of self compensation. However, the films grown on GaAs substrates showed conductive n-type layers which we believe is a result of diffusion of Ga from the GaAs substrate into the ZnSe deposit. The suitable temperature was found to be around $350^\circ C$. In addition it was found that the conductivity increased with the layer thickness. In some cases HCl was also used as a carrier gas with hydrogen. We now discuss the sequence of growth of ZnSe on Si and GaAs substrates.

4.52 Steps Involved in the Growth Process :

- 1) Both silicon and gallium arsenide substrates were thoroughly cleaned chemically using proper reagents as outlined before. The substrate was mounted on the graphite susceptor and thermally etched at relatively high temperatures in the presence of a carrier gas.

2) Arsine flow was initiated over the substrate as the substrate was cooled to the temperature of growth (around 350°C) in order to prevent elemental arsenic out gassing in the vicinity of growth.

3) Appropriate flow rates of all the gases used in the process. The typical flow rates employed for the various growth rates are indicated below.

Hydrogen carrier gas	1 l/min.
Hydrochloric acid	0.8 ml/min.
Dimethylzinc	2.5 ml/min.
Hydrogen selenide	15 ml/min.
Substrate temperature	200 to 600°C for silicon 250 to 400°C for GaAs
Transport distance	9 to 6 cm.
Average growth rate	0.5 to 3.0 $\mu\text{m}/\text{h}$

4) Upon the termination of the deposition, the DMZ and the H₂Se gases were by-passed to the exhaust and the lines closed by shutting the inlet valves. The substrate was cooled to room temperature before the air let into the chamber.

5) The quartz reactor was dismantled and the walls thoroughly etched using dilute HCl to scrap off all the deposition along the surface, for further deposition use. The samples were then examined for electrical and optical characterization.

The next step in the process was the external contact to the epilayers for the electrical measurements.

4.53 Ohmic contact to GaAs:

In this study we used the indium contact to the substrate of GaAs. A thin layer of indium was evaporated to the back side of the wafer by a vacuum evaporation technique. Au:Ge alloy has also been widely used for contact to gallium arsenide substrate. After the indium evaporation, annealing was carried out as described below.

4.54 Ohmic contact to ZnSe:

Indium was also used as contact to ZnSe side because it makes a barrier of 0.91 eV with ZnSe which is the second lowest to aluminum which has a contact potential of 0.74 eV with ZnSe. But Al is not widely used owing to its readiness to oxidation. In order to make indium contact to ZnSe side, the wafer was wrapped in an aluminum foil which essentially serves as a mask, containing small openings of about 1 mm diameter at several places for indium evaporation.

After indium evaporation as stated before, the mask was removed from the surface. The sample was then heat treated in a small tube furnace at 250°C for five minutes in nitrogen atmosphere. This ensures the proper diffusion of indium in to both ZnSe and GaAs sides of the sample. The furnace was connected to the exhaust to avoid the toxic arsenic vapour that could emerge from ZnSe epilayers. The wafer was then cut carefully using a scribe into smaller segments of approximately 5*5 mm² to obtain few diodes of ZnSe:GaAs and ZnSe:Si respectively.

4.6 External Contacts :

External contacts for measurements, to the wafers were made by silver painting ends of copper wire and soldering them with indium to both sides of the samples. This completes the description of the growth process. In the next section we describe the characterization of these samples.

For characterization, different samples grown with varying conditions of growth have been used. The analysis is mainly based on the results obtained from the different characterization techniques discussed next in chapter 5.

CHAPTER 5

EXPERIMENTAL RESULTS

5.1 Thickness & X-ray Measurements :

After the growth of the film, the thickness of the samples were measured using a DEKTECK surface profiler. For this purpose samples were etched at one corner carefully with a suitable etchant and the thickness measured at the edge between the etched and the non-etched regions with the help of the moving probe. The measurement was recorded on the chart paper and the thickness determined from the step height. The samples were then studied for resistivity using the four point probe method. As stated earlier, in all the cases, the resistivity of the films grown by vacuum evaporation technique showed very high levels of resistivity on both glass and silicon substrates. The next step was to study the crystallinity and possible orientation of the grown films on the substrates. The X-ray diffraction spectra are shown in figures 5-1 to 5-3 for samples grown by vacuum evaporation.

X-ray Technique :

For ZnSe grown on glass sample SGZ 1, an intense peak was observed at $2\theta = 26.92^\circ$. Another peak with smaller intensity occurred at 13.1° and can be attributed to that corresponding to the silicate. However, no other peak was registered beyond 27° . Sample SGZ 2 (ZnSe + 5% In_2S_3) showed most intense peak at 27.02° and sample SGZ 3 (ZnSe + 3% In_2S_3) exhibited peaks at 27.38° .

INTENSITY (ARBITRARY UNITS)

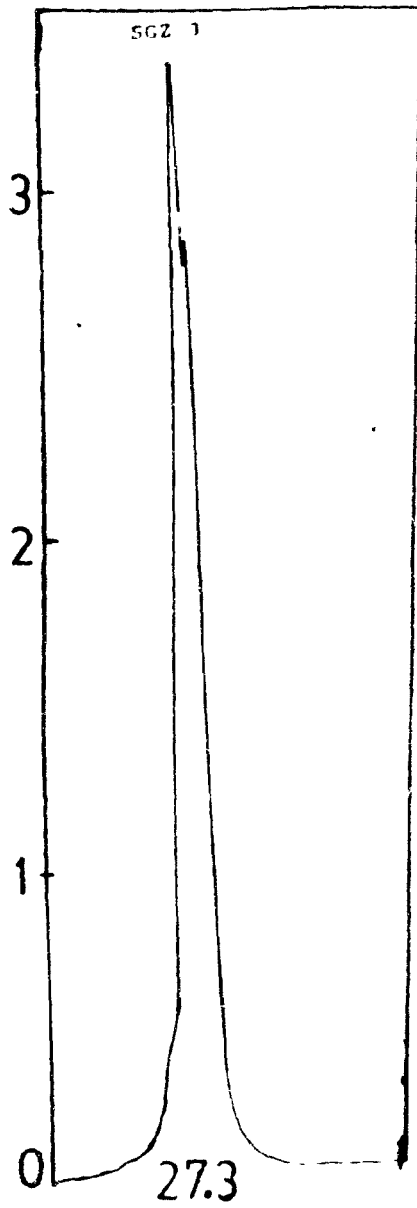


Fig. 5-3
X-ray spectra of SGZ 3.

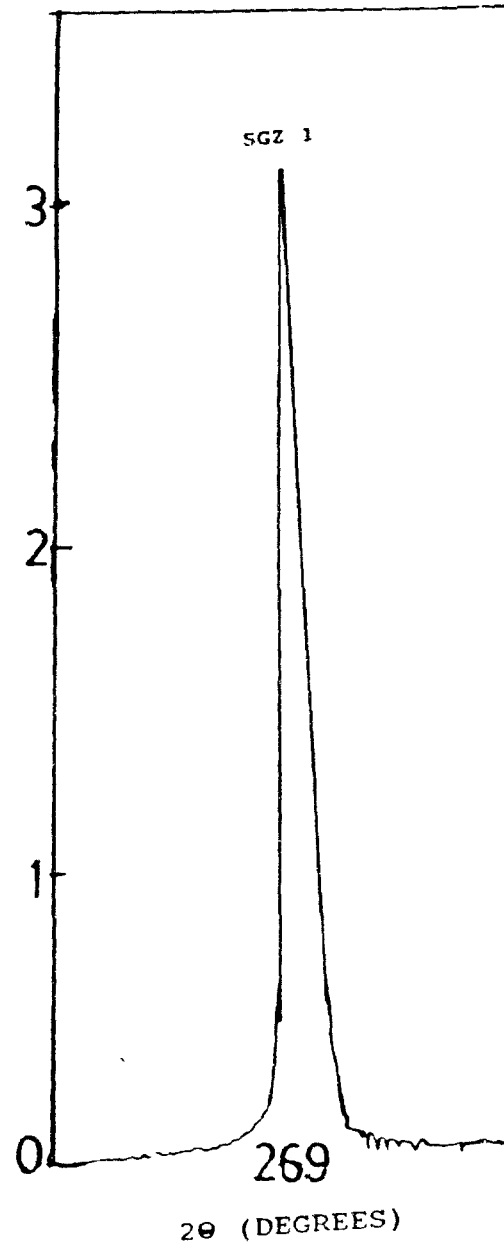


Fig. 5-1
X-ray spectra of SGZ 1.

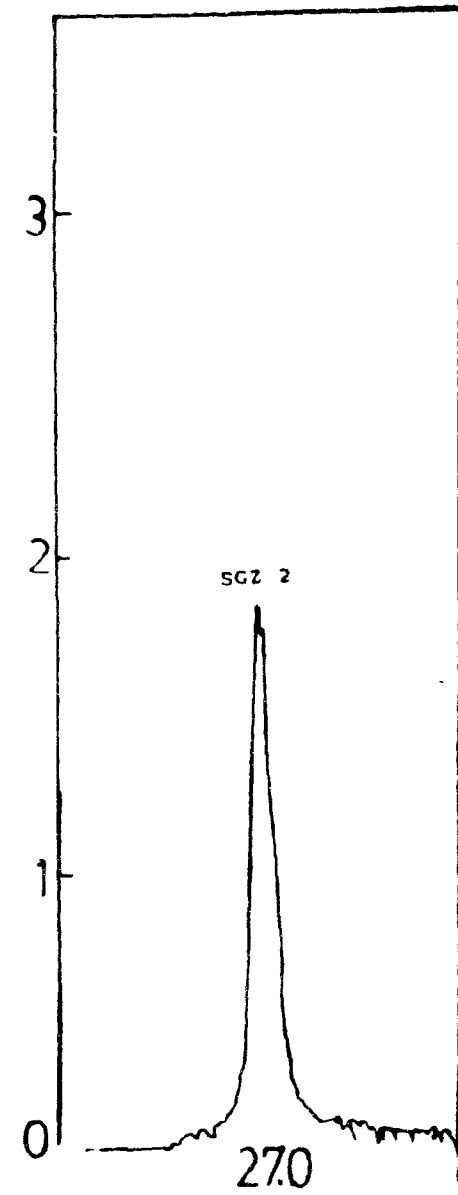


Fig. 5-2
X-ray spectra of SGZ 2.

All these results show a possibility of (111) growth of ZnSe on glass substrate. The off-set of the order of +0.3 degrees should be accounted to correct for the strain on the films during the crystal growth.

Figures 5-4 to 5-5 shows the x-ray spectra of ZnSe/Si grown using the vacuum evaporation technique on two silicon substrates having (100) orientation. The spectra exhibited several peaks at different angles. Two intense peaks were observed in both these samples, one at 26.8° corresponding to ZnSe (111) and the other at 65.9° corresponding to Si (400) substrate, indicating a growth of (111) ZnSe on these substrates. However, less intense peaks were observed at 44.9° and 53.3° degrees 2θ respectively which possibly could have resulted from different orientation such as (022) and (113) of the film. Only (111) peaks of ZnSe of these samples are shown on page 62.

The results of the diffraction studies on films grown on quartz and sapphire using OMCVD are also presented below. For the films grown on the quartz substrate four peaks are found: 27.2° (111), 42.35° (022), 53.65° (113) and 65.9° (004). All peaks correspond to ZnSe. The films grown on the sapphire also exhibited four peaks mainly at : 26.82, 44.92, 53.2 and 65.62 degrees respectively. These results suggest a possibility of monocrystalline growth of ZnSe films on these substrates. Figures 5-6 and 5-7 show the X-ray spectra of the above samples.

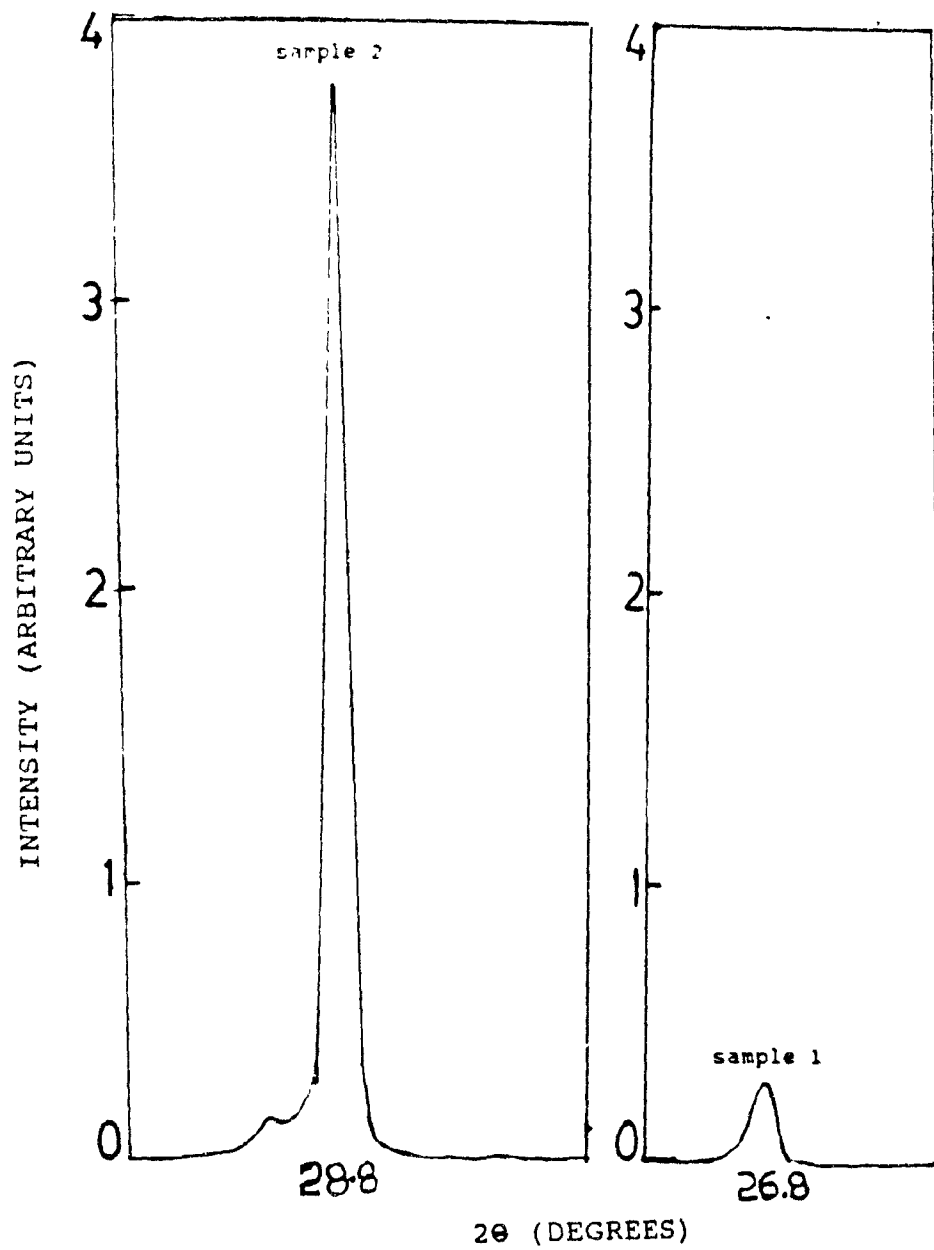


Fig. 5-4

X-ray spectra of sample 2.

Fig. 5-5

X-ray spectra of sample 1

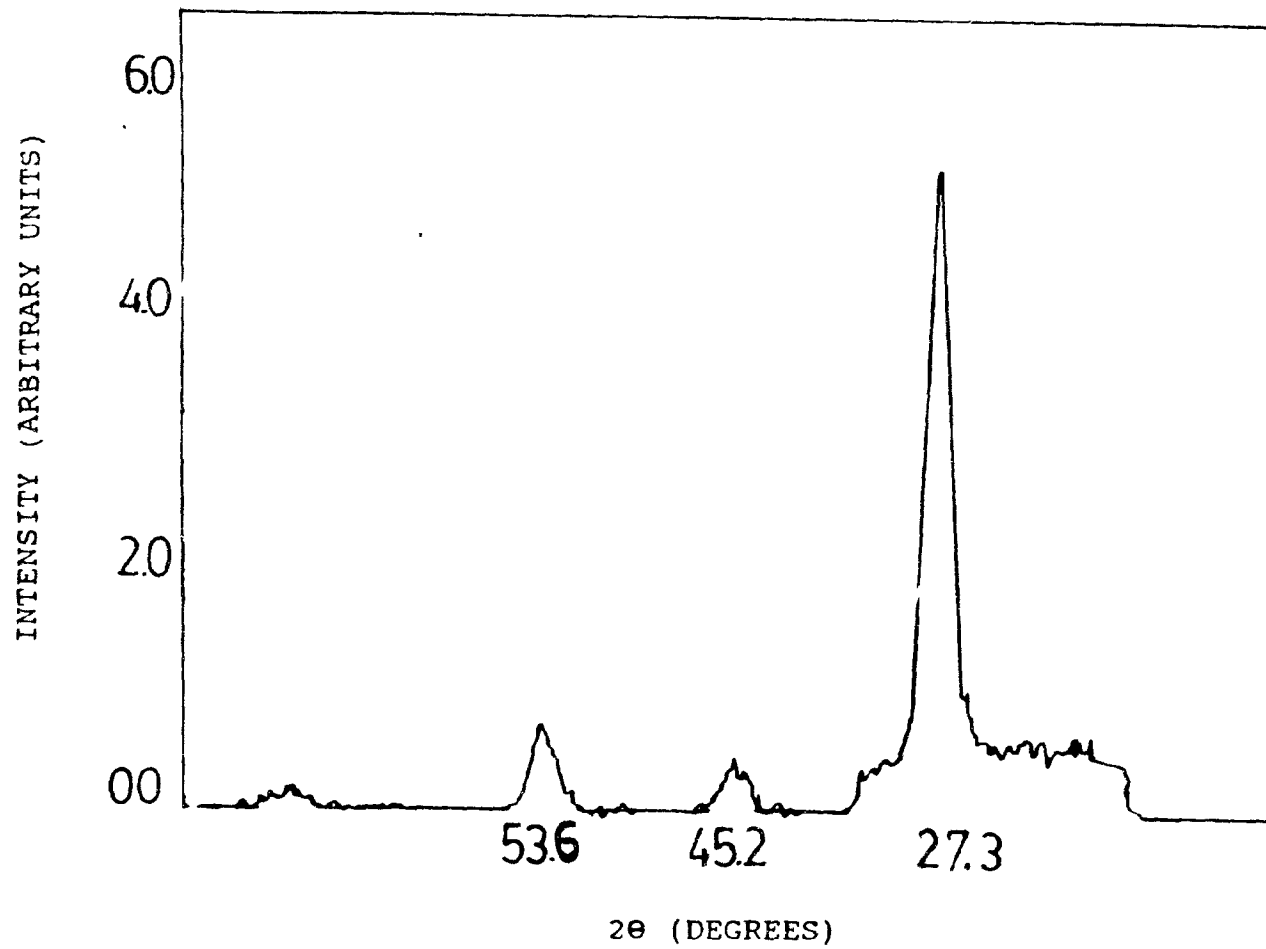


Fig. 5-6 X-ray spectra of ZnSe on quartz.

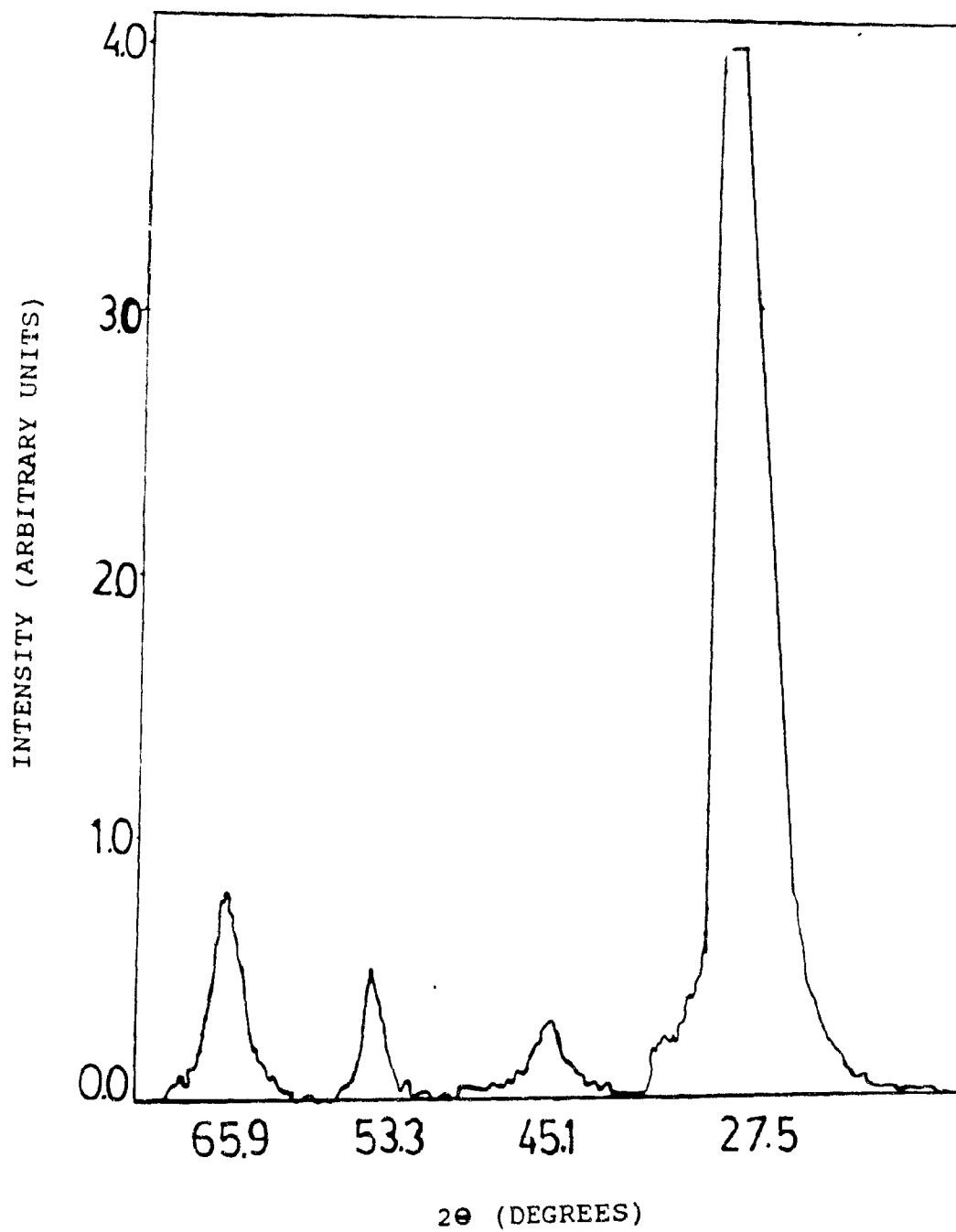


Fig. 5-7 X-ray spectra of ZnSe on sapphire.

The crystalline quality of the grown films were characterized by using X-ray diffraction technique. The X-ray pattern from a (400) plane (parallel to (100) plane in a real lattice) of the substrate and pattern from other orientation of the film has been discussed. The lattice mismatch between ZnSe and Si is approximately 4%. The substrates used were low resistivity Si with (100) orientation. The substrates were cleaned with the standard techniques as described before and chemically etched in the vacuum chamber at 800°C for 30 minutes in the presence of a carrier gas such as hydrogen to remove all surface oxides.

X-ray diffraction results of ZnSe grown on Si using OMCVD have been presented for six different temperatures starting from 200°C as shown in the figures 5-8 to 5-12. In all the cases the same x-ray beam intensity was maintained and the scans were run between $2\theta = 5$ to 70° in order to ensure all the major peaks that could be expected out of different orientations resulting from the film and the substrate. The substrates of silicon used in this study had the orientation of (100) in all the cases. The sample grown at 200°C shows an intense peak at 26.64° and a significantly less intense peak at higher angle of 53.3° . However no other peaks were observed in the range studied. This indicates that the film has an orientation of (111) on (100) Si substrate.

The X-ray spectra at 300°C shows very clearly two intense peaks one due to ZnSe at 26.9° and the other due to silicon at 68.8° indicating the growth of (111) ZnSe on (100) Si. Two other peaks

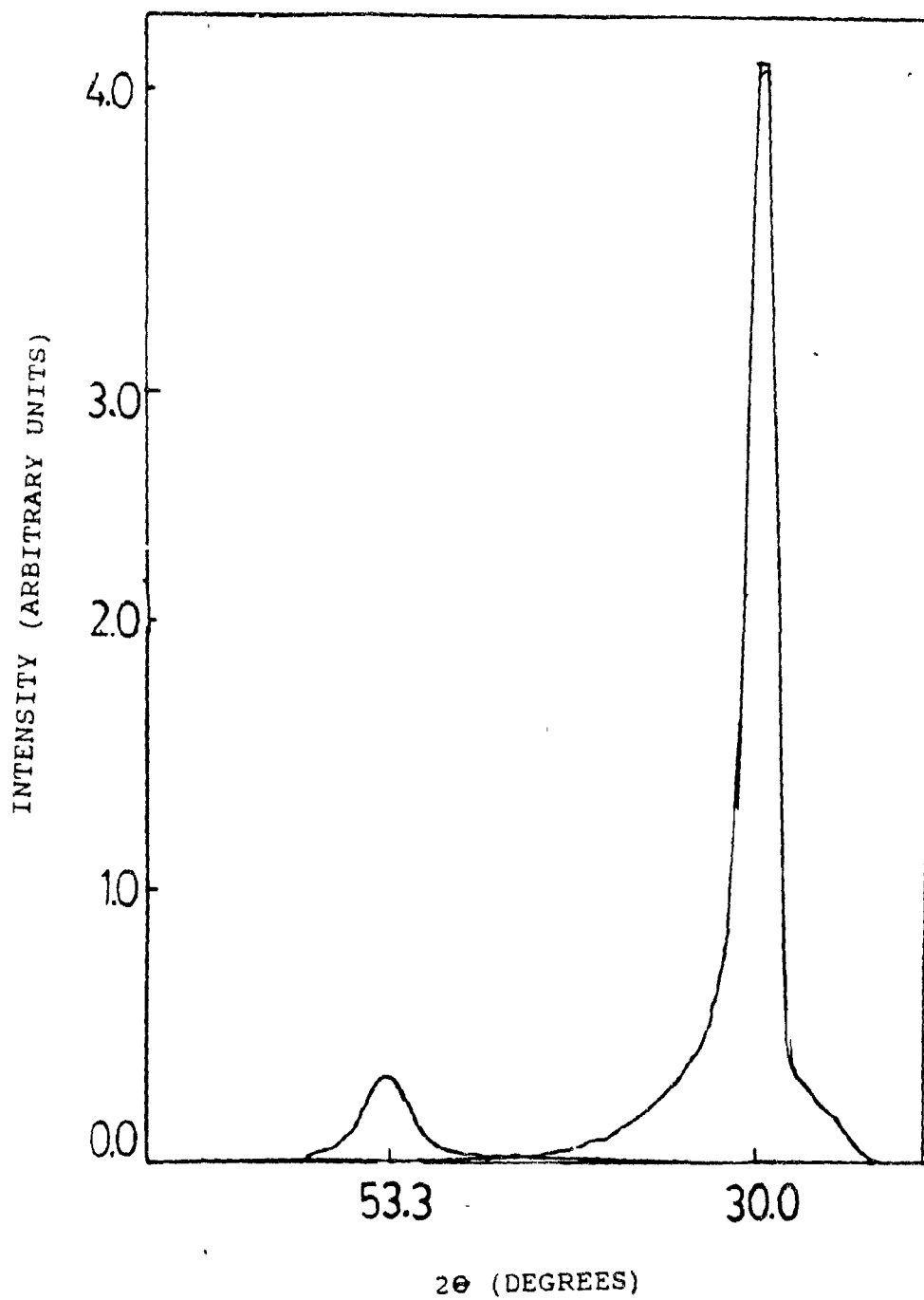


Fig. 5-8 X-ray spectra of ZnSe on Si <100> at 200°C.

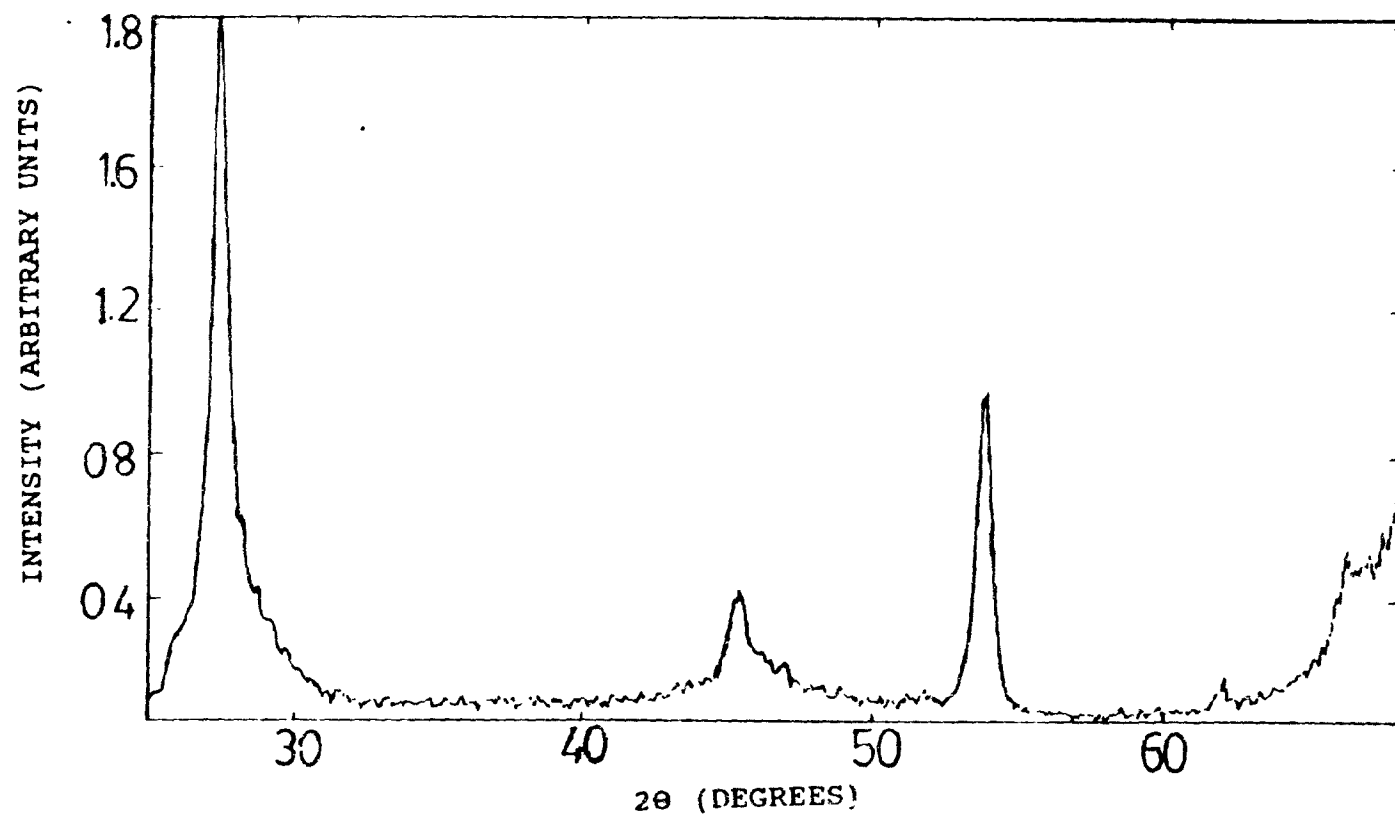


Fig. 5-9 X-ray spectra of ZnSe on Si <100> at 300°C.

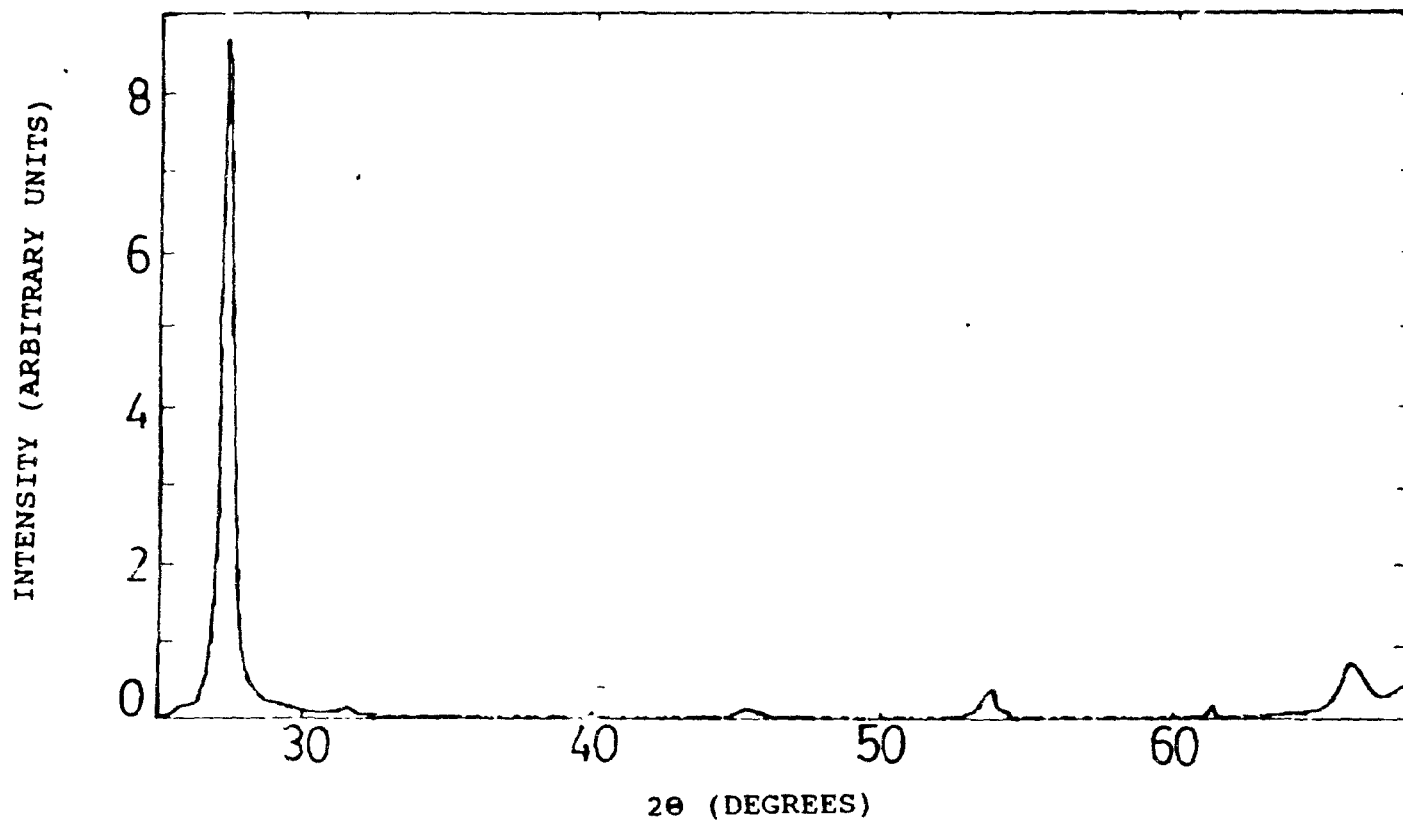


Fig. 5-10 X-ray spectra of ZnSe on Si <100> at 400°C.

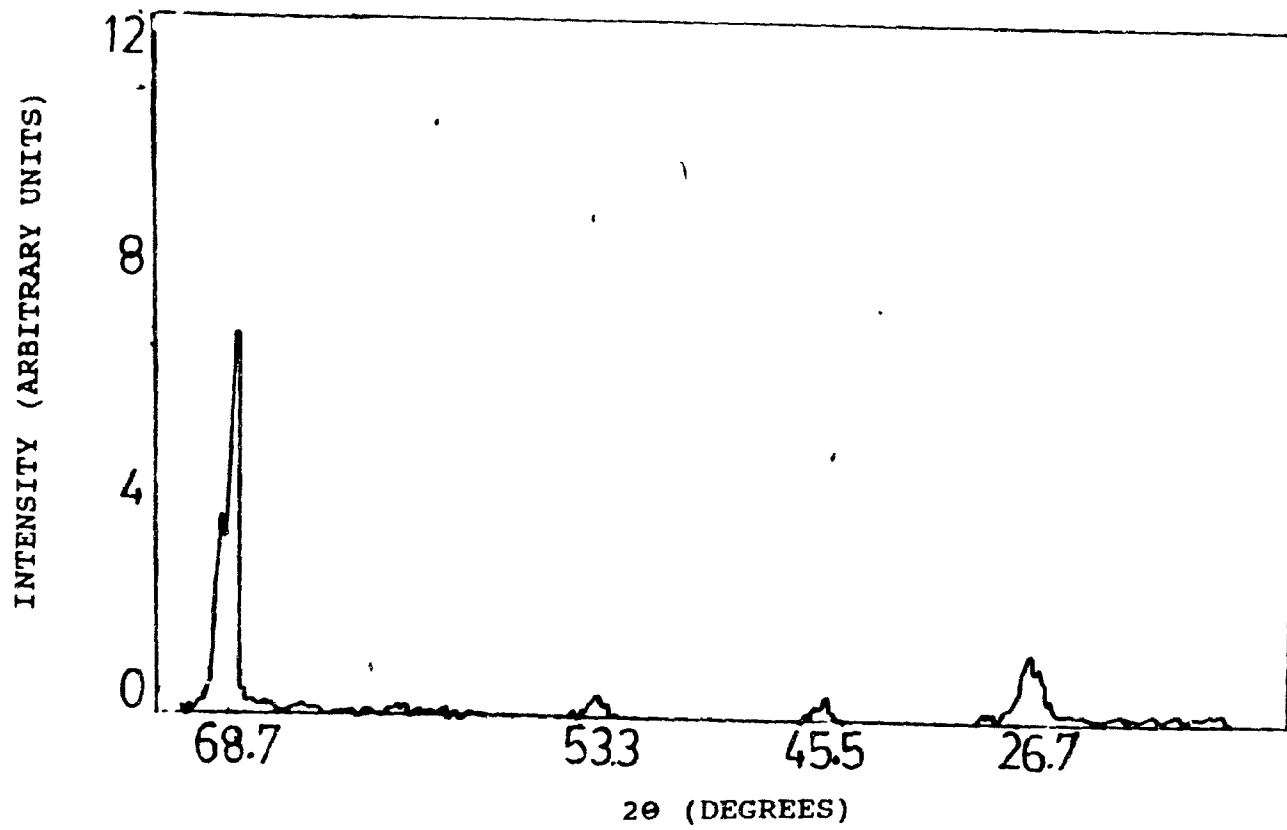


Fig. 5-11 X-ray spectra of ZnSe on Si <100> at 500°C.

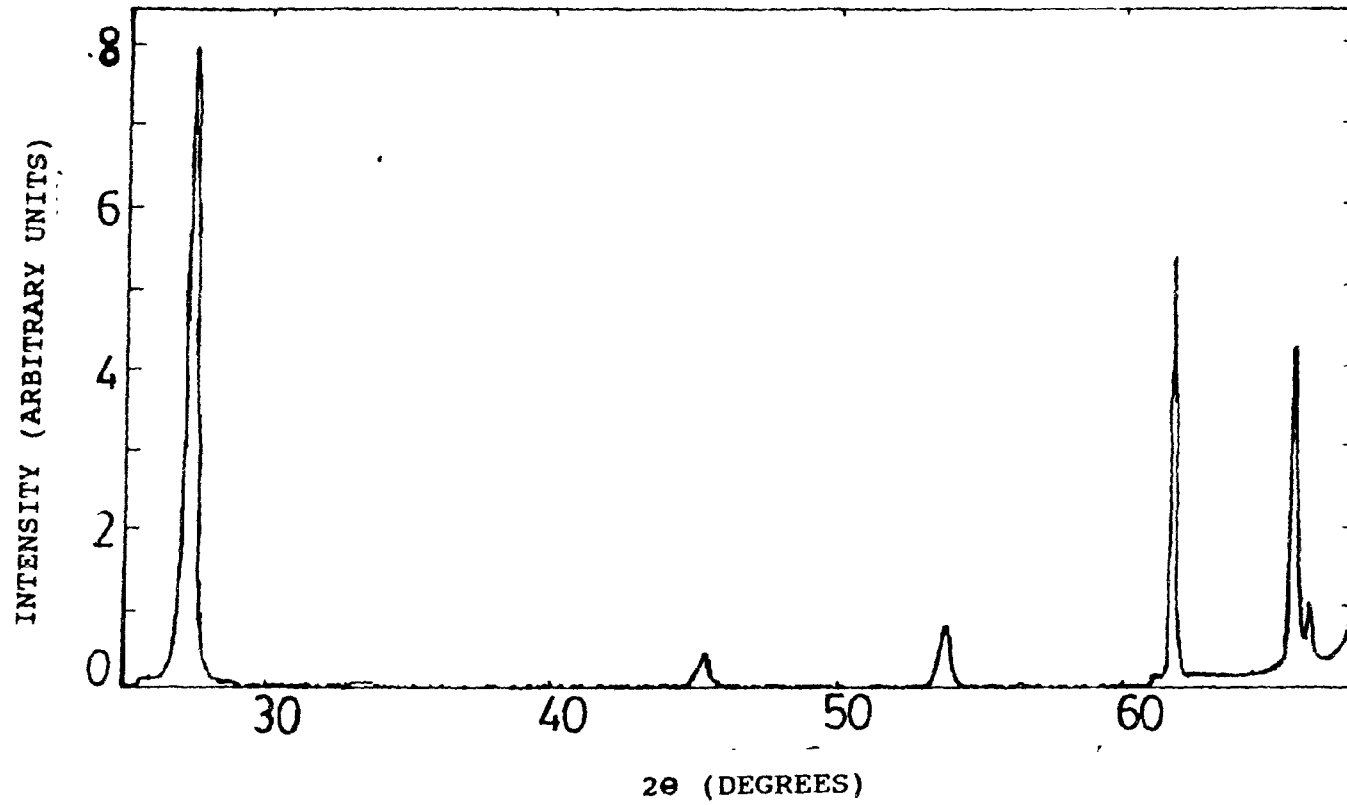


Fig. 5-12 X-ray spectra of ZnSe on Si <100> at 600°C.

of almost negligible intensity appeared as seen in the fig. 5-9. Also the peak heights were more pronounced than the one grown at 200°C.

The X-ray spectra of the sample grown at 400°C has been shown in figure 5-10. It is evident from the figure that all the peaks observed before appeared but this time the peak height variation was noticeable from the ZnSe (111) orientation and the Si(100) due to the substrates. The height of ZnSe peak lowered with the increase in the temperature and that of silicon increased correspondingly showing the affect of growth temperature on the degree of crystallinity of the film.

The X-ray spectra at 500 & 600°C show the further reduction in the peak height of ZnSe at (111) orientation and increase in Si(100) peak height are compared to what has been observed before for lower temperatures. These results are very useful to determine the optimum growth temperature range to grow good quality crystalline ZnSe films for further study. Figs. 5-11 and 5-12 show these spectra.

In order to determine the suitable growth temperatures, the ratios of peak heights with respect to (113) and (004) peak heights were considered. These ratios were then plotted as a function of temperature as shown in the figs. 5-13 and 5-14 respectively. The plots clearly indicate that the suitable growth temperature is around 300°C. Further growth experiments of ZnSe

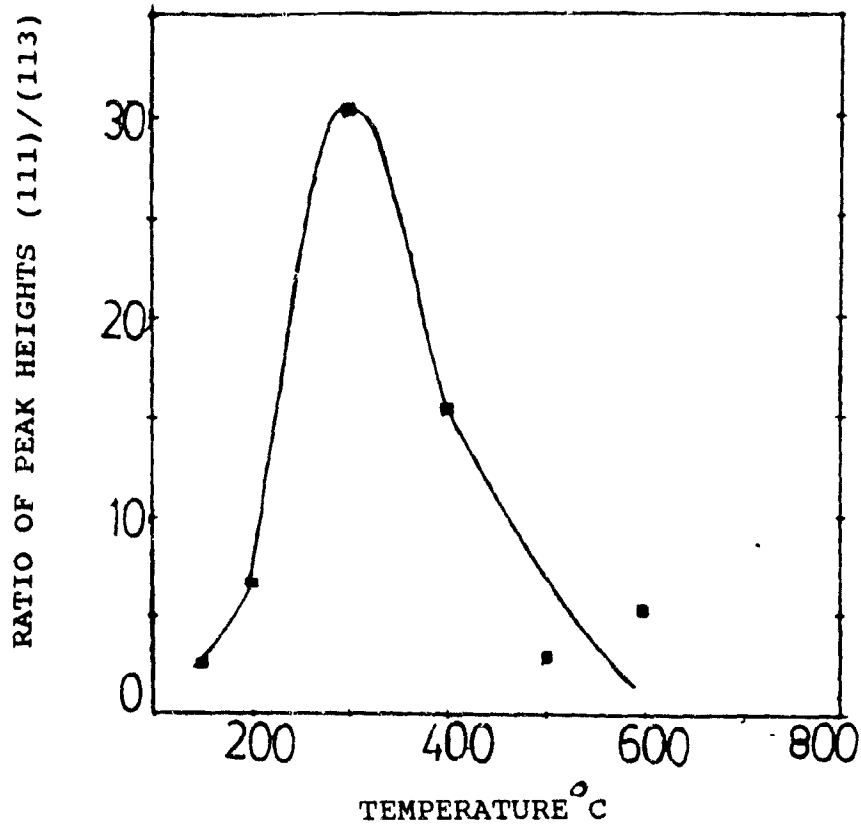


Fig. 5-13 Ratio of peak heights (111)/(113) vs. temperature

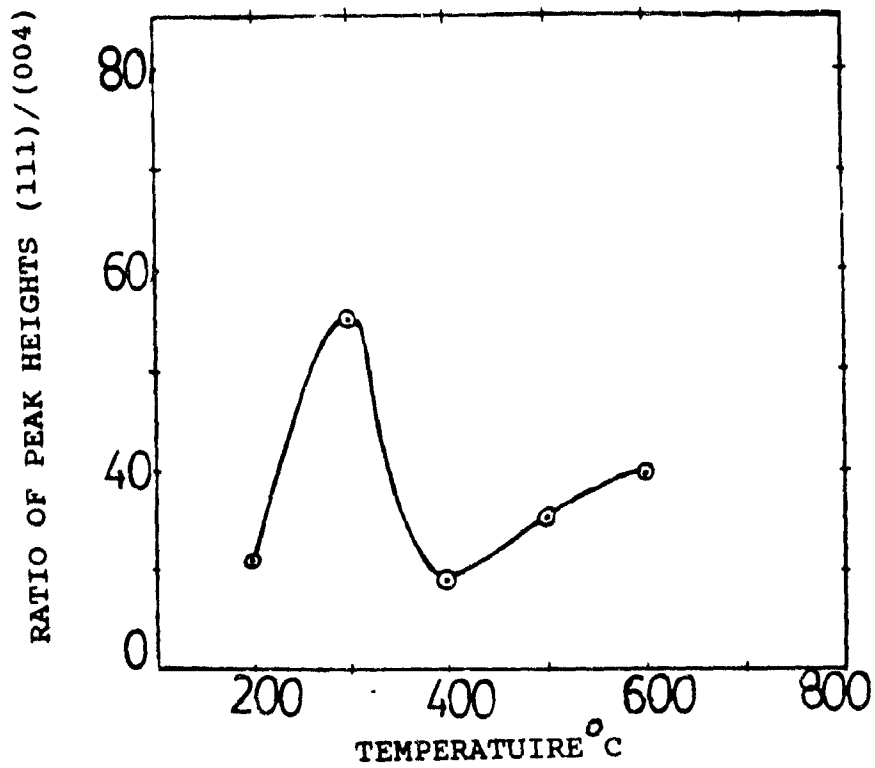


Fig. 5-14 Ratio of peak heights (111)/(022) vs. temperature.

were carried out at around 300 and 350°C. HCl was used as a carrier gas and a fairly thick layer of ZnSe (about 5 microns) was grown and the substrate was etched for 30 minutes at 900°C using a mixture of HCl+H₂ carrier gas prior to the growth of ZnSe. DMZ was used as a source of zinc. The x-ray results show a pronounced peak at 27.3° and other less intense peaks at different orientations indicating the good crystallinity of the films.

It was also noticed that annealing had a significant effect on the samples grown at 350°C. Before annealing the sample grown at 350°C showed less pronounced ZnSe peak than the one grown at the same temperature after annealing at 700°C for 30 minutes in the presence of H₂ carrier gas supplied at the rate of 1 litre/min. All these initial experiments gave a good idea about the different growth parameters to be used in order to grow good quality ZnSe films on the GaAs substrate as discussed further.

ZnSe films were grown on GaAs using pulsed OMCVD technique. The crystalline quality of the films were tested by x-ray analysis. The substrate had a orientation of (100) and the films showed a consistent structure with a (100) preferred orientation. The X-ray analysis was done in the range of 60 to 70° (2θ), where reflections from (400) planes of both substrate and the film can be resolved very distinctly. Fig.5-15 shows three peaks very distinctly resulting from a 3 micron thick layer of ZnSe on GaAs. These three peaks are due to the combination of the two X-ray line $k\alpha_1$ and $k\alpha_2$ and of the (004) planes of ZnSe and GaAs with a

0.3° off-set, possibly from the characteristics of the X-ray diffractometer used. This further suggests that the quality of the (100) ZnSe layer is good. The X-ray spectrograph of the sample 2 is also shown in figure 5-16. The splitting of the lines appeared at the same angles as observed in the first case with an off-set of 0.3°.

5.2 PHOTO-ELECTRIC MEASUREMENTS :

The photo-electric properties were obtained by shining light on the above samples as shown in the figure 5-17. The range of wavelength was from 400 to 1000 nm. Both short circuit photo-current and open circuit photo-voltage measurements were made on these samples. Figure 5-18 shows the normalized open circuit photovoltage of a layer deposited on an n-type GaAs layer with $n = 10^{16} \text{ cm}^{-3}$. The curve shows a sharp increase of photo voltage with wavelength upto 550 nm and shows nearly a saturation until 850 nm corresponding to the band edge of GaAs and then drops abruptly to almost zero volts around 1000 nm as seen from the plot. The photovoltage observed for energies below the band edge of GaAs can be attributed either to donor impurity band in the GaAs or to deep levels present within the ZnSe. However, the actual mechanism is not understood. The voltage corresponds to positive polarity on the ZnSe side and the negative polarity on the GaAs side of the junction. Fig. 5-19 shows the corresponding short circuit photocurrent of this diode. These results are consistent with the proposed model.

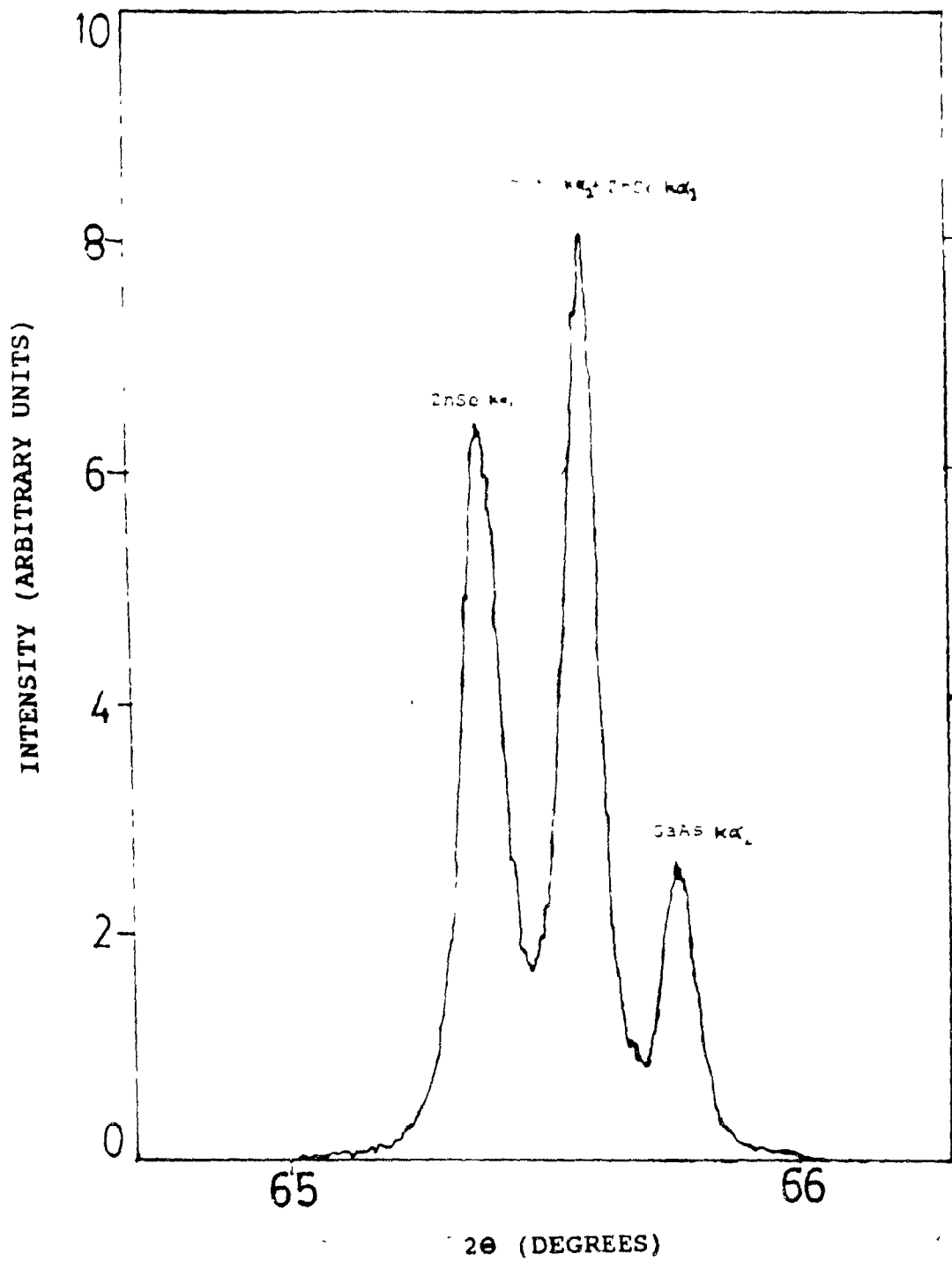


Fig. 5-15 X-ray diffraction spectra of ZnSe on (100) GaAs for diode 1.

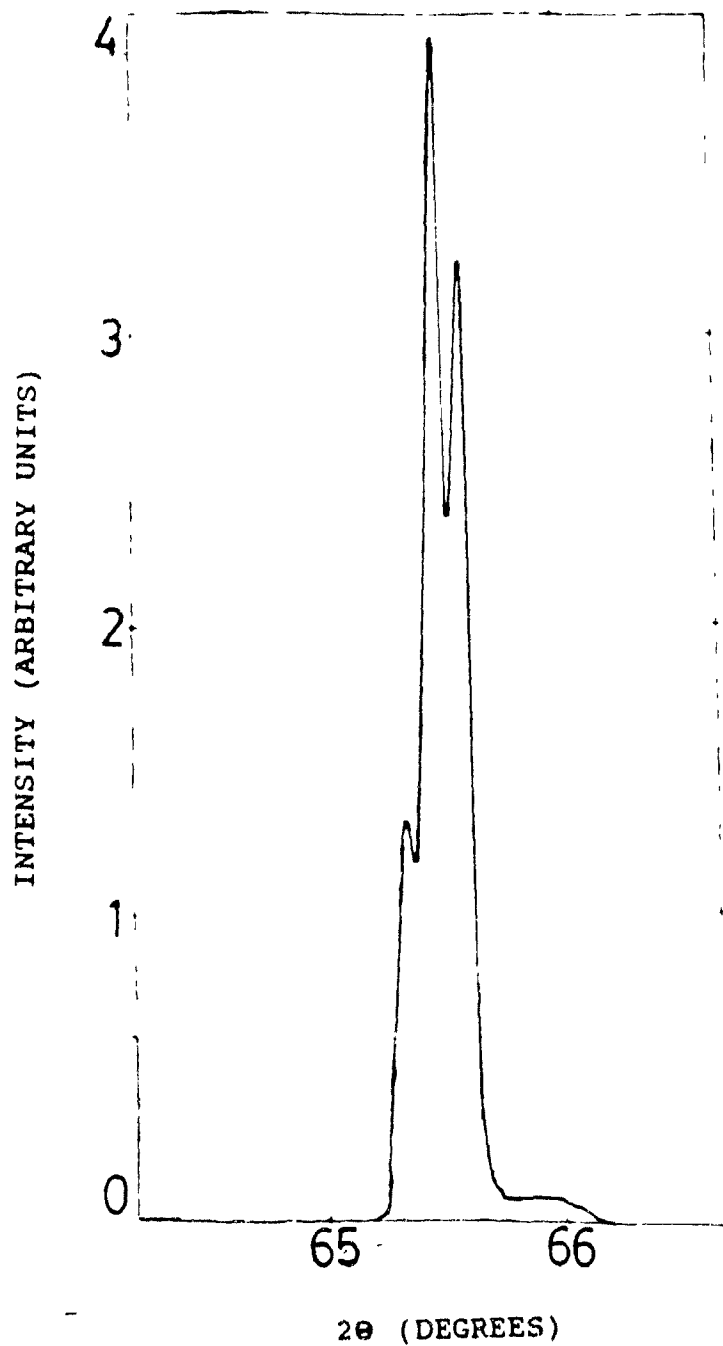


Fig. 5-16 X-ray diffraction spectra of ZnSe on (100)
GaAs for diode 2.

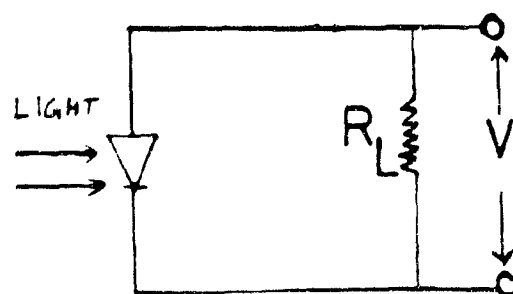
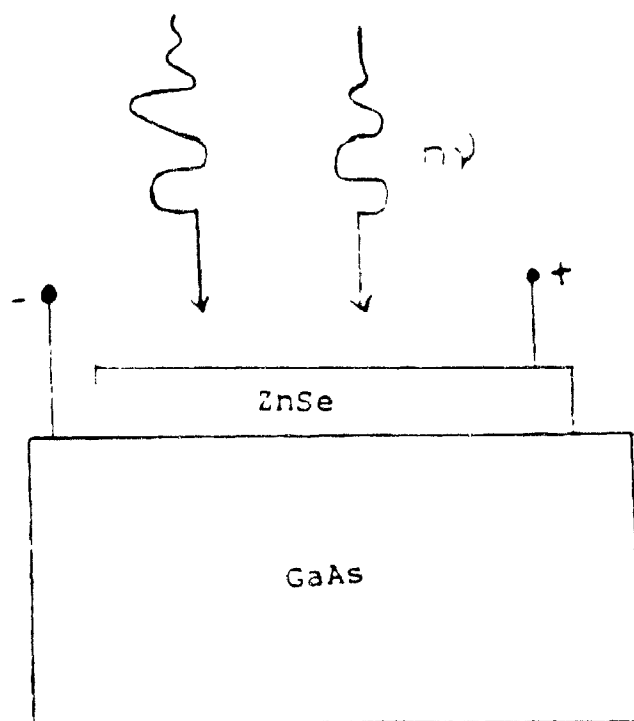


Fig. 5-17 Measurement set-up.

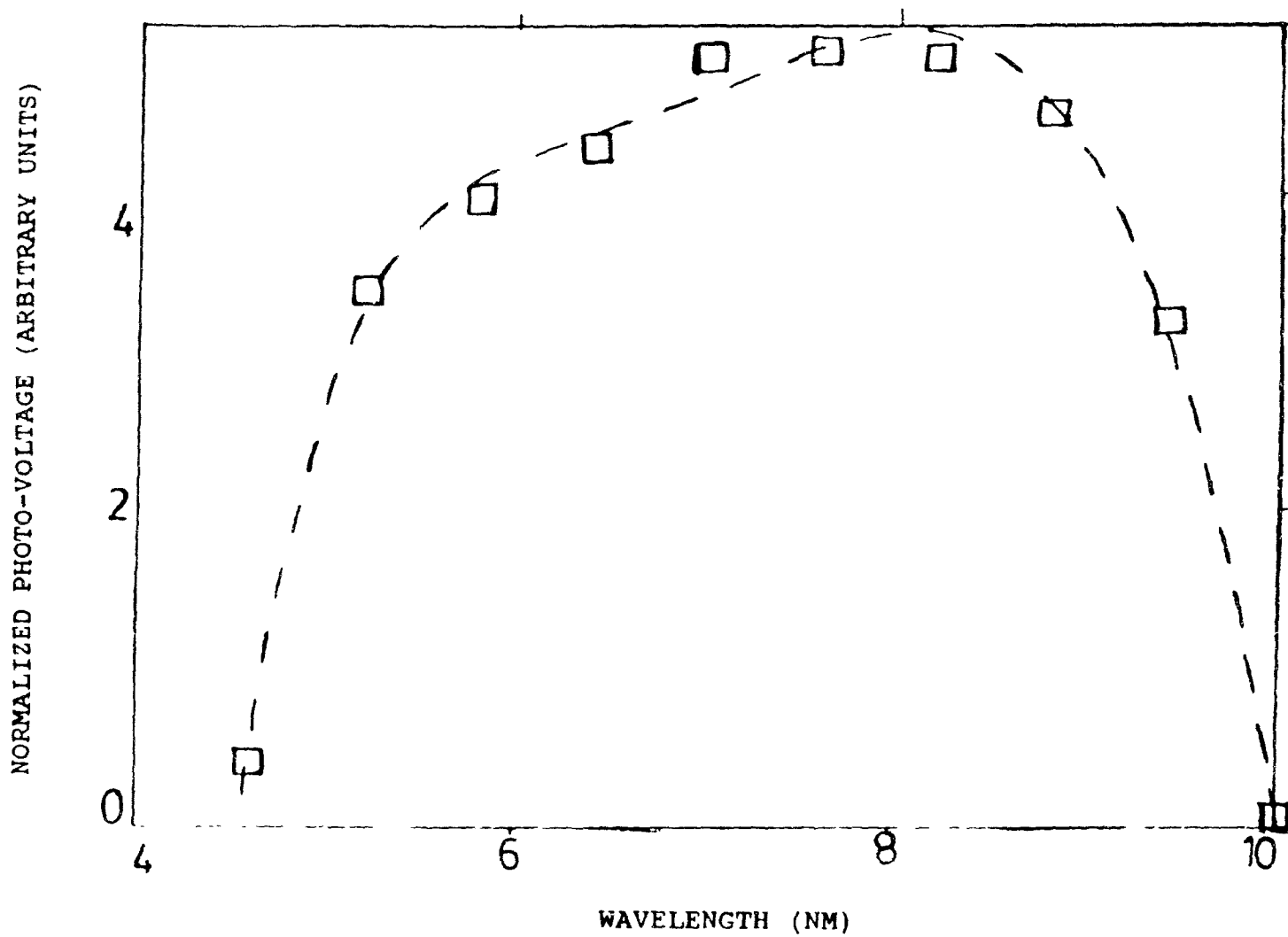


Fig. 5-18 Normalized photo-voltage vs. wavelength for diode 1.

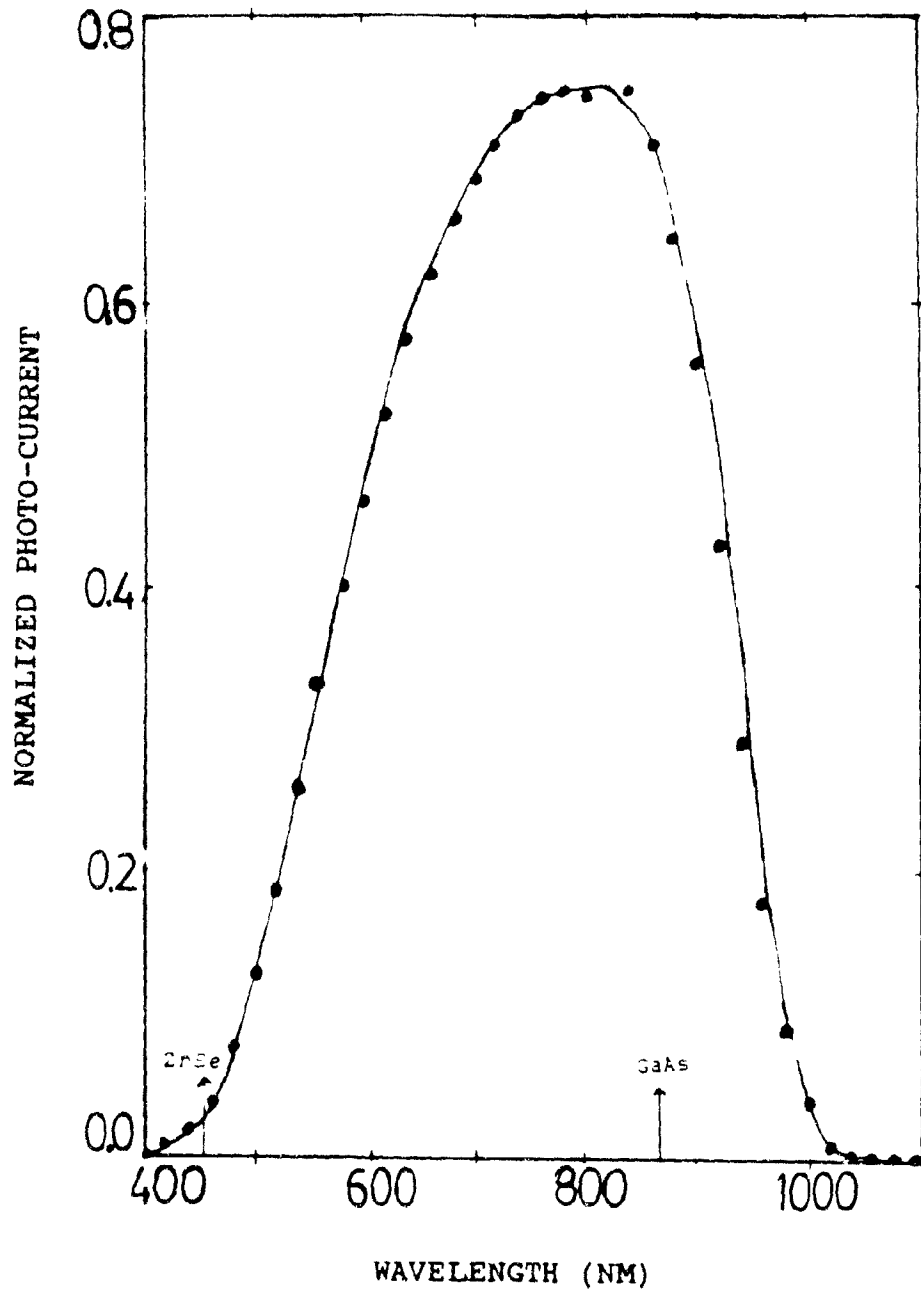


Fig. 5-19 Normalized photocurrent vs. wavelength
for diode 1 .

The photo-electric measurements made on sample 2 also exhibit the similar characteristics but the transition in the photocurrent seems to be more abrupt than the former. The open circuit photo voltage measurement on this sample shows a narrow peak compared to the first diode. These have been shown in figs. 5-20 & 5-21.

5.3 I-V CHARACTERIZATION :

The next step in this study was the electrical characterization of the diodes. For this purpose several diodes were fabricated by growing conducting n-type ZnSe films of different thickness ranging from 0.2 to 3 microns on SI GaAs substrates with (100) orientation. The doping of the ZnSe films was of the order of $n = 2 * 10^{19} \text{ cm}^{-3}$. Indium contacts were then alloyed to both ZnSe and GaAs sides of the diode using a low temperature soldering gun. The diodes had a surface area of 3 square mm. An attempt was made to heat treat the contacts in the presence of inert gas at 200°C for 3 minutes. However, no significant change in the electrical characteristics were observed as a result of heat treatment as seen from figs. 5-22 and 5-23, on a diode fabricated by growing a thin epilayer of ZnSe (of the order of 0.2 to 0.8 microns). The measured room temperature mobility was 300 cm² /volt. sec.

5.31 Forward Bias :

Figure 5-24 shows the I-V characteristic of diode 1 with a positive polarity on ZnSe side of the device. Linear I-V for this diode shows rectification. This diode shows an exponential current behaviour over a range of 5 decades. A simple diode

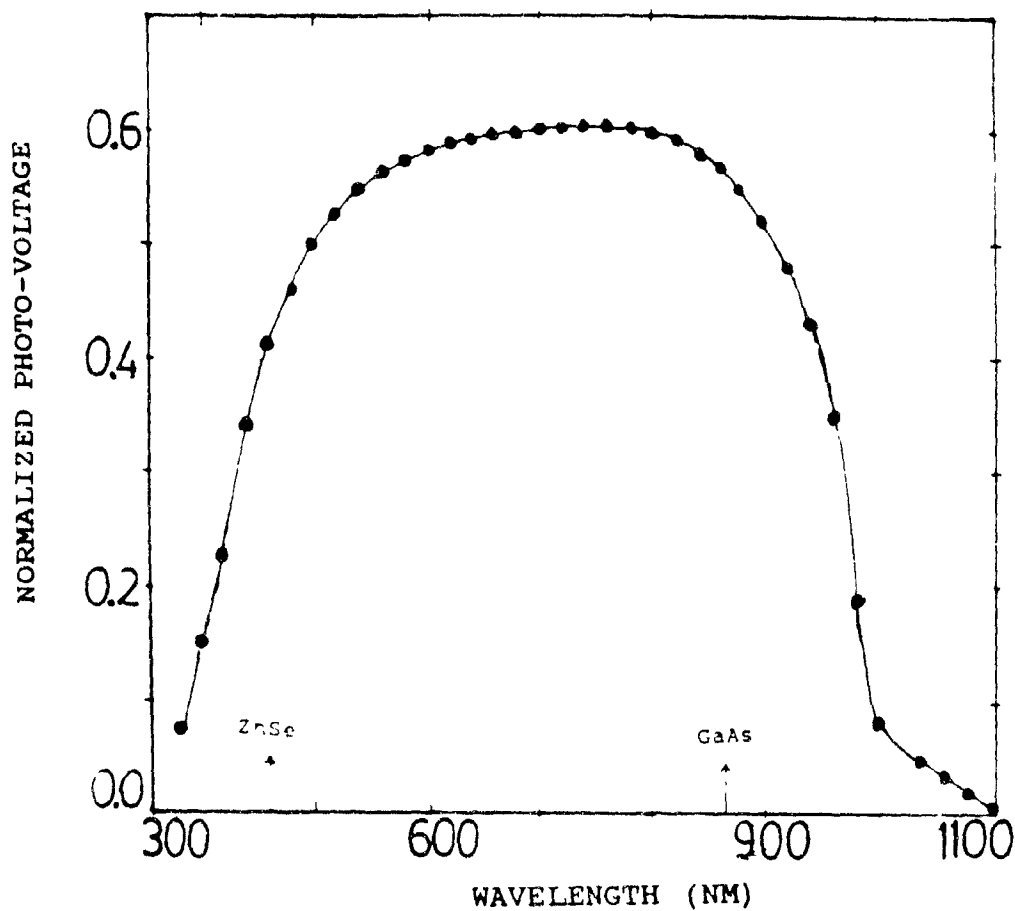


Fig. 5-20 Normalized photo-voltage vs. wavelength for diode 2.

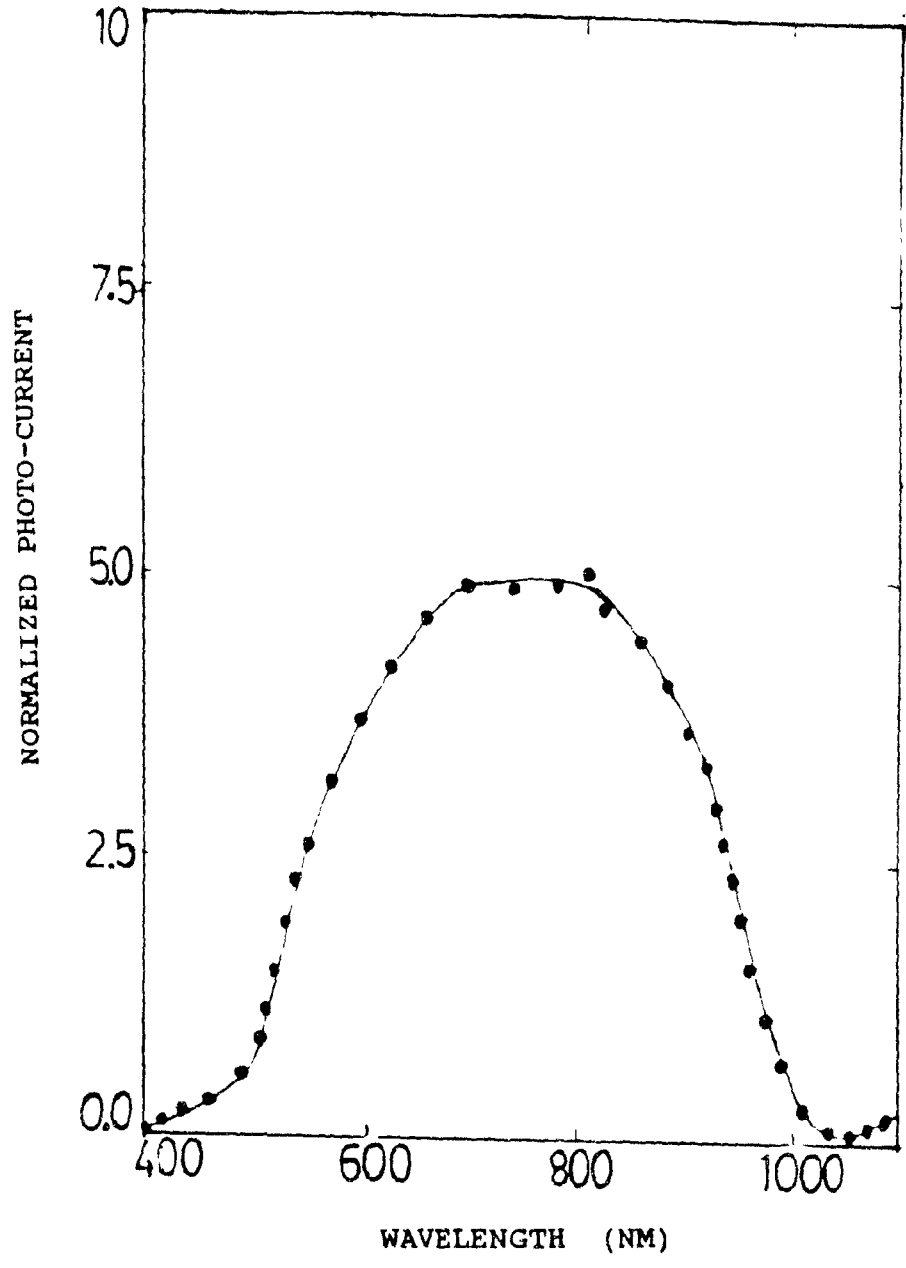


Fig. 5-21 Normalized photo-current vs. wavelength for diode 2.

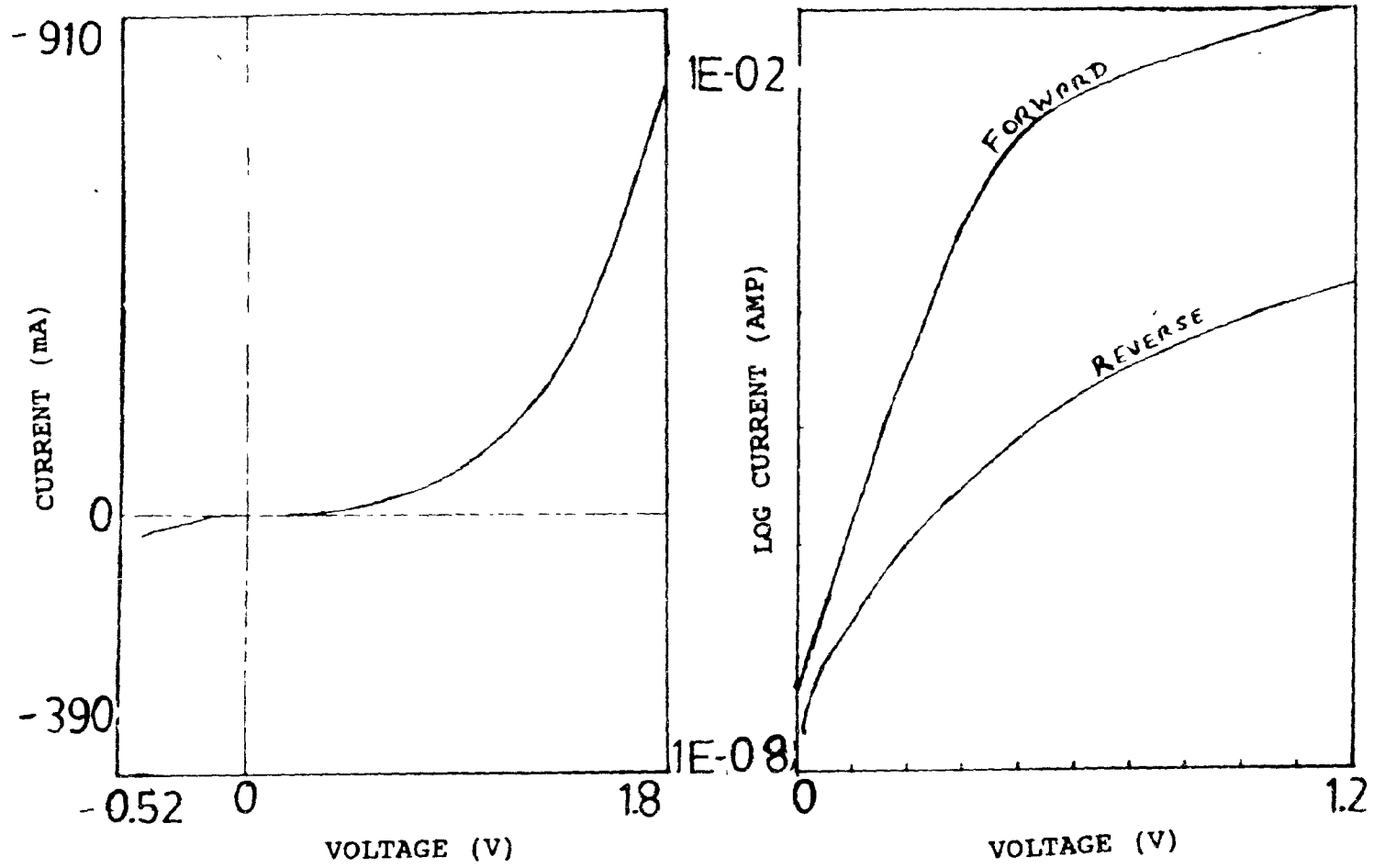


Fig. 5-22 Prior to the heat treatment of the contacts.

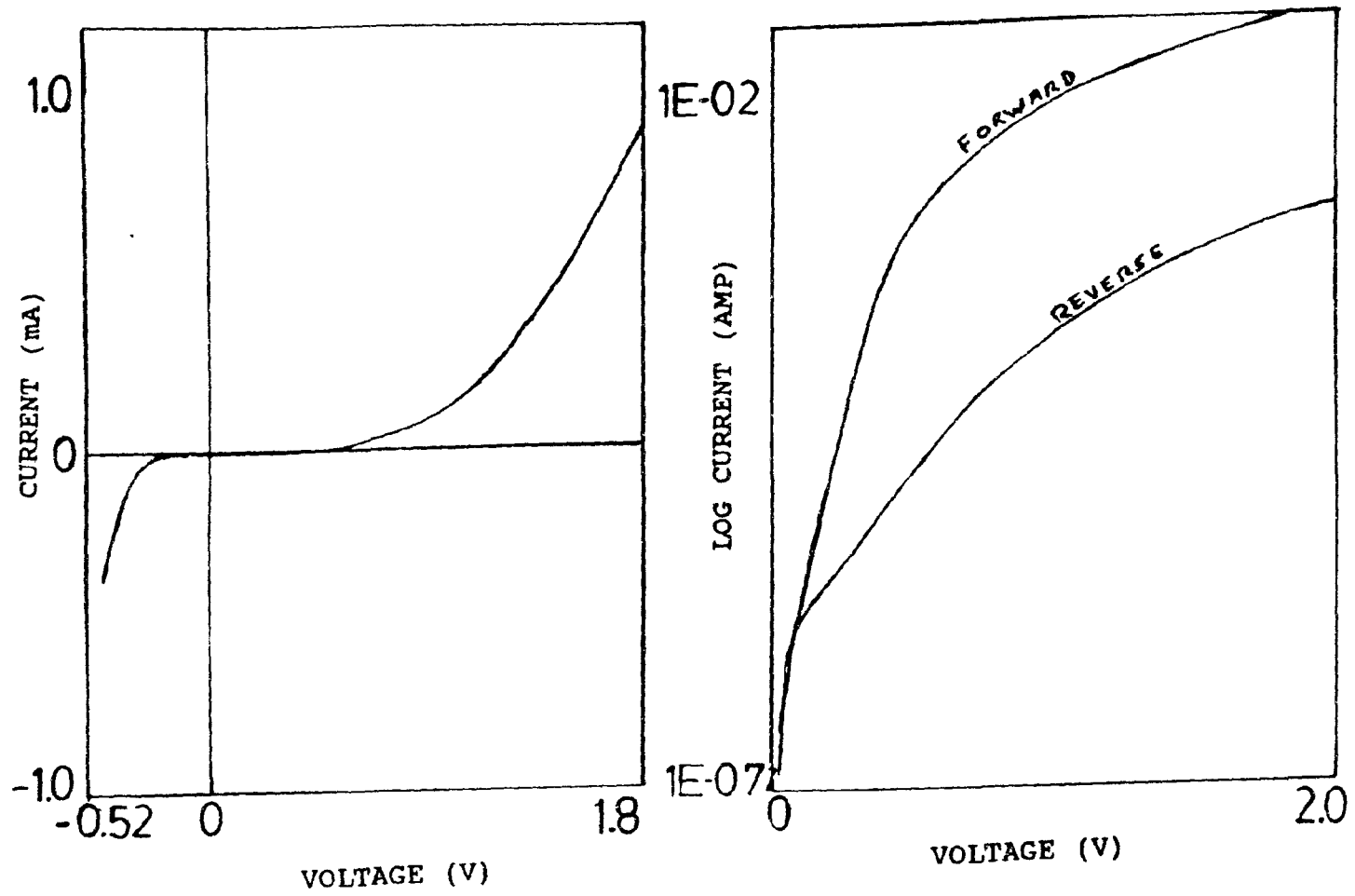


Fig. 5-23 After the heat treatment of contacts.

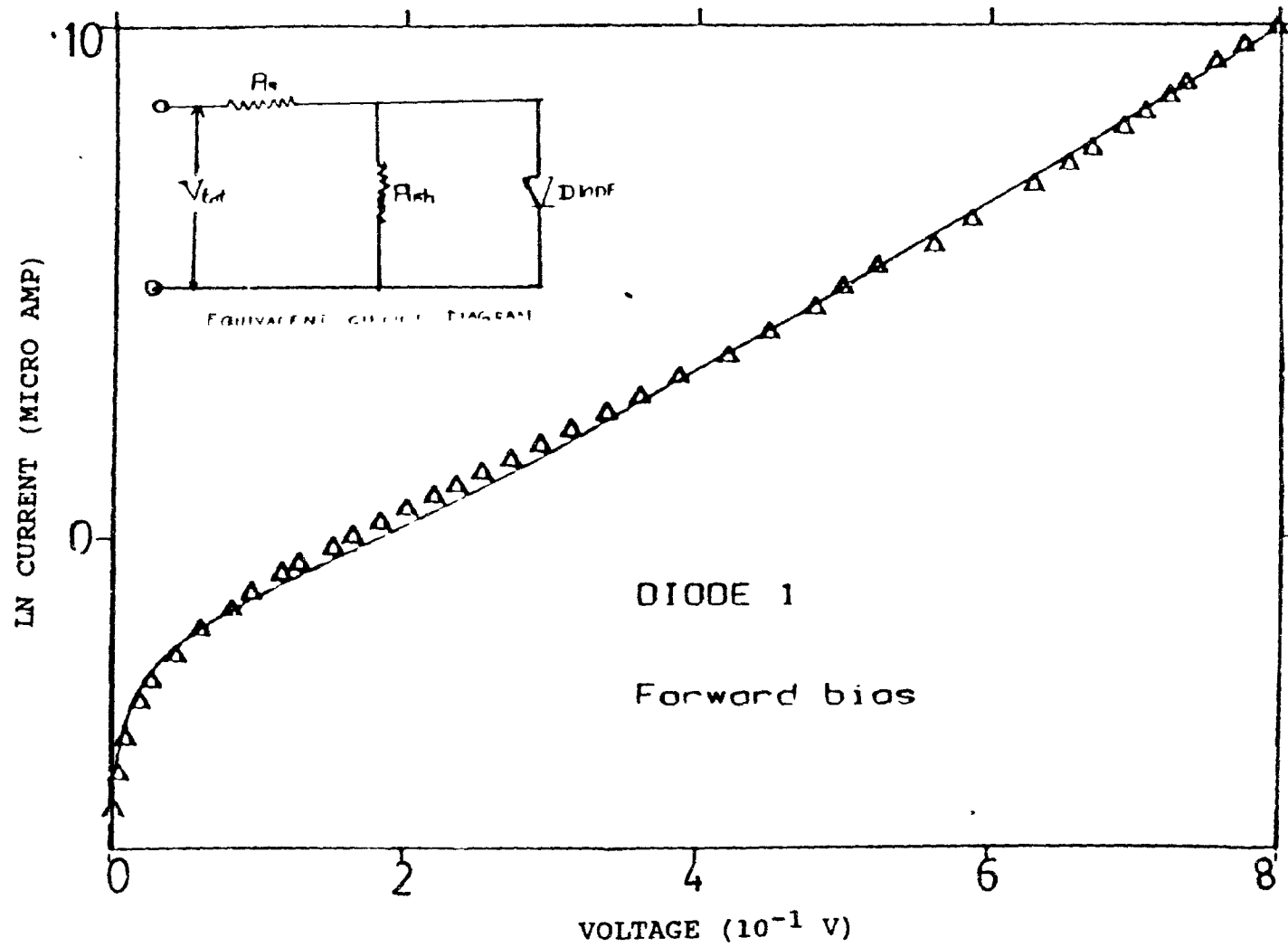


fig. 5-24 current vs. voltage of diode 1 in forward bias.

equation can be expressed as follows.

$$I = I_0 (\exp qV/nkT - 1)$$

where "n" is the ideality factor and the other symbols have their usual meaning. The ideality factor for a normal diode is 1.0.

In order to include the observed effects such as shunt resistance (R_{sh}) and series resistance (R_s), the above diode equation has to be modified. For this purpose, a modified empirical formula is used [39], which would fit the observed experimental data, for forward bias. The empirical analysis is based on the expression

$$I - V/R_{sh} = I_0 (\exp[qV/kT - qR_s/kT (I - V/R_{sh})] - 1) + V/R_{sh}$$

where the symbols have their usual meaning. This formula is in conjunction with the equivalent circuit model as shown in the insert of fig. 5-24 taking into account all the branch currents flowing through the network. However, for a given I-V plot, the values of R_s , R_{sh} , q/nkT and I_0 can be evaluated. The ideality factor for diode 1 was found to be 1.67 and was 2.05 for diode 2. For diode 1, as seen by the linearity of the curve, the exponential behaviour of current is upto 5 decades and the series resistance does not dominate the I-V characteristic. However, we notice that the shunt resistance has a pronounced effect on the I-V characteristics. With these parameters, the above expression can be used to fit the data. For diode 2, as shown in fig. 5-25 for the forward bias, the exponential behaviour of current is seen over about 4 decades and the series resistance effect seems to be dominant in the high current range. The leakage current in this case does not dominate the I-V characteristics and can be neglected. In figs. 5-24 and 5-25 the solid curve is the one

obtained by fitting the data using the above equation and the broken curve is the one obtained experimentally. It is evident that both the results agree very well. The following table summarizes the value of parameters that fit the data for these diodes.

Table 2 I-V Results for Forward Bias

	R_S (ohm)	R_{SH} (ohm)	$B(V^{-1})$	I_0 (amp)
Diode 1	1	$5 * 10^5$	16.8	$3.05 * 10^{-8}$
Diode 2	$5 * 10^3$	-	26.2	$1.77 * 10^{-3}$

5.32 Reverse Bias:

Fig. 5-26 shows the reverse biased characteristics for both diodes 1 and 2 respectively. The current does not saturate as it does in the case of a lightly or moderately doped p-n junction. The reverse currents were fitted to the data

$$I = I_{R0} \exp \left(-A/(V + V_0)^{1/2} \right)$$

where, V_0 is the barrier height and I_{R0} and A are adjustable parameters. This expression is deduced from the tunneling through a barrier of height V_0 . Both the diodes fit the data with the following values for the empirical parameters as shown in table 3 on the next page.

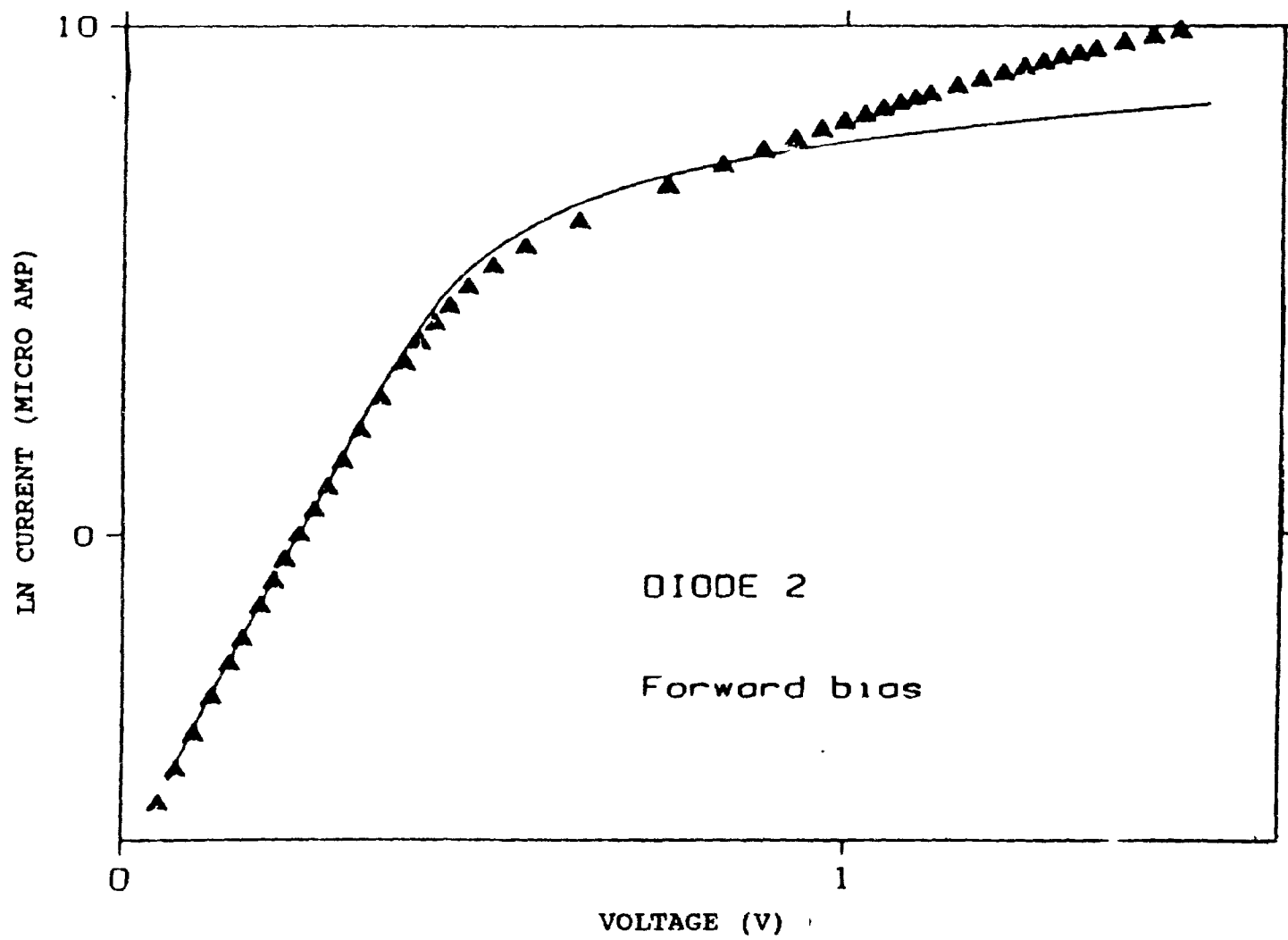


Fig. 5-25 Current vs. voltage of diode 2 in forward bias.

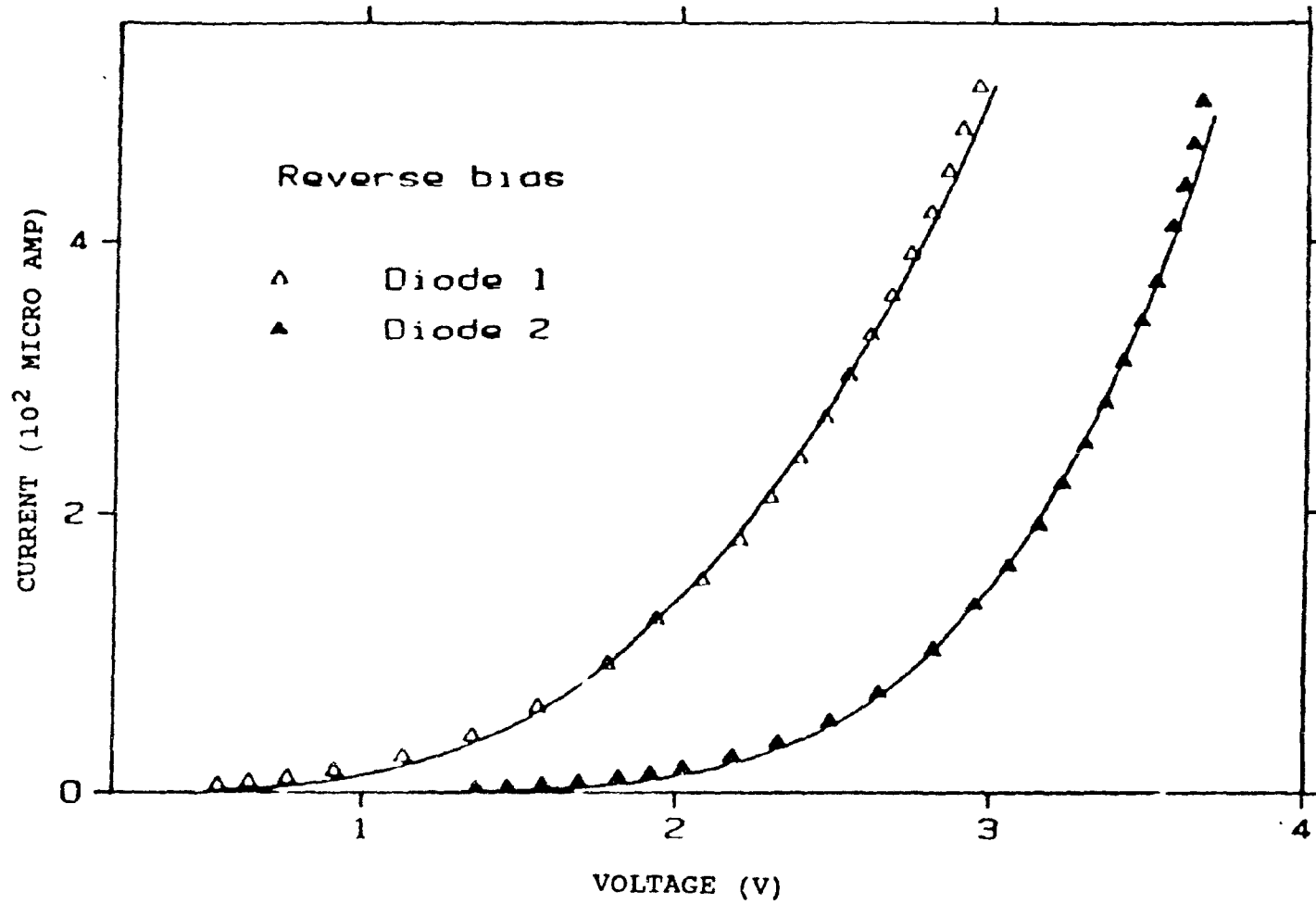


Fig. 5-26 Current vs. voltage of diodes 1 & 2 in reverse bias.

Table 3 I-V Results for Reversed Bias.

	$I_{ro}(\text{amp})$	$A(V^{1/2})$	$V_0(V)$
Diode 1	$1.29 * 10^{-6}$	15.1	0.7
Diode 2	$348.0 * 10^{-6}$	28.3	0.7

These values are consistent with the experimentally obtained values by Walsh et al. [40]. This value of V_0 is close to the value proposed earlier by Ludwig et al. [41] corresponding to $V_0 = 0.5$ V. Hence we believe that the reverse current is due to the the tunneling mechanism.

5.4 C-V MEASUREMENTS :

For the C-V measurements, a thin layer of ZnSe (1 micron) was deposited on the GaAs substrate. The carrier concentration as determined by the Hall effect was $2 * 10^{16} \text{ cm}^{-3}$. The measurements were carried out with the help of LCR meter and $1/C^{**2}$ value was computed for each voltage. The plotter connected to the system was used to plot the curve. Two diodes were tested for this purpose. The plots have been shown in the figs. 5-27 and 5-28 for diodes 1 and 2 respectively. These plots show that the capacitance decreases in both the cases as the value of reverse voltage is increased and increases for the forward bias. This is very well expected because the capacitance has a inverse square root dependence with the voltage. The slope of the straight line allows an evaluation of N_d while the extrapolated intercept with

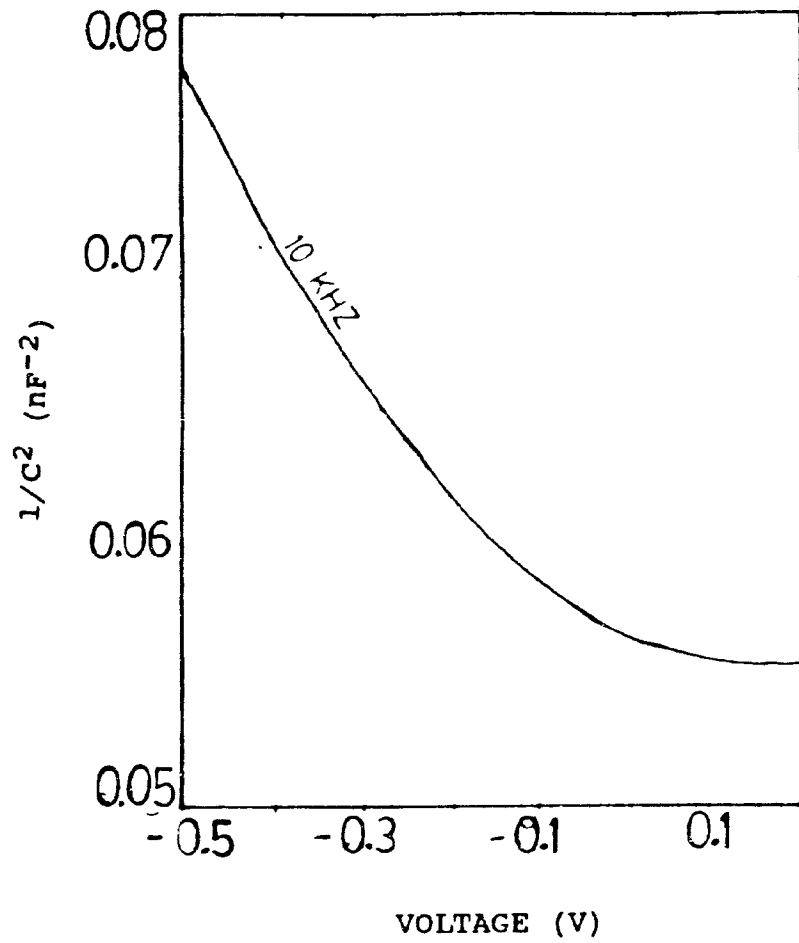


Fig. 5-27 Capacitance vs. voltage for diode 1.

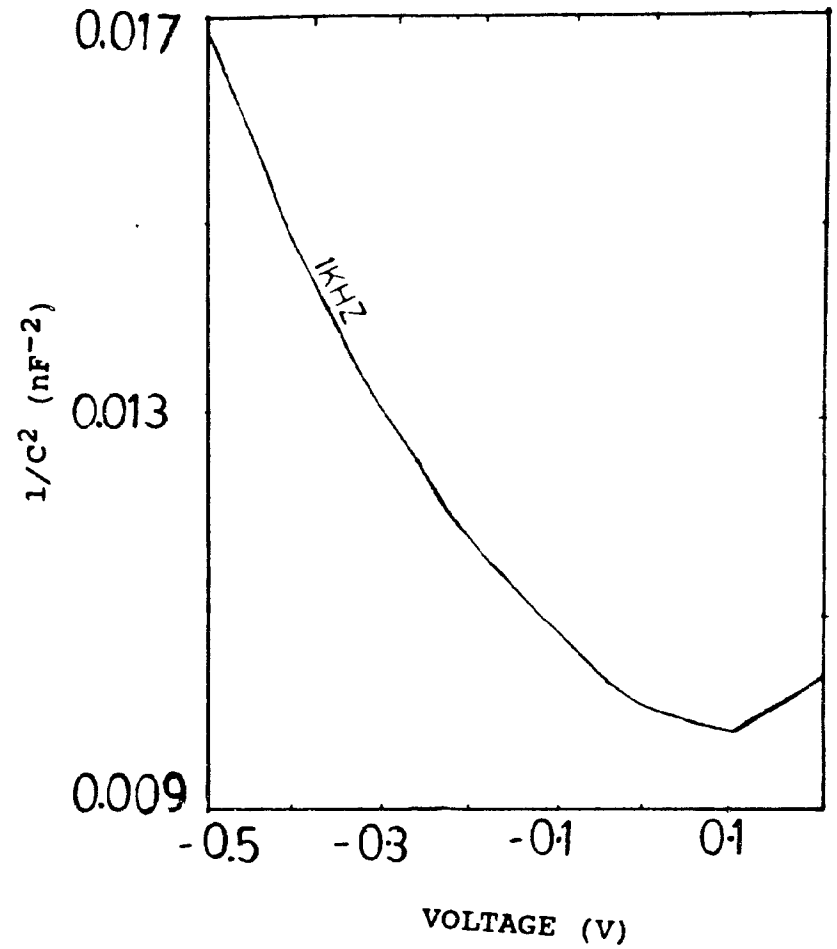


Fig. 5-28 Capacitance versus voltage for diode 2.

the abscissa gives the voltage. However, in the plot, we notice that the curve has more than one slope indicating different values of diffusion potential and also indicates that the donor concentration (N_D) is not quite uniform in the epilayer. This is due to the difficulty to achieve uniform doping in the growth. The values obtained from the experimental data for N_D are tabulated below.

Table 4 N_D values as determined by C-V analysis.

Diode 1	$0.16 * 10^{16} \text{ cm}^{-3}$
	$0.28 * 10^{16} \text{ cm}^{-3}$
Diode 2	$2.8 * 10^{16} \text{ cm}^{-3}$

5.5 PHOTOLUMINESCENCE SPECTRA (PL):

The analysis of PL spectra gives information about the impurities present and the native defects incorporated in the material. The spectra has been analysed in light of the standard spectra of bulk ZnSe as shown in insert of fig. 5-29. PL spectra of our samples were studied at low temperatures corresponding to 6 K and high temperature corresponding to 300 K.

Figure 5-29 shows the PL spectra of diode 1 at 6 K. This showed peaks at 2.80 eV due to free excitons and a second less intense peak at 2.79 eV due to bound exciton. At 300 K, a peak appeared at 2.70 eV due to edge emission (1LO) and a broad emission peak identified as self-activated (SA) emission spectra at 2.108 eV.

This shows the (SA) peak became negligible at low temperature. This spectra was obtained at low excitation conditions because low excitation is suitable for the assessment of the deep centres in ZnSe. Also, the presence of intense peak at 6 K indicates that the sample has a shallow donor impurity of about 10^{16} cm^{-3} . The PL spectra of the same diode obtained at 300 K has been shown in fig. 5-30.

Figure 5-31 shows the PL spectra of diode 2 at 7 K. Two pronounced peaks were observed in the short wavelength region, one at 2.80 eV and the other at 2.78 eV. From the standard analysis, it is evident that the first peak is due to the radiative recombinations of free excitons (X). The second intense peak is due to the radiative recombination of bound excitons at a neutral donor (D^0, X). This peak is generally associated with the impurities such as Ga, As and Al added in the film during the growth, to improve conductivity. The same sample showed three peaks at 300 K at 2.69, 2.60 and 2.56 eV respectively as shown in fig. 5-32. From comparison, we can see that these peaks fall in the band edge emission region and arise from the radiative recombination of electron and hole bound to a distant donor-acceptor pair. In comparison with the bulk ZnSe spectra, OMCVD grown ZnSe has no detectable acceptor impurities (A like) and also shows only small concentrations of impurities.

It has been reported [42] that the peak intensity ratio 'R' between narrow near band edge (NBE) and SA luminescence for OMCVD

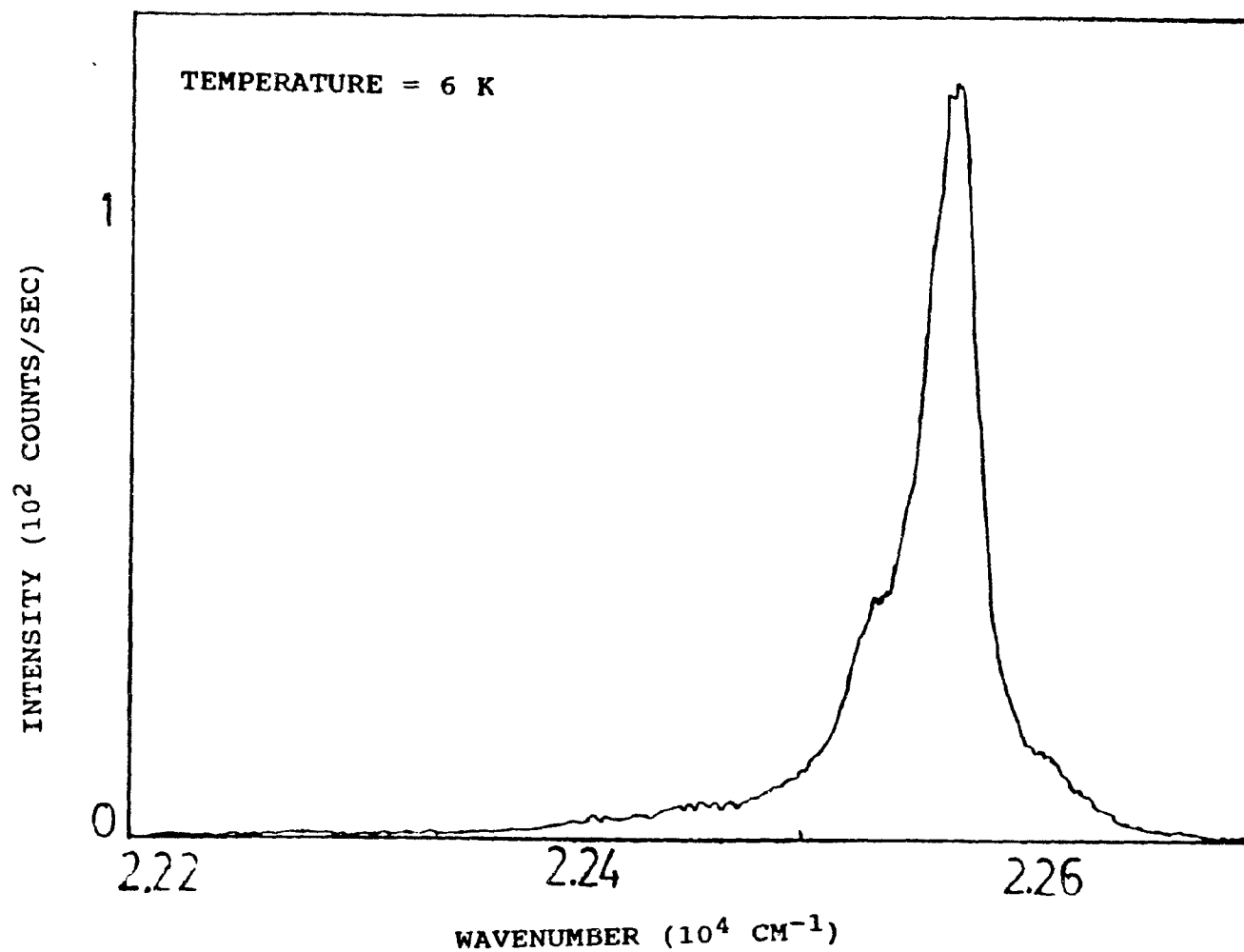


Fig. 5-29 PL intensity vs.wavenumber for diode 1 at 6 K.

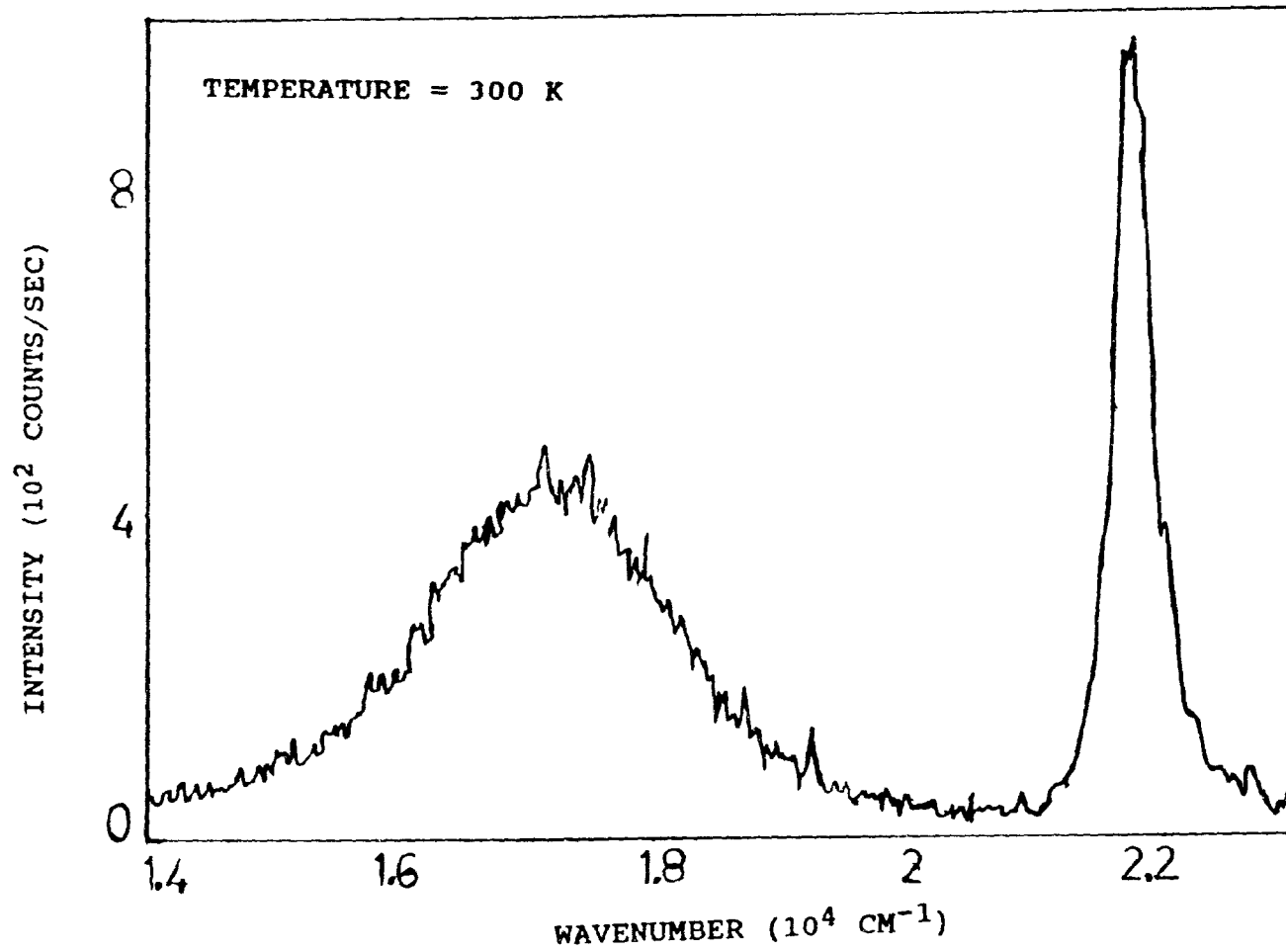


Fig 5-30 PL intensity vs. wavenumber for diode 1 at 300 K

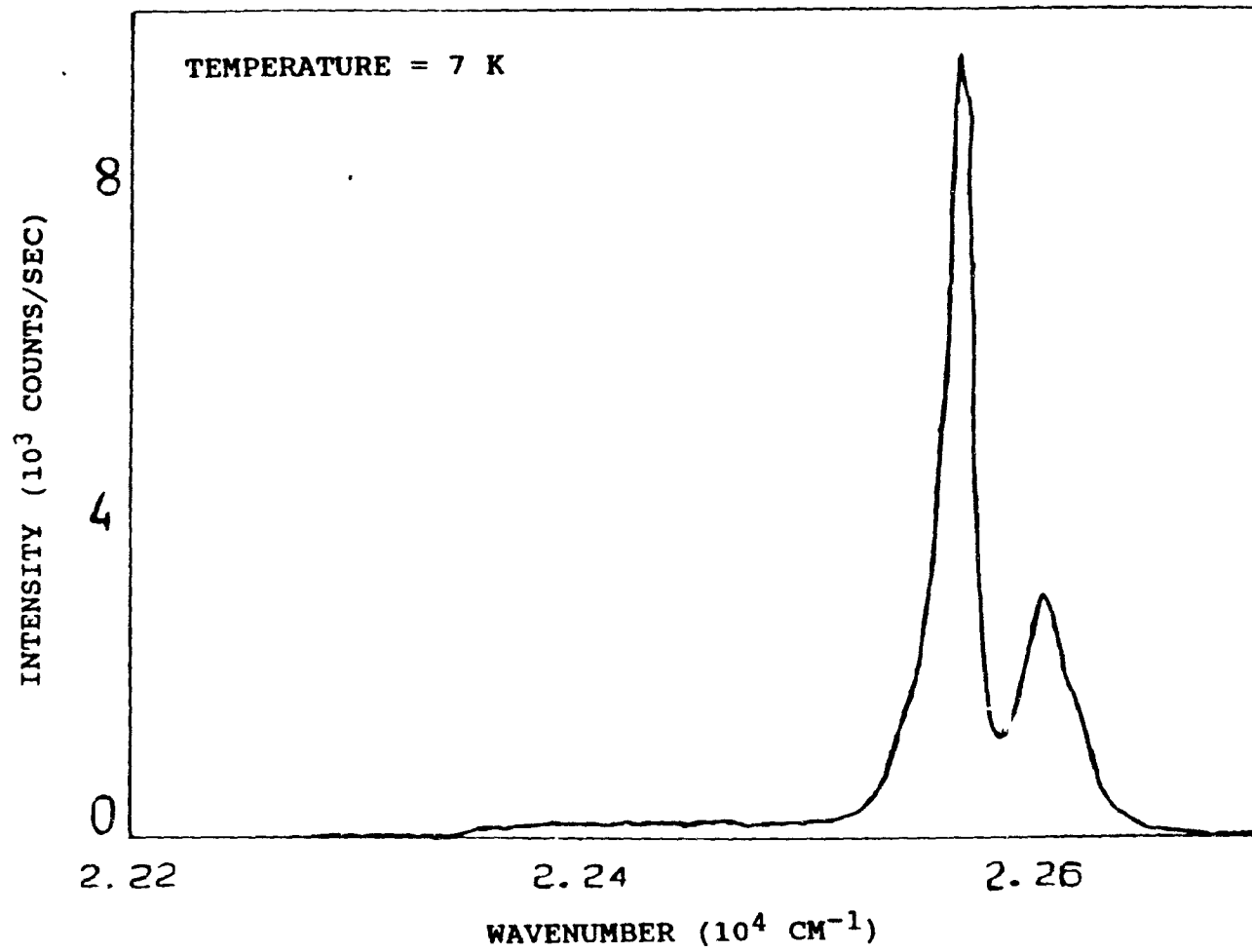


Fig. 5-31 PL intensity vs. wavenumber for diode 2 at 7 K.

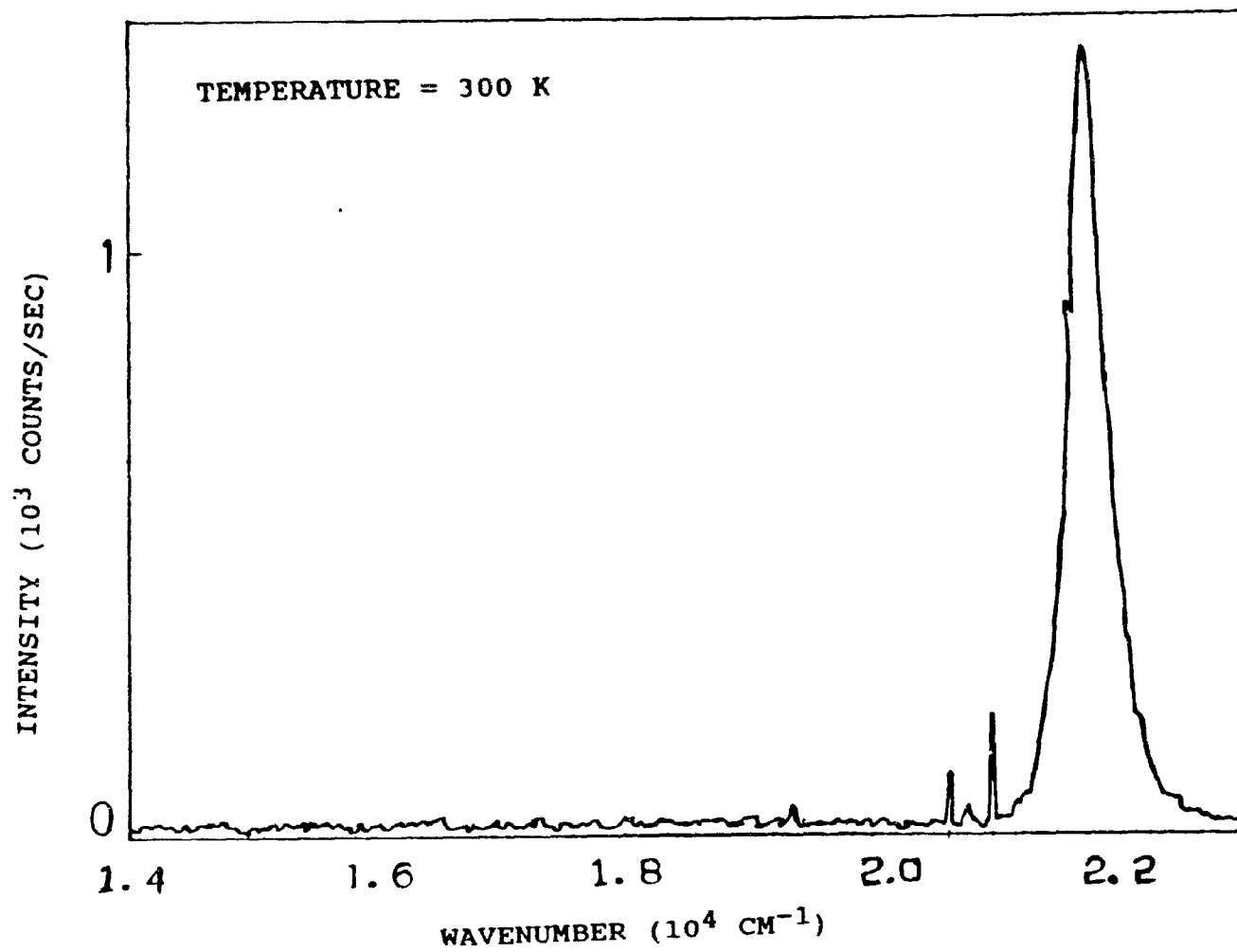


Fig. 5-32 PL intensity vs. wavenumber for diode 2 at 300 K.

ZnSe is $\ll 25$, indicating thereby a low concentration of crystalline defects. This can be greatly attributed to the low growth temperatures (typical growth temperature was 300°C).

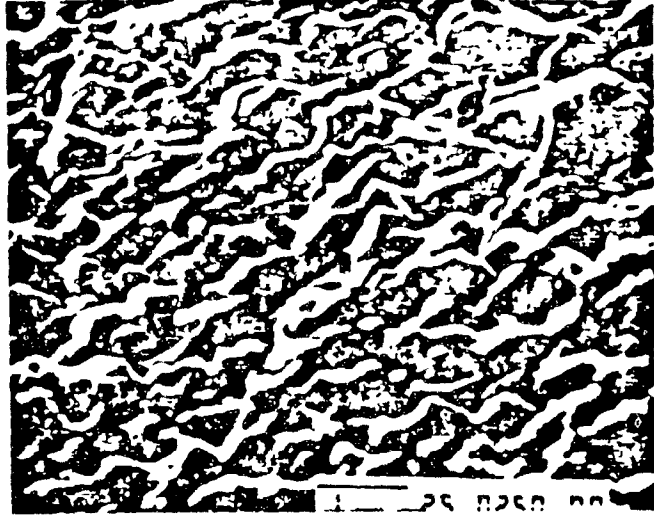
These facts are also seen for diode 2, which shows relatively smaller concentrations of SA centres and V_{Zn} defects at 300 K.

5.6 SEM ANALYSIS :

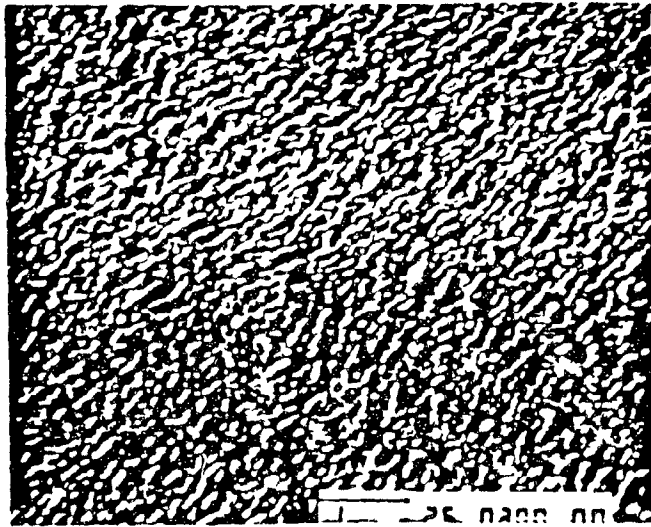
A typical photomicrograph of the ZnSe thin films (thickness 3 microns) on a (100) Si at 250°C is shown in the fig. 5-33a. It is seen that the surface is rough at this growth temperature. Below 250°C , we noticed a twin formation on the surface. Also shown is a photomicrograph of a second sample grown at 300°C in figure 5-33b. Good quality ZnSe films were obtained between 250 and 400°C indicating the proper growth temperature. This concludes the discussion on various characterization.

5.7 ENERGY BAND MODEL :

Based on the above described experimental results, a band model is proposed for the ZnSe:GaAs structure (fig. 5-34). The energy band model for the junction is consistent with the structure first proposed by Mach and Ludwig [42]. In this model, the GaAs side is depleted of electrons and the ZnSe side with accumulation of electrons. The calculation presented in this work yielded a barrier height of 0.7 V which agrees well with the above value reported by other workers.



$T = 250^{\circ}\text{C}$



$T = 300^{\circ}\text{C}$

Fig. 5-33 SEM micrograph of ZnSe on (100) Si.

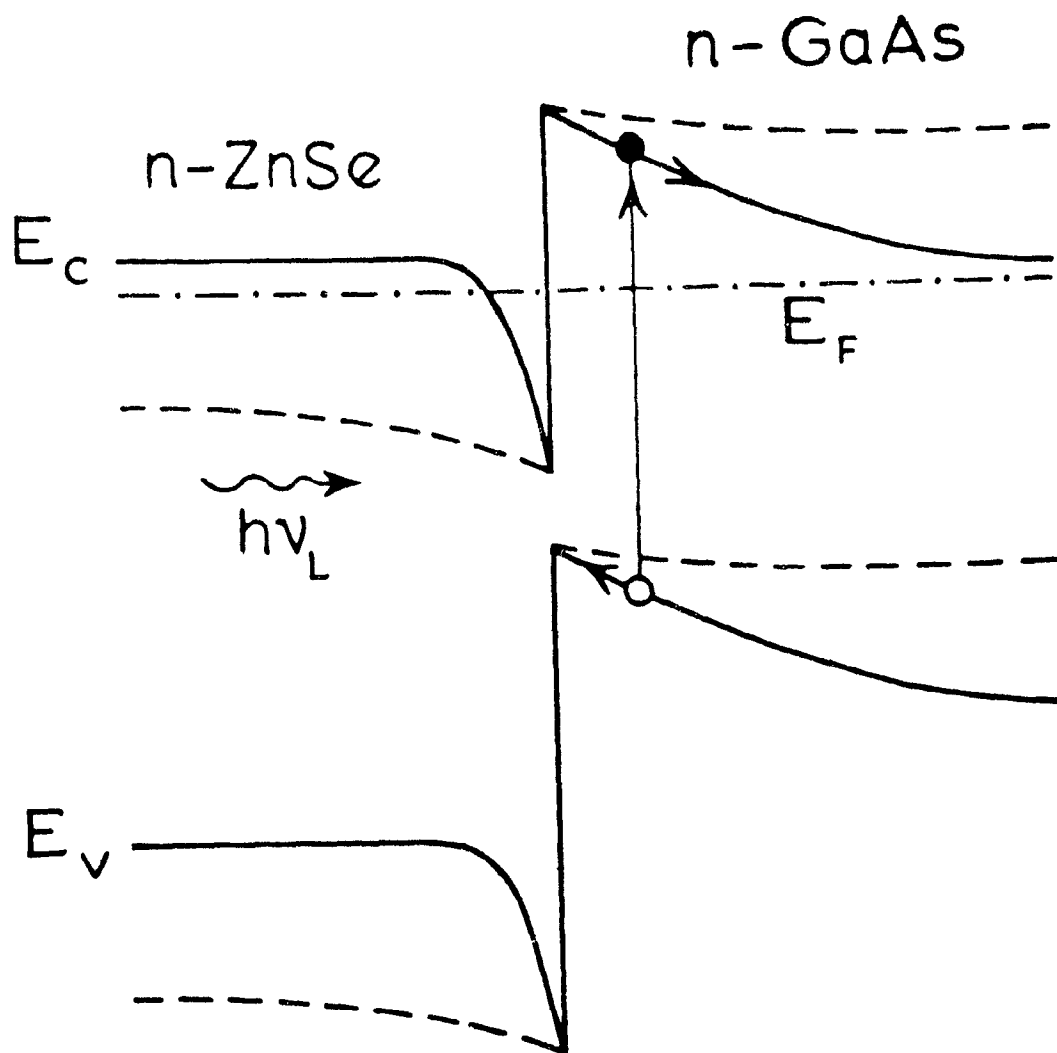


Fig. 5-34 Proposed Energy-Band model of ZnSe : GaAs structure.

CHAPTER 6 CONCLUSIONS

Growth and characterization of ZnSe layers on GaAs and Si substrates have been reported. The physical parameters of GaAs and ZnSe as described in the previous chapters are useful for the understanding of the material properties. ZnSe thin films grown on silicon and GaAs are shown to be high quality as determined by X-ray diffraction technique. The films grown using vacuum evaporation technique helped in understanding the basic nature of the ZnSe thin films on different substrates.

A literature review gave an insight into all the aspects involved in the OMCVD technique for growing a good quality epitaxial layer. We were able to produce good quality films with a minimal residual impurity as determined by the PL spectra. The C-V characterization allowed us to estimate the donor concentration. We noticed that the carrier concentration over the entire layer is not very uniform. The photoresponse and the I-V characteristics are consistent with the proposed band model for the n-ZnSe:n-GaAs structure. The morphology of the OMCVD grown ZnSe on Si substrates showed a uniform growth at 250 and 300°C.

Although the above analysis shows satisfactory results, it is extremely difficult to obtain reproducible growth. There are many factors in the growth process that needs attention. Some of them are outlined below :

- 1] Cleanliness at every stage of fabrication is extremely

important because any contamination in the film could drastically affect the electrical characteristics.

2] Ohmic contacts to the epilayers are very important in determining the properties.

3] If the system pressure is not maintained properly, there could be a danger of oxide contamination in the grown layer. In fact some of the films appeared to be rough and the morphology was poor.

All these factors together make it important to exercise lot of care at all the stages of growth and characterization. We believe that the hetero structures such as ZnSe:GaAs will find applications in opto-electronic devices because of the blue light emitting properties.

REFERENCES

- 1] A.G. Milnes, *Deep Impurities in Semiconductors* (Academic Press, New York).
- 2] V. M. Goldschmidt, *Tran. Faraday Soc.* V25, (1929) 253.
- 3] A.N. Goryunova, *'The Chemistry of Semiconductors'* McGraw Hill, New York.
- 4] E. Nelson, *Jour. of elect. chem soc.* V112, (1963). 1020
- 5] & 6] J.J. Tietjen, J.A. Amik, *J. electrochem. soc.* V113, (1966) 724
- 7] H.M. Manasevit, *Appl. Phys. Lett.* V12, (1968) 156.
- 8] *The Tech. & Phys. of MBE* by E.H.C. Parker, Plenum Press, NY.
- 9] Gunther P., *PL spectra of II-VI compounds*, Plenum Press, NY.
- 10] K.L. Chopra, *Thin film Tech.* McGraw Hill, NY.
- 11] R.C. Miller and W.C. Tsang, *Appl. Phys. Lett.* v39 (1981) 334
- 12] Kane E.O., *J. Phys & Chem. of Solids*, v1 (1957) 249.
- 13] M.H. Cohen and T.K. Bergstresser, *Phy. Rev.* v141 (1966) 789.
- 14] S. Fugita. and Y. Tomonura, *Jap. J. Appl. Phys.*, v22 (1983) L583.
- 15] Y.P. Varshni, *Physica*, v34 (1977).
- 16] H. Kroemer, *Proc. IEEE*, v70 (1982) 13.
- 17] N. Mutsukuru and Yoshimachi, *Jpn. J. Appl. Phys.*, v18 (1979) 233.
- 18] R. Fornari, P. Franzosi, *J. Cryst. Growth*, v72 (1985) 717.
- 19] Holt D.B. and Muir M.D., *Academic Press* (1974) 335.
- 20] Hiroshi M. and R.J. Roedel, *Appl. Phys. Lett.* v34 (1979) 476.
- 21] Willams G.F. and Capasso F., *IEEE Elect. Div. Lett*, v3 (1982).

- 22] S.J. Bass, *Inst. Phy. Conf. series*, v33 (1977).
- 23] P.J. Wright and B. Cockayne, *J.Cryst.Growth*, v59 (1982) 142.
- 24] P. Besomi, B.W. Wessel, *Appl. Phy. Lett.*, v37 (1980) 955.
- 25] *Thin Film Tech.*, by Chopra K.L., Mc-Graw Hill Inc., NY.
- 26] Y. Shirakawa, *J. Appl. Phys.*, v51 (1980) 2014.
- 27] Hishachi s., Koukitu A., *Jpn. J. Appl. Phys.* v24 (1985) p458.
- 28] A. Koukitu, T. Suzuki, *J.Cryst. Growth*, v74 (1986) 181.
- 29] Novikova S. and P.G. Strelkov, *Sov.Phy.* v1 (1959) 1687.
- 30] R.L. Anderson, *solid state elect.*, v5 (1982) 341.
- 31] Swank G.F. and Williams W., *IEEE Devices lett.* v3 (1982) 71.
- 32] R.N. Bhargava, *J. Cryst. Growth*, v59 (1982) 15.
- 33] *The Crystalline State*, by Lawarance Bragg, Cornell Univ. Press, Itahca, NY.
- 34] G.K. Wehner, *Phys. Rev.*, v114 (1959) 1270.
- 35] S. Iida., T. Sugimoto, *J. Cryst.Growth*, v72 (1985) 51.
- 36] G. Jones, *J. Lumin.* v9 (1974) 389.
- 37] D.M. Matiox and J.E. Macdonald, *comunnications*, (1964) 2493.
- 38] S. Sritharan and K.A. Jones, *J. Cryst. Growth.*, v66 (1984) p656.
- 39] K. Mazuruk, M. Benzaquen, D. Walsh, B. Makuc, H. Jayatirtha and H. Aharoni, *proc. conf. sol. state tech. Ottawa 1988.*
- 40] D. Walsh, K. Mazuruk, M. Benzaquen and P. Weissfloch *semicond. sci. tech.* v3 (1988) L33.
- 41] R. Mach, W. Ludwig, *Phys. stat. solidi A*, v1 (1970) 701.
- 42] W. Stadius, *Appl. Phys. Lett.*, v33 (1978) 656.